THE EFFECT OF β-GLUCAN STRUCTURE ON THE RHEOLOGICAL PROPERTIES OF YEAST CELL WALLS

by

SPIROS JAMAS

S.B., Chemical Engineering
University of Manchester Institute of Science and Technology
(1981)

Submitted to the Department of
Nutrition and Food Science
in Partial Fulfillment of the
Requirements of the Degree of

MASTER OF SCIENCE

at the

MASSACHUSETTS INSTITUTE OF TECHNOLOGY

May, 1983

Signature of Author: _____
Department of Nutrition and Food Science, May 18, 1983

Certified by: _____
Thesis Supervisor

Accepted by: _____
Chairman, Committee on Graduate Students,
Department of Nutrition and Food Science

THE EFFECT OF β-GLUCAN STRUCTURE ON THE RHEOLOGICAL PROPERTIES OF YEAST CELL WALLS

by

SPIROS JAMAS

Submitted to the Department of Nutrition and Food Science on May 18, 1983 in partial fulfillment of the requirements for the degree of Master of Science in Food Science

ABSTRACT

The structure-function relationships of yeast glucans were studied. Rheological measurements were performed on whole glucan and on glucan subjected to chemical and enzymatic modification. A linear model has been developed to analyse these measurements. Thus, the hydrodynamic properties of the yeast glucan samples have been determined quantitatively. These results enable us to gain valuable insight to the 3-dimensional (tertiary) structure of the yeast glucan matrix.

Glucan samples were isolated from Saccharomyces cerevisiae A364A (wild type) and its cell division cycle mutants, 374 (cdc8) and 377 (cdc11). Whole glucan from the two mutants exhibit higher thickening properties than the wild type glucan. The thickening properties of the mutants' glucan can be enhanced by chemically extracting the interchain crosslinks. Furthermore, glucans from strains 374 and 377 consist of a denser matrix than the wild type glucan with a high degree of crosslinking. This crosslinking plays an important structural role.

Treatment by a lytic enzyme (laminarinase) generally causes a decrease in the thickening properties, however, this effect is less pronounced in 374 and 377 glucan.

Depending on the required application (eg. food thickening) the structure-function relationships of yeast glucan can be adjusted by chemical and enzymatic modification. The linear model will provide the qualitative standards in the process.

Thesis Supervisor: Dr. Anthony J, Sinskey.

Title: Professor of Applied Microbiology

ACKNOWLEDGMENTS

I would like to dedicate this thesis to my mother and father. Their continuous support and encouragement has been unsurpassed by anyone in my student years.

I wish to express my appreciation to Professor Anthony J. Sinskey for his guidance and patience throughout my two years at M.I.T. I would also like to thank Dr. Chokyun Rha and her group for their valuable cooperation and criticism of this work.

Finally, I would like to thank all the inhabitants of laboratories 16-222 and 16-210 for their friendship, their constructive criticism and their destructive criticism. I would like to thank Cheryl O'Brien for maintaining a level of human insanity in the lab.

My trainee laboratory technician Marianne Wenckheim deserves special mention for her valuable technique of test tube mixing.

This project was funded by the Center for Biotechnology Research. I acknowledge the Center's support and interest in this work.

TABLE OF CONTENTS

	Page
ABSTRACT	2
LIST OF TABLES	5
LIST OF FIGURES	6
1. INTRODUCTION	10
2. LITERATURE SURVEY	19
3. DEVELOPMENT AND APPLICATION OF THEORY TO VISCOMETRY STUDIES	40
4. MATERIALS AND METHODS	50
4.1 Strains	50
4.2 Growth Media	50
4.3 Yeast Fermentation	51
4.4 Glucan Extraction	52
4.5 Infra-red Spectroscopy	53
4.6 Capillary Viscometry	53
4.7 Laminarinase Digest	54
4.8 Acetic Acid Extraction	55
4.9 Total Carbohydrate Assay	56
5. RESULTS AND DISCUSSION	57
6. SUMMARY AND CONCLUSIONS	126
7. SUGGESTIONS FOR FUTURE RESEARCH	128
REFERENCES	130

LIST OF TABLES

Table No.	Title	Page
1.	Chemical Composition of Yeast Cells.....	12
2.	Chemical Composition of Yeast Cell Walls.....	12
3.	Composition of Media.....	51
4.	Yeast Fermentation.....	57
5.	Glucan Extraction.....	77
6.	Hydrodynamic Properties of Whole Yeast Glucan...	98
7.	Hydrodynamic Properties of Glucan after Acetic Acid Extraction.....	109
8.	Extraction of β(1-6) Glucan.....	111
9.	Hydrodynamic Properties of Glucan after Laminarinase Digest.....	119
10.	Effect of Laminarinase digestion time on the Hydrodynamic Properties of A364A Glucan.....	121

LIST OF FIGURES

Figure No.	Title	Page
1.	Viscosity Profiles of Three Different Morphologies	13
2.	Summary of Viscosity Profiles of Yeast Cells and Cell Wall Suspensions	14
3.	Viscosity Profile of Cell Wall Suspensions of *S. cerevisiae* A364A	15
4.	Viscosity Profile of Cell Wall Suspensions of *S. cerevisiae* JD7 Grown in SDC	16
5.	Viscosity Profile of Cell Wall Suspensions of Mycelium-like *S. cerevisiae* JD7	17
6.	Yield Stress-Concentration Relationships of Mycelium-like Cell Wall Suspensions and CMC	18
7.	Arrangement of Mannoprotein in the Yeast Cell Wall	21
8.	Pathways in Mannan Biosynthesis	23
9.	Arrangement of Glucan and Mannan in the Yeast Cell Wall	26
10.	General Structure of the Alkali Soluble Glucan Fraction	28
11.	General Structure of the Alkali Insoluble Glucan Fraction	30
12.	The Proposed Mechanism for Glucan Synthetase Regulation	36
13.	Growth Curve for *Saccharomyces cerevisiae* A364A.	58
14.	Growth Curve for *Saccharomyces cerevisiae* 374...	59
15.	Growth Curve for *Saccharomyces cerevisiae* 377...	60
16.	Morphology of *Saccharomyces cerevisiae* A364A....	61

17[a]. Morphology of Saccharomyces cerevisiae 374 Grown at 28°C..... 63

17[b]. Morphology of Saccharomyces cerevisiae 374 after 4 hours at 37°C..... 65

18[a]. Morphology of Saccharomyces cerevisiae 377 Grown at 28°C..... 67

18[b]. Morphology of Saccharomyces cerevisiae 377 after 4 hours at 37°C..... 69

19. A364A Glucan..... 71

20. 374 Glucan..... 73

21. 377 Glucan..... 75

22. I.R. Spectrum of Laminarin (2% w/w sample concentration)..... 79

23. I.R. Spectrum of β-Gentiobiose (2% w/w sample concentration)..... 80

24. I.R. Spectrum of A364A Glucan (2% w/w sample concentration)..... 81

25. I.R. Spectrum of 374 Glucan (2% sample concentration)..... 82

26. I.R. Spectrum of 377 Glucan (2% w/w sample concentration)..... 83

27. I.R. Spectrum of A364A Glucan (8% w/w sample concentration)..... 84

28. I.R. Spectrum of 374 Glucan (8% w/w sample concentration)..... 85

29. I.R. Spectrum of 377 Glucan (8% w/w sample concentration)..... 86

30. I.R. Spectrum of A364A Glucan after Acetic Acid Extraction (8% w/w)..... 87

31. I.R. Spectrum of 374 Glucan after Acetic Acid Extraction (8% w/w)..... 88

32. I.R. Spectrum of 377 Glucan after Acetic Acid Extraction (8% w/w)..... 89

33. Cooperative Hydrogen Bonding in Adjacent Cellulose Molecules..... 90

34. Inter-Molecular Hydrogen Bonding within a β(1-3) Glucan Molecule..... 90

35. Viscosity Profiles of Yeast Glucan Comparing Different Cell Morphologies..... 94

36. Plot of the Modified Mooney Equation for A364A Glucan..... 95

37. Plot of the Modified Mooney Equation for 374 Glucan..... 96

38. Plot of the Modified Mooney Equation for 377 Glucan..... 97

39. Viscosity Profile of A364A Glucan Showing the Effect of 3h. Extraction in Acetic Acid..... 100

40. Viscosity Profile of 374 Glucan Showing the Effect of 3h. Extraction in Acetic Acid..... 101

41. Viscosity Profile of 377 Glucan Showing the Effect of 3h. Extraction in Acetic Acid..... 102

42. Plot of the Modified Mooney Equation for A364A Glucan..... 103

43. Plot of the Modified Mooney Equation for A364A Glucan after 3h. Extaction in Acetic Acid. 104

44. Plot of the Modified Mooney Equation for 374 Glucan..... 105

45. Plot of the Modified Mooney Equation for 374 Glucan after 3h. Extraction in Acetic Acid.. 106

46. Plot of the Modified Mooney Equation for 377 Glucan after 3h. Extraction in Acetic Acid.. 107

47. Viscosity Profile of A364A Glucan Showing the Effect of 4h. Laminarinase Digest..... 113

48. Viscosity Profile of 374 Glucan Showing the Effect of 4h. Lamminarinase Digest..... 114

49. Viscosity Profile of 377 Glucan Showing the Effect of 4h. Laminarinase Digest..... 115

50. Plot of the Modified Mooney Equation for A364A Glucan after 4h. Laminarinase Digest..... 116

51. Plot of the Modified Mooney Equation for 374 Glucan after Laminarinase Digest..... 117

52. Plot of the Modified Mooney Equation for 377 Glucan after 4h. Laminarinase Digest..... 118

53. Viscosity Profile of A364A Glucan Showing the Effect of Incubation Time with Laminarinase..... 122

54. Plot of the Modified Mooney Equation for A364A Glucan - the Effect of Incubation Time with Laminarinase..... 123

55. Linear Correlation of a Hydrodynamic Parameter of A364A Glucan to Incubation Time with Laminarinase..... 124

1. INTRODUCTION

The study of structure-function relationships of biopolymers is becoming a field of increasing importance. With the advent of genetic engineering, biopolymers can be modified *in vivo* to produce molecules with altered physical properties.

Polysaccharides which form the bulk of biopolymers in the microbial world have already been noted for their structural importance and are responsible for maintaining the integrity of bacteria and fungi.

An initial study performed by Liu (S.M. Thesis, Dept. of Food Science, M.I.T., 1981) compared the rheological properties of *Saccharomyces cervisiae* A364A and its morphological mutant JD7. The results indicate that the branched and elongated cells of JD7 impart a higher viscosity in solution than the spherical A364A cells and also have a lower critical concentration (see Figs. 1,2,3,4,5,6). Furthermore, the cell wall components exhibit viscosities 3-4 times higher than the whole cells and the yield stress of the cell wall components was comparable to other hydrocolloidal polysaccharides.

These cell wall components consisted mainly of glucan, and it was also observed that the morphological mutant JD7 had a higher glucan content than the yeast-like A364A (Table 1,2).

This study is therefore directed to investigate the

structure-function relationships of yeast glucan as a first phase in the development of a scheme to produce glucan with desirable physical properties through directed biosynthesis.

For this study, morphological mutants with a block in their cell division cycle were chosen in order to elucidate the changes in glucan structure that occur when a morphological change is induced. This is important since genetically directed biosynthesis can be achieved only once we have understood the machinery and information that the cell requires to synthesize new glucan.

Various processing procedures can be used to remove the outer mannan and glycogen components of yeast cell walls and obtain either soluble (2) or insoluble (3,4) fractions of glucan. For the initial phases of this study, the alkali-insoluble glucan fraction has been used. This fraction generally contains a major component (about 85%) of a branched β(1-3) glucan which 3% β(1-6) interchain links (3) and a minor component which is a β(1-6) glucan.

Studies on rheological properties and structure was obtained for these glucan samples.

Table 1

Chemical Composition of Yeast Cells (1)

(%)	JD7-YPD*	JD7-SDC	A364A-YPD	A364A-SDC
Trehalose	4.5±0.4	3.2±0.8	10.1±0.6	5
Alkali-soluble Glycogen	5.4±0.7	6.4±1.1	5.7±0.2	9
Total Glycogen	17.3	18.2	13.8	20.3
Mannan	12.8±0.1	11.6±0.4	16.3±0.4	12.1
Glucan	14.6±0.9	13.8±o.3	12.1±0.5	11.5
Total Carbo-hydrate	50	43	49	41
Protein	54	45	52	43

* Strain-Medium

Table 2

Chemical Composition of Yeast Cell Wall(1)

Composition(%)	JD7-YPD*	JD7-SDC	A364A-YPD
Trehalose	-	-	-
Alkali-soluble Glycogen	0.7	1.4	1.6
Acid-soluble Glycogen	39.8	31.2	37.9
Total Glycogen	40.5	35.6	38.3
Mannan	ND	ND	ND
Glucan	39.5	35.9	38.3
Total carbohydrate	78	75	80
Protein	ND	ND	ND

ND - not detected
*strain-medium

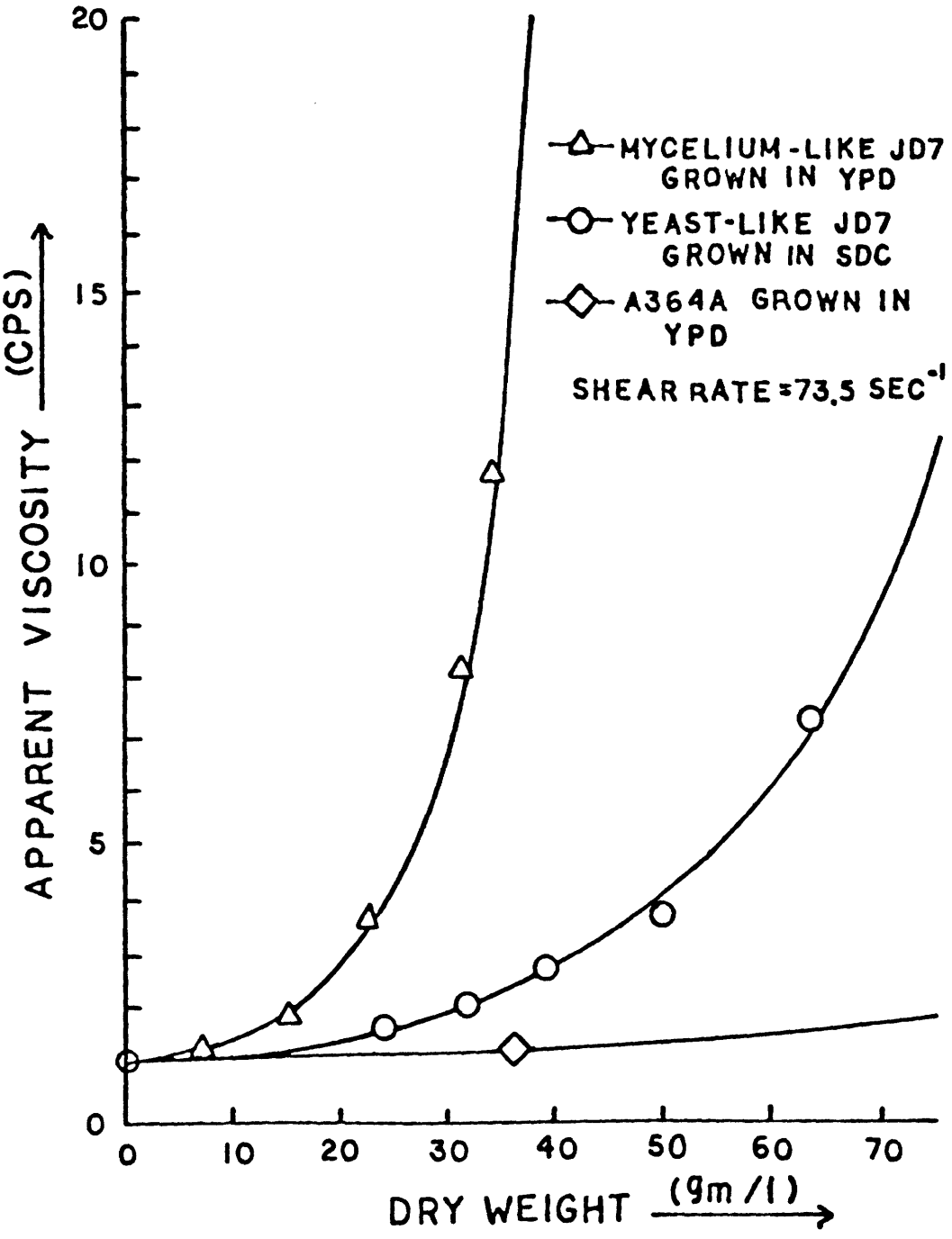

Figure 1: Viscosity Profiles of Three Different Morphologies

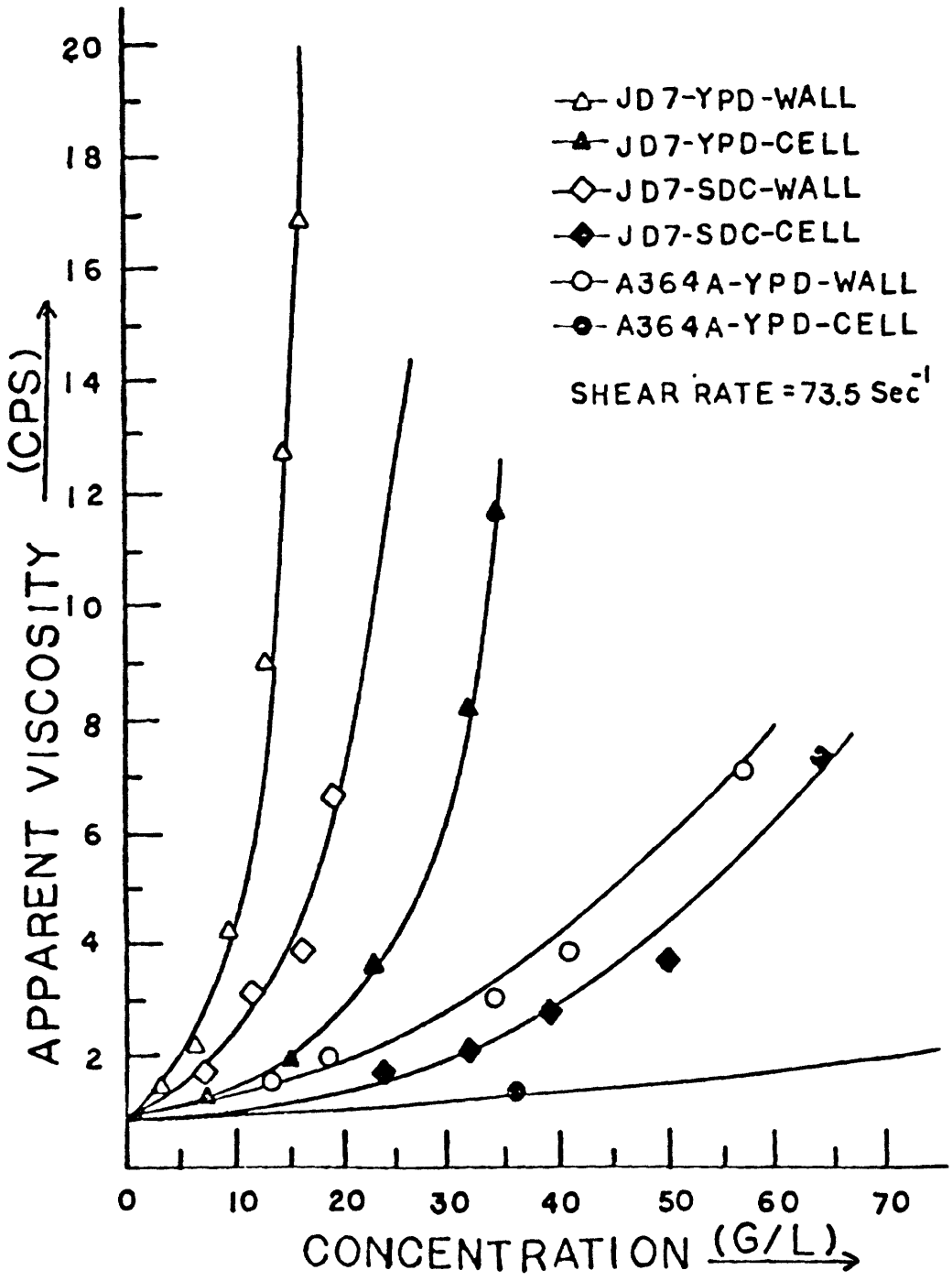

Figure 2: Summary of Viscosity Profiles of Yeast Cells and Cell Walls Suspensions

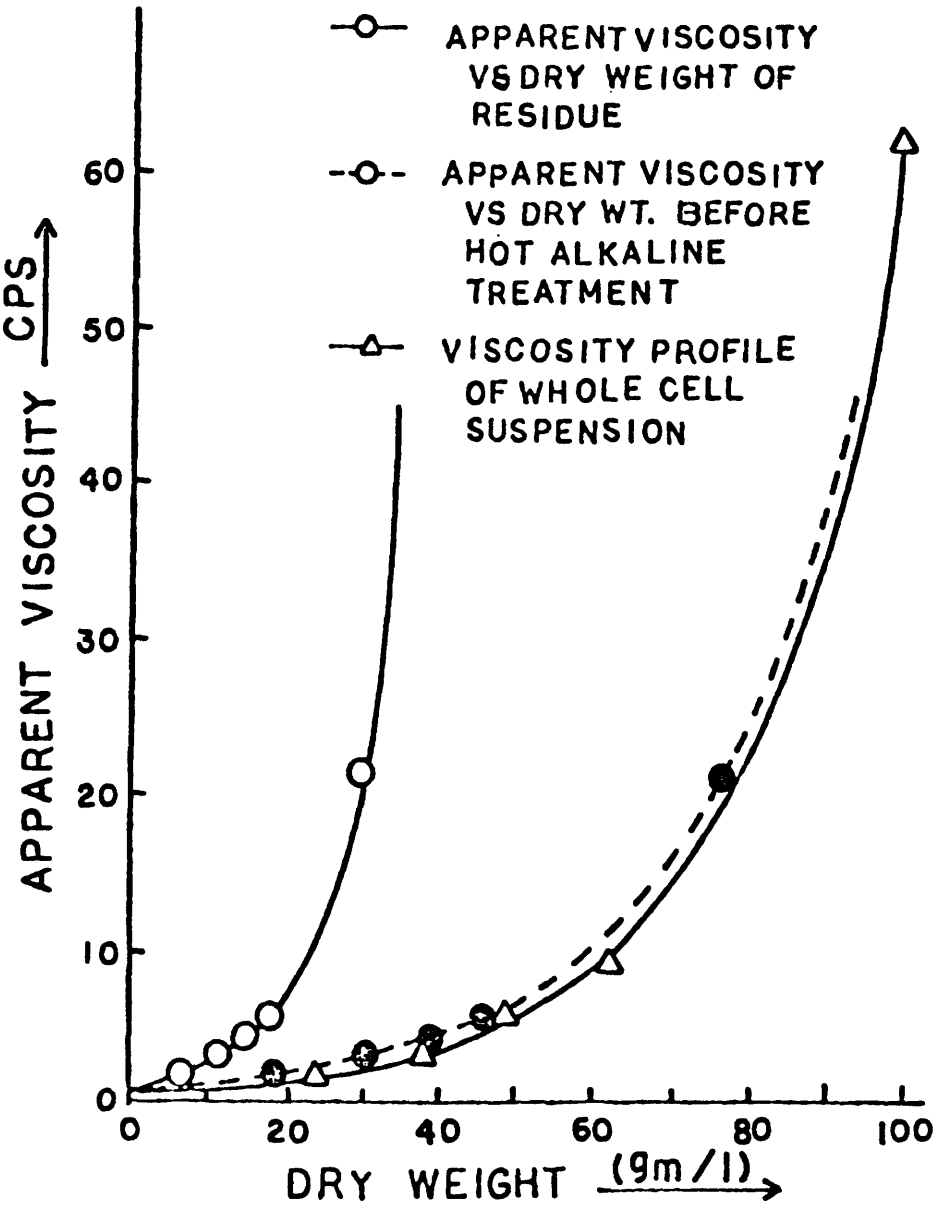

Figure 3: Viscosity Profile of Cell Wall Suspensions of Saccharomyces cerevisiae A364A

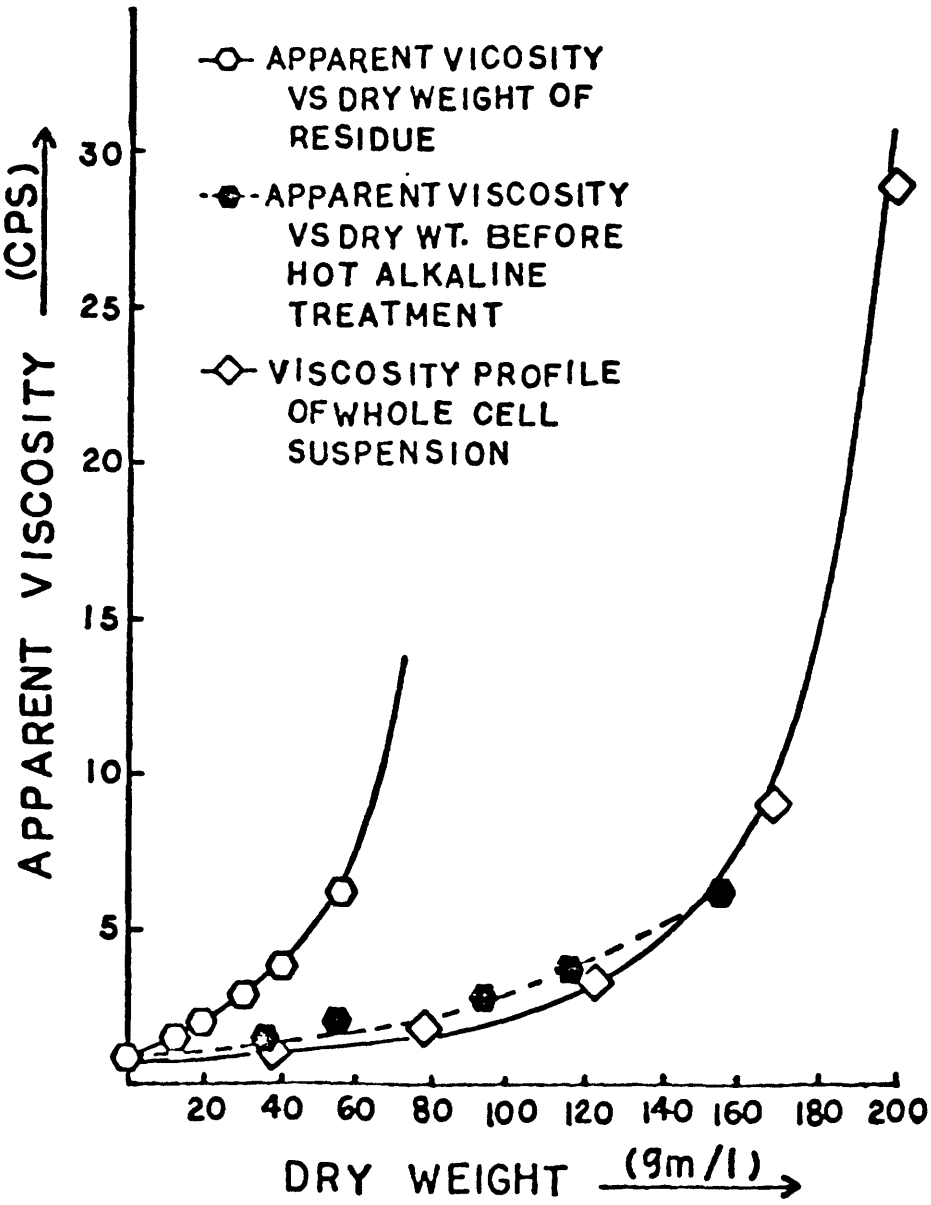

Figure 4: **Viscosity Profile of Cell Wall Suspensions of** *Saccharomyces cerevisaie* **JD7 Grown in SDC**

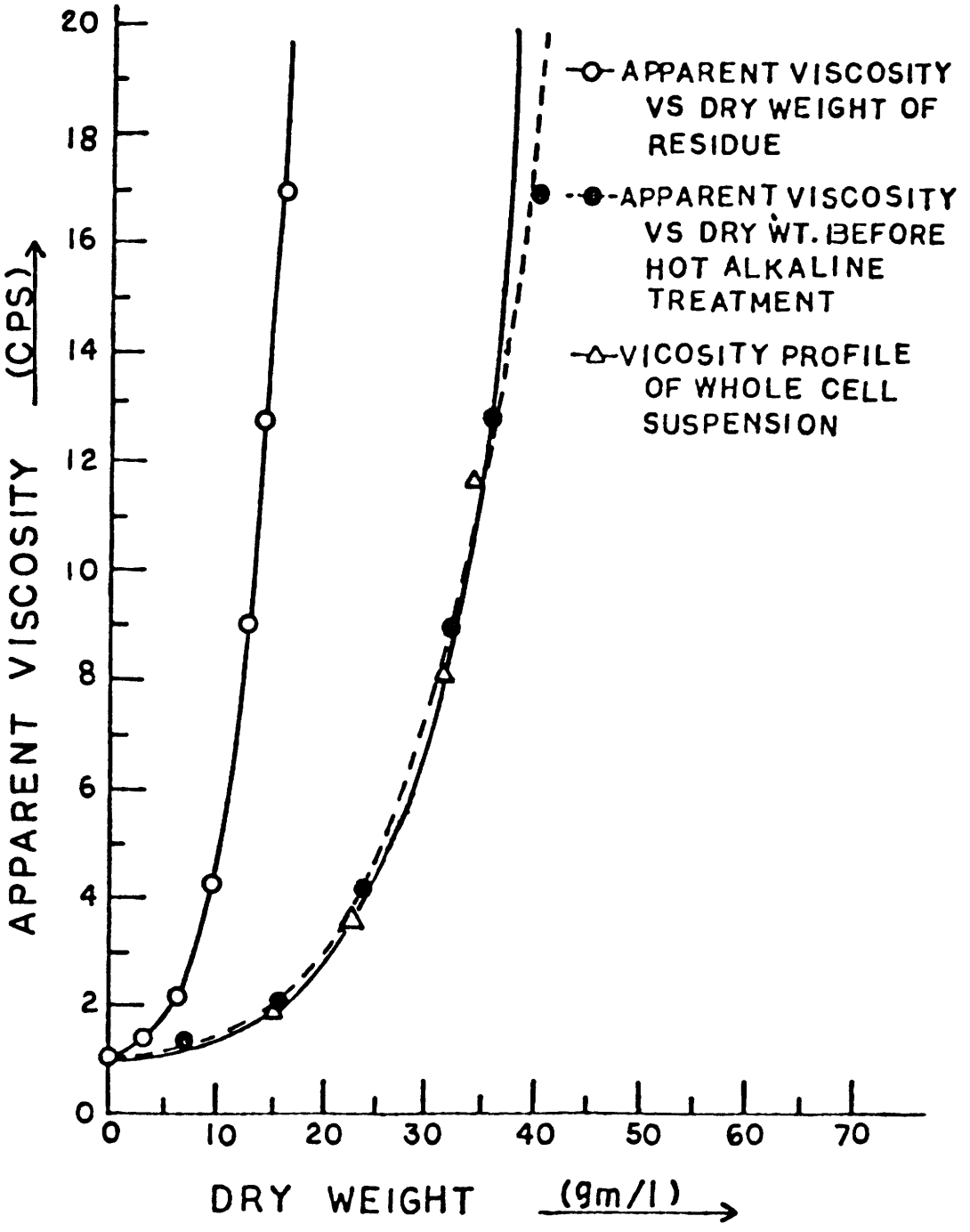

Figure 5: Viscosity Profile of Cell Wall Suspensions of Mycelium-like Saccharomyces cerevisiae JD7

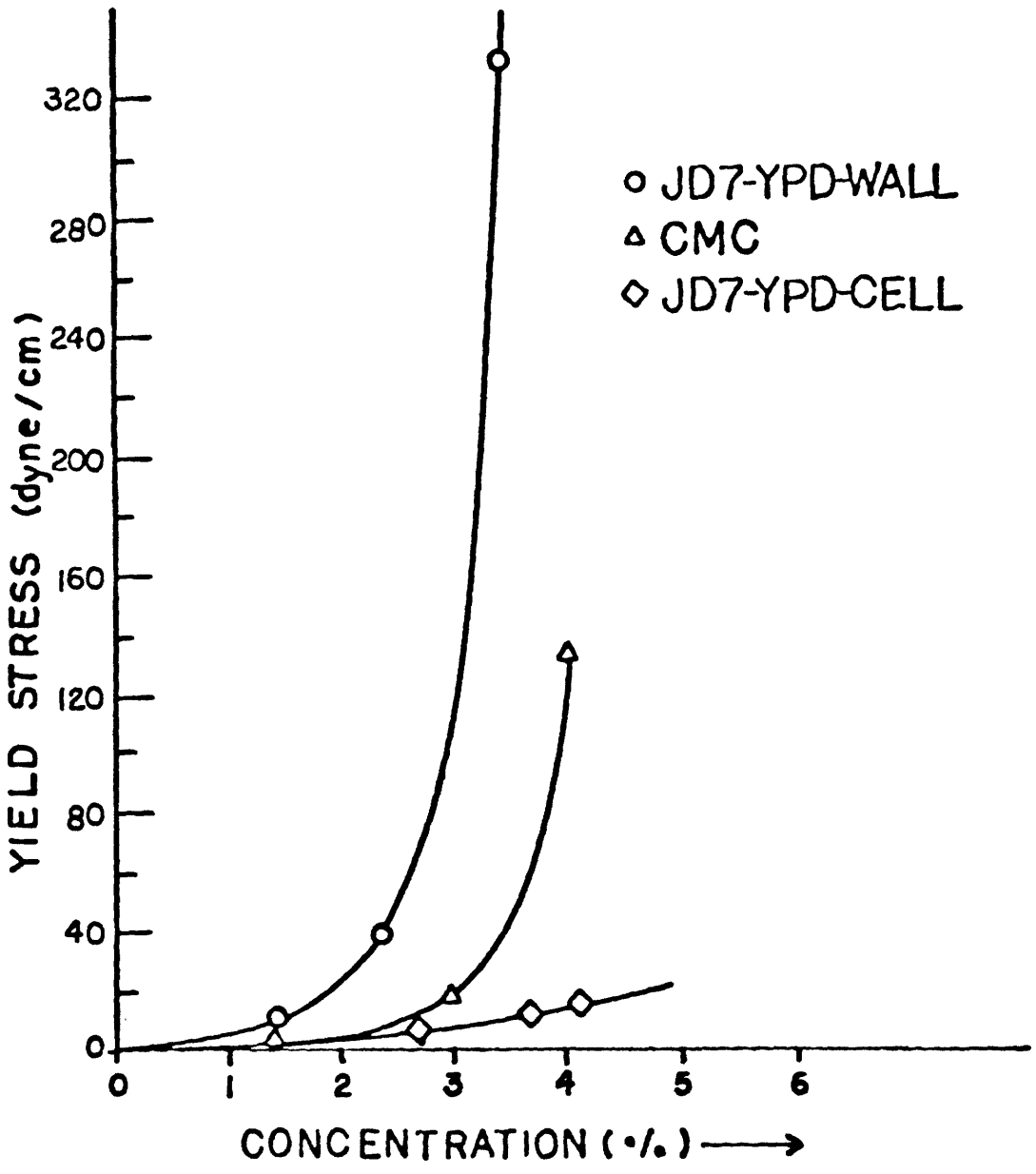

Figure 6: Yield Stress-Concentration Relationships of Mycelium-like Cell Wall Suspensions and CMC

2. LITERATURE SURVEY

2.1 The Yeast Cell Wall

Yeast cells are encapsulated in a rigid wall consisting almost entirely of three polysaccharide components. The chemical structure of the components is relatively simple but unique to each. Hence, with this careful tuning of structure the cell is able to assign specific physical functions (structure-function properties) to these polysaccharides.

The three components are homopolysaccharides of glucose, mannose and N-acetylglucosamine and occur as independent structures in the cell wall. Only mannan (mannose polymer) is known(5) to be covalently linked to a short peptide moiety. However, recent studies(6,7) provide evidence for a possible linkage between chitin and glucan-either directly or through short peptide sequences containing mainly lysine and citrulline.

Glucan (the glucose polymer) provides the structural rigidity of yeast cell walls and hence maintains the morphology of yeasts. A detailed review on the structure and biosynthesis of yeast glucan will be included below.

The mannoprotein component can be extracted from whole cells by heating in citrate buffer (pH 7.Ø) or in dilute alkali. This treatment solubilizes the mannoprotein and

depending on the exact procedure fragments with various degrees of disruption are obtained(5). The mannan fragments have molecular weights ranging from 25,000 to $1x10^6$. The heterogenous fractions of mannoprotein obtained can be assigned to two groups on the basis of their functionaal role in the cell wall. The first is the structural component. It is interspersed throughout the cell wall and also covers the surface(8) acting as a cement. The second is the enzyme bound component. Mannan provides a matrix for the location of cell wall expansion enzymes (exoenzymes) such as invertase and acid phosphatase(5). In Saccharomyces cerevisiae an outer mannan core and an inner mannan core have been distinguished(8). The inner mannan core consists of a chain of 15-17 α(1-6) linked mannose units. This main chain is highly branched through α(1-2) and α(1-3) bonds to oligomannose residues varying in length. The terminal mannose unit in the inner core is linked through β(1-4) bonds to the asparagine unit(5) of the peptide through an acetylglucosamine bridge. In addition the inner core consists of short oligomannoside chains linked directly to the serine and threonine of the proteins(5).

The outer core mannan chain consists of a much longer α(1-6) linked backbone with heterogenous branching through α(1-2) and α(1-3) linkages. Phosphodiester bonds are also found linking the side-chains(8).

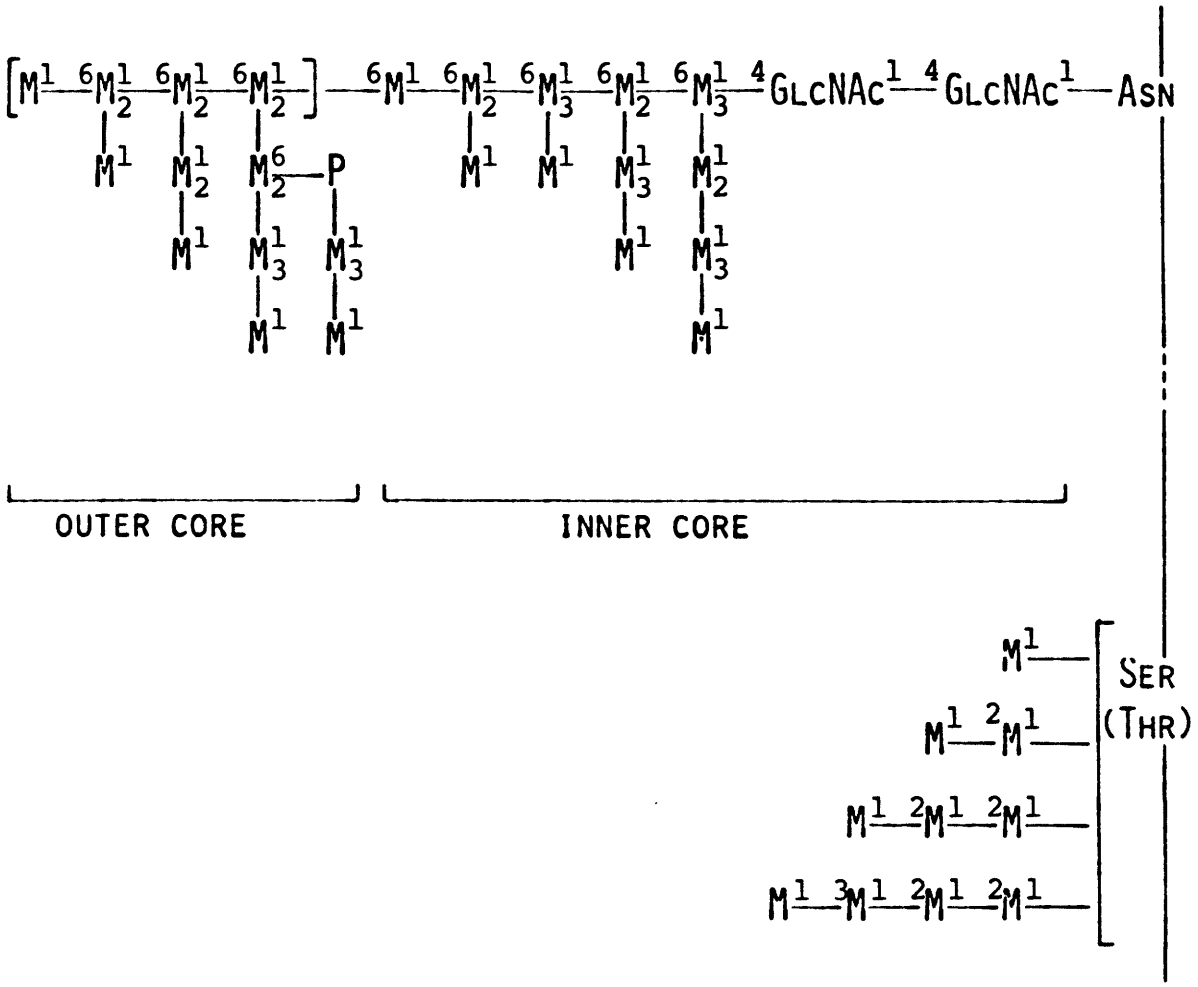

Figure 7. Arrangement of Mannoprotein in the Yeast Cell Wall

The biosynthesis of mannan follows rather more complex pathways than chitin and glucan. In fact, lipid-linked intermediates are known(8) to be involved in mannan biosynthesis. Also, the fact that mannan is the only component in the yeast cell wall to be of glycoprotein nature complicated the elucidation of these pathways further.

The isolation and characterization of mannan mutants of

Saccharomyces cerevisiae along with the finding that antibiotic tunicamyacin(9) inhibits mannan biosynthesis in yeast protoplasts played an important role in clarifying the structure and biosynthetic pathways involved.

Initial studies on mannan biosynthesis investigated the formation of the carbohydrate portion. Enzyme preperations from lysed protoplasts of Saccharomyces carlsrbergensis (8,9) were shown to catalyse the transfer of mannose residues from a nucleotide precursor to form mannan. The enzyme preparation is specific for the precursor GDP-mannose however, no primer is required. The presence of Mn^{2+} is essential. The acetolysis fragments of the synthesized mannan revealed a structure resembling that found in vivo . Studies on the effects of cations(9) provided evidence for the involvement of lipid bound intermediates in mannan biosynthesis. It was observed that in the presence of either Mn^{2+} or Mg^{2+} as the only cation a mannosyl-lipid intermediate was formed from GDP-mannose but no mannan was produced(9). In the presence of both cations mannosyl residues were transfered from the nucleotide-sugar precursor to the lipid bound intermediate and then to mannan.

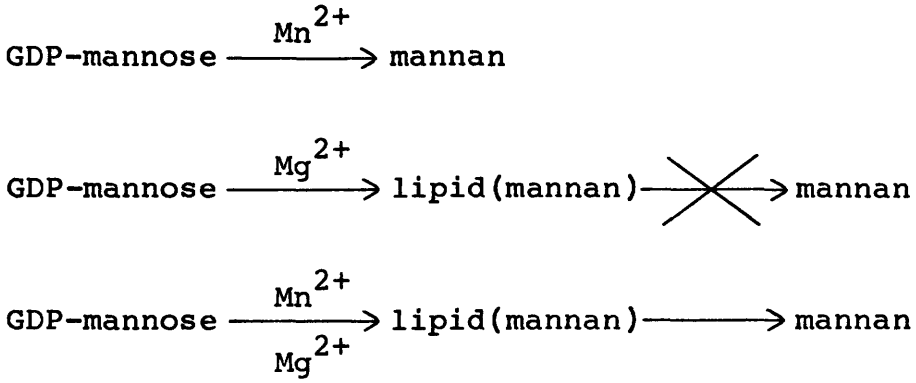

Figure 8. Pathways in mannan biosynthesis.

The lipid intermediate was identified(9) to be dolichyl-monophosphate-mannose (DMP-mannose). Recently the role of DMP-mannose in the formation of mannoproteins was clarified(9). In the short mannan sequences linked to serine and threonine residues of the protein, only the mannosyl residue directly linked to the protein is incorporated from the lipid intermediate. The subsequent addition of mannose units occurs directly from the nucleotide-sugar precursor. However, the complete role of the lipid intermediate in the synthesis of the high molecular weight mannan of the inner and outer core has not been understood. The current working hypothesis is that an oligosaccharide moiety which represents part of the inner core is first N-glucosidically linked to the protein's asparagine residue in a lipid intermediate involving step. Once this step is completed further mannosylation occurs by direct transfer from GDP-mannose. The formation of the

specific bonds (α(1-2), α(1-3), α(1-6)) in the outer core and branches is controlled by specific mannosyl transferases(9).

Most of the chitin found in yeast (Saccharomyces) cell walls is located in the bud scars and constitutes the primary septum. Although chitin is a major component of fungal walls it only constitutes approximately 1% of the yeast cell wall polysaccharides. It is a linear polymer of α(1-4) linked N-acetylglucosamine residues. The structure of chitin has been chracterized in detail(8). In yeasts the α crystalline form occurs. In this form chitin chains run antiparallel to each other thus allowing extensive intramolecular hydrogen bonding to occur. Hence, chitin is resistant to chemical extraction and insoluble in water.

As mentioned above over 90% of the chitin found in yeast is located in the bud scar region(10). During early budding, chitin appears as a ring surrounding the neck between the mother and daughter cells. Before each cell division chitin grows over the annulus between the two cells forming a disc-shaped cross-wall. However, studies by Molano et al (10) on purified septa showed the presence of an anthrone reacting agent in the septal disc. This material constituted approximately 15% of the septa and could possibly be glucan. The remaining fraction of chitin is distributed as lozenge-shaped particles over the entire

cell wall.

Chitin synthesis is not necessarily localised at the budding region of a cell. In fact, studies made on yeast with a block in the cdc24 gene(8) revealed that chitin was synthesized randomly over the entire surface of unbudding cells.

The biosynthesis of chitin involves the enzyme chitin synthetase which is inactive in the native state(9). The enzyme can be activated by mild proteolysis in the presence of an unknown activating factor or trypsin. The existing tentative mechanism is that activation of chitin synthetase occurs by proteolytic destruction of an inhibitor which is tightly bound to the enzyme. The pathway for chitin synthesis resembles the mannan pathway in that a nucleotide precursor transfers the sugar residues to an endogenous receptor. In yeasts Mg^{2+} and Mn^{2+} cations are essential for this pathway(8).

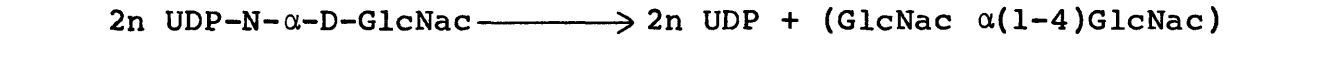

The endogenous acceptor is chitin itself however, it is not known if an acceptor is required for the initiation of chitin synthesis. Oligomers of N-acetylglucosamine clearly stimulated the enzyme preparation from fungi(9) however, their exact role as primers of chitin synthesis is not clear.

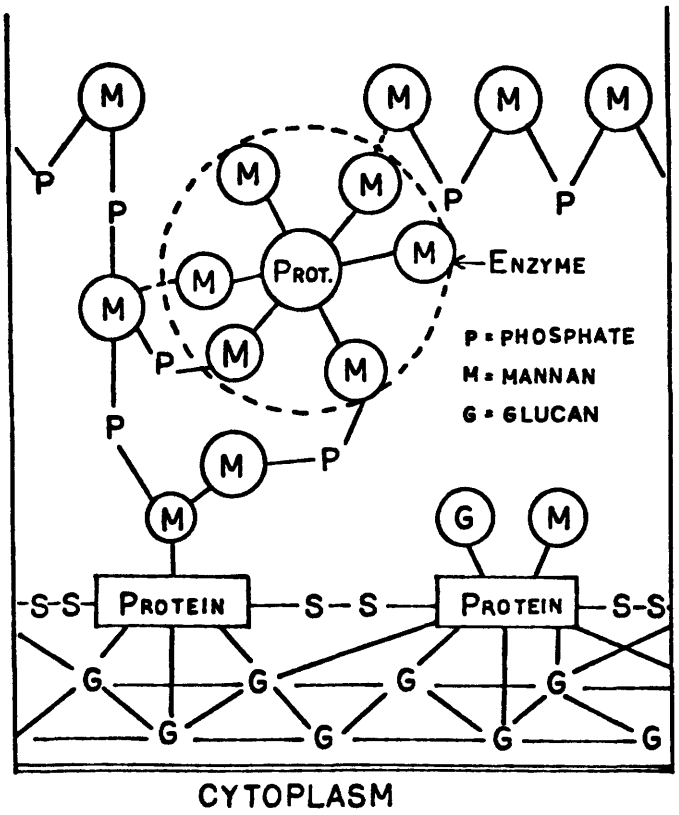

Figure 9. Arrangement of Glucan and Mannan in the Yeast Cell Wall

2.2. The Structure of Yeast Glucan

Glucan, the major structural polymer in yeast cell walls is a polymer of glucose linked through either β(1-3) or β(1-6) glucosidic linkages. The role of glucan in yeast cell walls was understood after removal of mannan, chitin and a soluble glucan component from cell walls by chemical and enzymatic treatment had no effect on the cell morphology(9).

As shown in Figure 3., and determined by Kopecka et al (11) β(1-3) linked glucan forms a fine fibrillar layer in the cell wall adjacent to the cytoplasm. The β(1-6) branches and other polysaccharides are located on this inner fibrillar layer. However, the yeast cell wall must not be considered as a structure containing seperate polysaccharide layers. The glucan provides a gross structural matrix onto which the other polysaccharide components are located.

Treatment of yeast (Saccharomyces) cell walls with β(1-3) and β(1-6) glucanase enzymes(11) revealed that digestion began at the outer bud scar regions and then proceeded in all directions. This observation agrees with that of Molano et al(9) that glucan is present in yeast septa.

Glucans are grouped on the basis of their solublity in alkali. Three fractions of glucan have been identified(12,13,14). These are an alkali soluble component, an insoluble component consisting mainly of (1-3) linkages and a highly branched component, consisting mainly of β(1-6) linkages, which is tightly associated with the former.

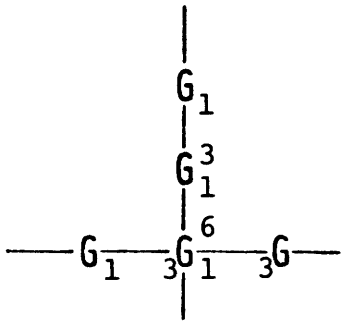

Figure 1Ø. General Structure of the Alkali Soluble Glucan Fraction

The minor alkali soluble component is of little structural importance to the cell wall. When extracted with cold dilute sodium hydroxide this component comprises about 2Ø% of the cell wall(2). Structural analyses showed that this glucan consisted of 8Ø-85% β(1-3) linkages, 8-12% β(1-6) linkages and 3-4% heterogenous branches. This glucan has a degree of polymerization of approximately 1,5ØØ and a molecular weight of 25Ø,ØØØ , thus, it is very similar to the alkali insoluble fraction. Furthermore, both glucans show approximately 3-4% branching through β(1-3) and β(1-6) linkages. Thus the only structural difference explaining the solubility characteristics of the two glucans is that the soluble fraction contains 8-12% β(1-6) linked residues. Consequently, the arrangement of these linkages is important in determining the physical properties of glucans. The results of Smith-degradation(2) on this glucan suggested the

general structure shown in Figure 10.

The major insoluble glucan fraction accounts for 85% of the total yeast glucan. This glucan consists of a β(1-3) linked backbone of high molecular weight containing 3% β(1-6) interchain linkages(3). The molecular weight of the β(1-3) linked backbone after extraction in acetic acid is 240,000. However comparison of the results obtained by Bacon et al (3) and Manners et al (3) indicate that the β(1-6) linkages have an insignificant effect on the final evaluation of the molecular weight, showing that these linkages are present in minor quantities.

The ability of glucan to provide the cell with an insoluble envelope clearly depends on fine tuning its structure. The length of the β(1-3) backbone has a significant effect on the solubility of the molecule. For example, laminarin which has an average degree of polymerization of 10(3) and a low degree of branching is soluble in water. But, linear laminarin molecules containing 20 glucose residues are insoluble in water. Therefore, by applying this knowledge to yeast glucan Manners et al (3) assumed that the high molecular weight β(1-3) glucan molecules were essentially linear and by the appropriate inter-chain and intra-molecular β(1-6) crosslinking an insoluble matrix is formed. With the information available to date on glucan structure it can be

postulated that the insoluble β(1-3) component forms a two dimensional random tree-type structure resembling that proposed for amylopectin. Evidence for yeast glucan existing wholly or partially in a triple-helical form has not been found. The degree of polymerization of this glucan was found to be about 1500 (3). Hence, it can be calculated that each glucan molecule contains approximately 50 side chains. The glucan structure proposed by Manners et al (3) is illustrated below.

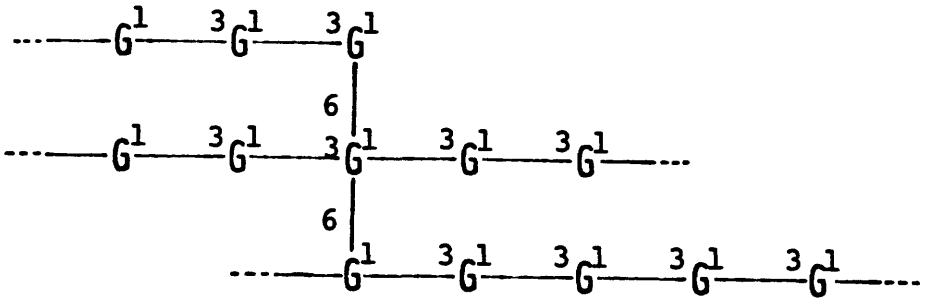

Figure 11. General Structure of the Alkali Insoluble Glucan Fraction

The minor insoluble component isolated from Saccharomyces cerevisiae is a highly branched glucan with a degree of polymerization in the range 130-140. This molecule has a high proportion of β(1-6) linkages with a smaller proportion (19%) of β(1-3) glucosidic linkages(4). This component can be isolated either by selective enzymolysis (endo- β-(1-3) glucanase) of a whole glucan sample or by extraction in hot acetic acid. Both procedures

yield very similar glucan structures. The resistance of this glucan fraction to degradation by endo-β -(1-3) glucanase shows that adjacent β(1-3) glucosidic linkages are absent. Therefore, the 19% β(1-3) linkages present act as inter-chain or intra-molecular linkages(4).

Extraction of this fraction in hot acetic acid revealed that it is soluble in aqueous solution. This is possibly due to the high degree of branching in the molecule which prevents the suitable allignment of adjacent molecules to form an insoluble matrix.

In the above review of the structure of insoluble β-glucan attempts were made to explain the solubility properties on the basis of inter-chain and intra-molecular branching. The structure of β-glucans definitely plays an important role on these properties. However, recent evidence shows that the solubility of β-glucans is affected by a possible covalent linkage with chitin. Sietsma and Wessels(6) first proposed the existance of this linkage after studying the effects of selective enzymatic hydrolysis and chemical treatment on cell wall preparations of the fungus Schizophyllum commune. Degradation of the chitin present in the alkali insoluble fraction of the cell walls caused a significant increase in the solubility of the β-glucan. Chitin was removed either by digestion with a purified chitinase or by deacetylation with alkali followed

by depolymerization in nitrous acid. Both methods released two β-glucan components, an alkali insoluble component with single glucose unit branches, and a highly branched water soluble component.

Treatment of the glucan/chitin complex with β(1-3) glucanase dissolved 90% of the β-glucan and the remaining residue could be hydrolysed with chitinase to yield N-acetylglucosamine and an N-acetylglucosamine-lysine-citrulline complex. The glucan/chitin complex was found to contain 50% lysine, 20% citrulline and approximately 12.5% glutamic acid(6).

Recently, Sietsma and Wessels(7) obtained similar evidence for the covalent glucan-chitin linkage in Saccharomyces cerevisiae. The glucan fraction remaining insoluble after extraction in 40% sodium hydroxide at 100°C could be solubilized after treatment with nitrous acid. Since nitrous acid depolymerises the acetylated chitin the possibility of a glucan/chitin linkage is supported.

2.3 Glucan Biosynthesis

The presence of three distinct, and chemically related glucans in the cell walls of yeast hinders the complete understanding of their respective functions and modes of biosynthesis. In contrast to the structural importance of this compound in yeast cell walls, little information

concerning glucan biosynthesis is available. Initially, incorporation studies using whole cells were used to obtain information on the overall biosynthetic pathway. Sentandreu et al (13) used Saccharomyces cerevisiae cells permeabilized by treatment with toluene and ethanol. On incubation of the cells with labelled UDP-[U- ^{14}C]glucose , synthesis of a labelled β(1-3)glucan was observed. No labelled lipids were detected.

The next step in understanding glucan biosynthesis was a study performed by Elorza et al (14). The workers investigated glucan biosynthesis at the translational and transcriptional level by employing Saccharomyces cerevisiae ts(-136). RNA synthesis is blocked by incubation at the non-permissive temperature (37 ^{o}C). Cycloheximide was used to block protein synthesis. After shifting log phase cells to the non-permissive temperature a decrease in mannan formation was observed however glucan synthesis continued for a further 5 hours. This observation indicated that mRNA's of the wall peptides have a relatively slow decay rate. By blocking protein synthesis with cycloheximide mannan formation was blocked after a few minutes whereas glucan formation was unaffected. This result suggests a high degree of stability for the glucan synthetases.

Lopez-Romero and Ruiz-Herera(15) demonstrated that cell free extracts from Saccharomyces cerevisiae could synthesize glucan containing both β(1-3) and β(1-6) linkages. The

incorporation of glycosyl residues from UDP-(U-^{14}C)glucose and GDP-(U-^{14}C)glucose was investigated. Only trace amounts of glucose were incorporated from the latter, however a glucan containing both β(1-3) and β(1-6) linkages was synthesized from the UDP-sugar precursor. Membrane and cell-wall fractions were used, however activity was higher in the cell wall fraction.

An interesting point that arose from this study was that a mixed membrane preparation catalysed the formation of a glucan containing Ø.6% β(1-6) linkages whereas a glucan containing 2.5% β(1-6) linkages was formed using the cell wall fraction. The glucan synthesized from the latter resembles the major alkali insoluble glucan fraction found in vivo . However, the in vitro synthesized glucan is soluble in alkali possibly due to a lower molecular weight. From these results it can be assumed that the β(1-6)glucosyl transferase is mostly associated with the cell walls. Biosynthesis of β-glucan was specific for UDP-glucose.

The regulation of β(1-3)-glucosidic bond formation in glucan was studied in detail by Shematek and Cabib(16) using a membrane preparation from Saccharomyces cerevisiae . UDP-glucose was used as the sugar donor and the reaction addition of glycerol, bovine serum albumin and ATP or GTP to activate the membrane preparation. Under optimal conditions the workers obtained 2Ø-5Ø% incorporation of the substrate

in 20 minutes. The glucan produced was water insoluble and alkali soluble, and was characterized to be a β(1-3) glucan of degree of polymerization 60 to 80. No evidence for the requirement of a primer was found and no lipid linked intermediate was involved in the synthesis of the glucan. Equivalent amounts of UDP were liberated for each glucose unit transfered hence, the following equation can be written:

$$\text{UDP-glucose} + (\beta(1\text{-}3)\text{glucose})_n \longrightarrow \text{UDP} + (\beta(1\text{-}3)\text{glucose})_{n+1}$$

In contrast to mannan and chitin biosynthesis, the transfer of the sugar from the nucleotide-sugar precursor does not require the presence of divalent cations.

During the yeast cell cycle the synthesis of wall material is not evenly distributed over the cell wall. For example, during budding cell wall synthesis is quiescent in the mother cell whereas new cell wall material is actively synthesized at the growing bud. The need for a reversible activation/inactivation scheme for glucan synthesis is therefore implied. A regulatory mechanism for the membrane bound β(1-3) synthetase is essential to localize the enzyme activity where required.

Shematek and Cabib(17) observed that the membrane bound synthetase is stimulated by ATP or GTP. ATP activation is inhibited by the presence of EDTA whereas GTP activation

requires EDTA. Several GTP analogs which are unable to transfer the γ-phosphate also acted as stimulants of the enzyme preparation indicating that the γ-phosphate of GTP is not involved in enzyme activation. The simple working hypothesis derived from these observations is:

GTP stimulation occurs by binding to a site on the membrane while ATP converts a loosely bound phosphorylated substrate into a product tightly bound to the enzyme. In the presence of Mg an endogenous hydrolytic enzyme converts the ATP product back into the ATP substrate hence allowing reversible activation/inactivation of the enzyme.

Now, to simplify this mechanism it can be assumed that the phosphorylated substrate and the product are GDP (or GMP) and GTP, respectively.

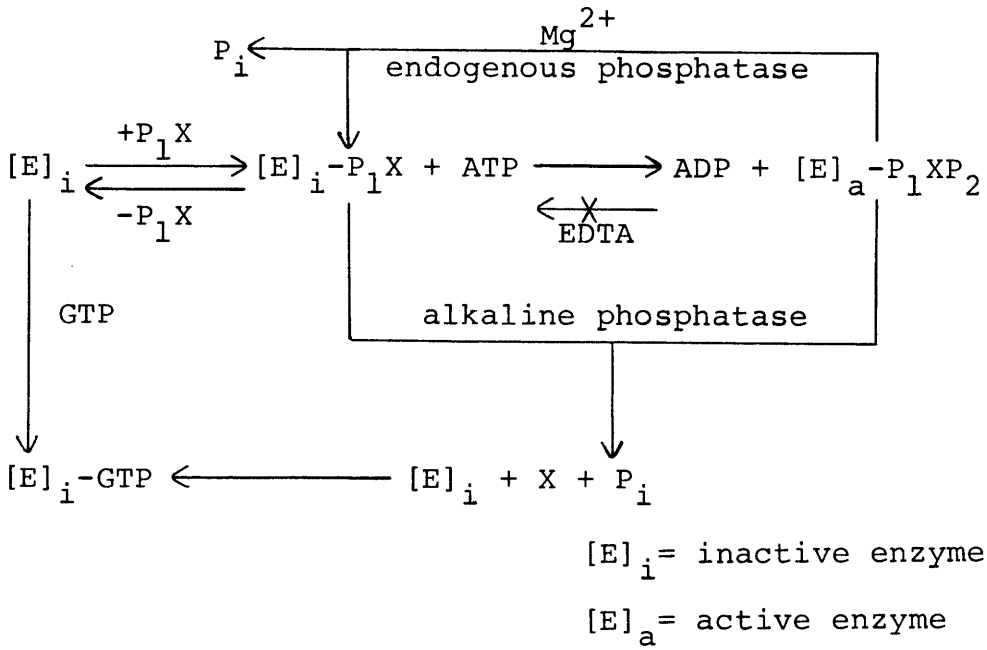

Figure 12. The Proposed Mechanism for Glucan Synthetase Regulation(17).

2.4 Cell Division Cycle Mutants

Saccharomyces cerevisiae is a yeast that reproduces by mitosis or budding. A single cell begins the mitotic cycle by initiating a bud on its surface and this bud grows in size throughout the cell division cycle. The size of the bud reveals the position of the cell in the cell division cycle. The mitotic cycle progresses through a series of events which include DNA replication at the beginning of the cell cycle, nuclear division when the bud is about three quarters the size of the mother cell, and cell separation when the bud and the mother cell are approximately the same size. Thus, mechanisms that control cell size must be closely related to those that control cell wall synthesis. Now, since the size of the bud indicates the position of the cell in the cell division cycle, it has been made possible to screen temperature sensitive (ts) mutants of yeast that are defective in genes that are induced at specific times during the cell division cycle(18). This technique allows us to determine the time in the cell division cycle that the particular gene product completes its function and more relevantly the biosynthetic step in cell wall synthesis involved. About 150 such mutants wre isolated that defined 32 genes in the cell division cycle(19).

In the Saccharomyces cerevisiae cell cycle two dependent sequence of events have been identified(20).

These are DNA replication and nuclear division in one sequence, and bud emergence, nuclear migration and cytokinesis in the second sequence. In other words, in the dependent sequence, each event can proceed only upon completion of the preceeding event. The cell cycle is made up of a large number of these ordered events(20).

It must be noted however, that most of the gene-controlled functions implied above are not rate controlling for the cell cycle progress. This can be illustrated by various temperature sensitive, cell division cycle mutants of Saccharomyces cerevisiae which undergo several cell cycles before total arrest. In these mutants the synthesis of the gene product is the temperature dependent event hence, material synthesized before the shift in temperature remains functional(20). This supposition explains the observation of continuous cell wall synthesis in these ts mutants most appropriately.

In yeasts, the major rate controlling step in the cell cycle is the actual rate of increase of cell mass. In other words, the cell division cycle is initiated once a critical mass is obtained. Saccharomyces cerevisiae cells for example, form buds only when a certain size is reached.

Blocks at various stages in the cell division cycle of yeasts affects the cell morphology and hence the synthesis of the structural polymers in the cell walls. Hence, the employment of ts cell division cycle mutants may prove to be

a useful tool in elucidating the structural and functional properties of these polymers.

3. DEVELOPMENT AND APPLICATION OF THEORY TO GLUCAN VISCOMETRY STUDIES

3.1 Rheology of Suspensions

The glucan extraction process used in this work yields cell ghosts composed of a rigid matrix containing mainly -glucans. These glucan particles have maintained the original cell morphology and have a very narrow discrete size range (2.Ø-5.Ø m) as determined by coulter counter.

In the studies on rheological properties of these glucans, dispersed system models have been used to analyze the results.

The experimental apparatus used was the Cannon-Fenske capillary viscometer (size 75). Glucan dispersions in distilled, deionized water were used. This system can be modelled as one in which the solid glucan particles are much larger than solvent molecules but smaller than the dimensions of the experimental apparatus. In a dispersion of this nature the microscopic viscosity (consider an element of solvent not occupied by glucan particles) remains unchanged, i.e., the solvent viscosity is governing. This condition is based on the assumption that the suspended phase is not soluble to any degree in the solvent. Therefore, the results obtained from the capillary viscometer are a measure of the macroscopic viscosity. This

viscosity is the result of distorted flow lines due to the large suspended particle.

The three dimensional equation of flow(21) has been used to calculate the effect of a large suspended particle on the flow of a fluid. Using Stoke's equation to simplify the equation of flow and the following boundary conditions:

1. Flow velocity u, at all points far removed from the suspended particles have an assigned value determined by the rate of flow.
2. Flow velocity u, at the surface of the particle is equal to the particle velocity in magnitude and direction.

Einstein (22) obtained the following equation for the macroscopic viscosity of a dilute suspension of rigid spheres:

$$n = n_o(1 + 2.5\phi)$$

where, n = macroscopic viscosity of the suspension

n_o = viscosity of the solvent

ϕ = volume fraction of suspended paricles

This treatment was extended to apply to asymmetric particles. In this case the orientation of the particles with respect to the flow lines is an important parameter.

At low velocity gradients one can assume that the particles are randomly oriented. For this case the Einstein-Simha equation describes the macroscopic viscosity,

$$n = n_o(1 + V\phi)$$

where, V = shape factor
V = 2.5 for spheres
V > 2.5 for ellipsoids

This equation, however, can only be used for very dilute systems in which $\phi < 0.02$.

Mooney (23) extended Einstein's equation to apply to a suspension of finite concentration ($\phi < 0.2$)

$$n_r = \frac{n}{n_o} = \exp\left[\frac{V\phi}{1 - \phi/\phi_m} \right]$$

where, n_r = relative viscosity
ϕ_m = maximum packing fraction

The term, ϕ , is experimentally difficult to determine, hence we can substitute $\phi = c\bar{v}$ into Mooney's equation,

where, c = concentration
$\bar{v}$ = hydrodynamic volume

Hence, Mooney's equation becomes:

$$n_r = \exp\left[\frac{Vc\bar{v}}{1 - c\bar{v}/\phi_m} \right]$$

In order to employ this equation to obtain meaningful values for the rheological parameters of glucans, the following algebraic manipulations must be made to the above equation.

Take $\log_e$: $\ln(n_r) = \dfrac{Vc\bar{v}}{1 - c\bar{v}/\phi_m}$

Now, for a particular glucan sample assume that v = constant in the operating range of c. Hence, the equation can be expressed solely in terms of c by defining two constants, k_1, k_2.

$$\ln(n_r) = \frac{k_1 c}{1 - k_2 c}$$

where, $k_1 = V\bar{v}$

$$k_2 = \frac{\bar{v}}{\phi_m}$$

Expanding the above equation yields:

$$\ln(n_r) - k_2 c \ln(n_r) = k_1 c$$

$$\ln(n_r) = k_1 c + k_2 c \ln(n_r)$$

$$\ln(n_r) = [\, k_1 + k_2 \ln(n_r)]c$$

$$c = \frac{\ln(n_r)}{k_1 + k_2 \ln(n_r)}$$

Inverting:

$$\frac{1}{c} = \frac{k_1 + k_2 \ln(n_r)}{\ln(n_r)}$$

Therefore:

$$\frac{1}{c} = k_1 \frac{1}{\ln(n_r)} + k_2$$

Hence, Mooney's equation has been used to obtain a linear model relating reciprocal concentration to the reciprocal $\log_e$(relative viscosity).

The above equation was used as a model for the rheological studies on the glucan dispersions. The resulting correlations enabled the determination of the parameters k_1, k_2. Upon microscopic observation of the samples mean values of the aspect ratio (length dimension/width dimension) of each sample were determined

hence using the equation (24):

$$V = 0.4075\left(\frac{L}{D} - 1\right)^{1.5} + 2.5$$

where, $\frac{L}{D}$ = aspect ratio of the suspended particle

exact values of the shape factor, V were calculated. Hence, the values $\bar{v}$, ϕ_m were determined from the plots of $1/c$ vs $1/\ln(n_r)$.

3.2 Capillary Viscometry

As discussed above, the time taken for a suspension of particles to flow through a capillary is proportional to the macroscopic viscosity of this suspension.

Ideal conditions are considered in the development of the theory for capillary viscometers(25). Therefore, the following assumptions must be made:

1. Steady flow
2. No radial or tangential components of fluid velocity, i.e., laminar flow
3. Axial velocity is only a function of the radial coordinate
4. Boundary layer at capillary walls, i.e., fluid velocity is zero at wall
5. End effects are negligible
6. Incompressible fluid

7. No external forces

8. Isothermal conditions

9. Viscosity is not a function of the changing pressure down the capillary

To derive the relationship between efflux time and viscosity for the above ideal conditions, a force balance is made on an element of the capillary.

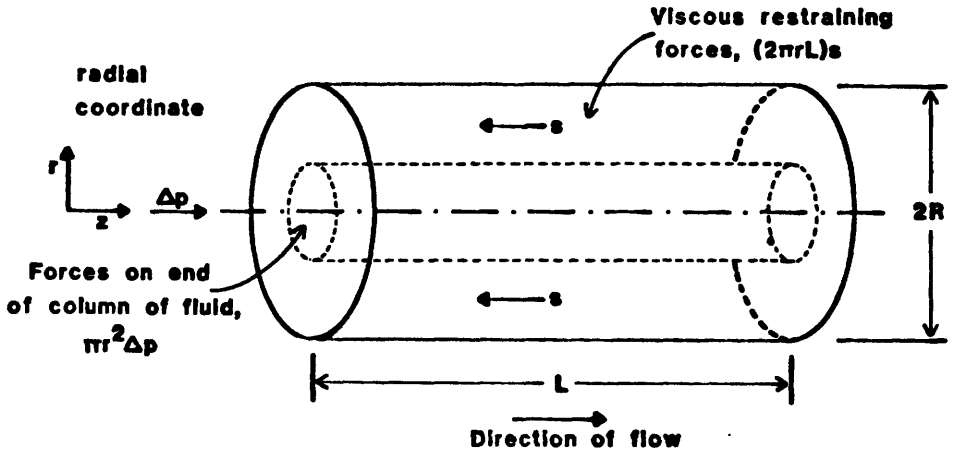

$$\pi r^2 \Delta p = (2\pi rL)s$$

where, s = shearing stress

L = capillary length

r = radial coordinate

p = pressure difference over the capillary

For a Newtonian fluid,

$$n = s/(-du/dr)$$

Now, $s = r\Delta p/L$

thus, $-du/dr = \Delta pr/2nL$

Integrating:

$$u(r) = (\Delta pR^2/4nL)(1 - (r/R)^2)$$

The volumetric flow rate, Q, can be expressed as the surface integral of the velocity over the cross-section of the capillary:

$$Q = \int_0^R 2\pi ru(r)dr$$

Hence, substituting for u(r) into the above equation and integrating, with respect to r:

$$Q = \pi R^4 \Delta p/8nL$$

Now let a total volume, V_T flow through the capillary in time t.

$$\frac{V_T}{t} = \pi R^4 \Delta p / 8nL$$

For a fluid flowing under gravity, $p = h\rho g$.

where, h = hydrostatic head

ρ = fluid density

g = acceleration due to gravity

hence, $$\frac{V_T}{t} = \frac{\pi R^4 hgt}{8nL}$$

Rearranging the equation gives,

$$\frac{n}{\rho} = \frac{\pi R^4 hgt}{8LV_T}$$

where, the term $\frac{n}{\rho}$ = kinematic viscosity

Since the term $\frac{\pi R^4 hg}{8LV_T}$ is constant for a given viscometer we can write:

$$\frac{n}{\rho} = Ct$$

Hence, by determining the density and efflux time of a

glucan suspension the macroscopic viscosity, n can be calculated.

However, since we are interested in the relative viscosity (n/n_o) where n_o is the viscosity of the solvent,

$$\frac{(n/\rho)}{(n_o/\rho_o)} = \frac{Ct}{Ct_o}$$

for the range of glucan concentration used it was determined that $\rho = \rho_o$

hence, $$n_r = \frac{n}{n_o} = \frac{t}{t_o}$$

The experimental results could therefore be directly converted to relative viscosity using the above equation.

4. MATERIALS AND METHODS

4.1 Strains

Saccharomyces cerevisiae A364A which has the genotype (a, adel, ade2, his7, tyrl, gall) was used as a control in these studies. S. cerevisiae 374 and 377 are ts mutant strains which have the same genotype as A364A but harbor the cell division cycle mutations cdc8 and cdcll, respectively. These mutants grow physiologically at the permissive temperature 28°C but when grown at the non-permissive temperature 37°C, a block in the cell division cycle leads to one or more elongated buds which remain attached to the parent cell.

4.2 Growth Media

Complex media YPG and YEPD were used for growth of the yeast strains. All media are kept at pH = 5.5

The yeast strains have been maintained on YPAD slants at 4°C.

The composition of the media is as follows:

Table 3

Component	% v/v
YPG	
Dextrose	2
Peptone	1
Yeast extract	Ø.3
YEPD	
Dextrose	2
Peptone	2
Yeast extract	1
YPAD	
Dextrose	2
Peptone	2
Yeast extract	1
Agar	2

4.3 Yeast Fermentation

The fermentations were all carried out under batch operation. The 1Ø1 culture medium was sterilized in the fermenter itself. The inoculum size was 25Ø ml of an overnight culture. The operating conditions were:

Stirrer speed, N = 4ØØ RPM

Aeration, Q = 1 vvm

pH = 5.5 (maintained with 1Ø M NaOH)

Temperature = 28°C (or 37°C after shift for 374, 377)

Growth of the cells was followed by removing 1Ø ml samples and measuring turbidity in a Klett-Summerson colorimeter.

Cells were harvested by centrifugation at 12,ØØØ RPM for 2Ø minutes.

4.4 Glucan Extraction

In order to obtain a glucan sample representative of glucan as found *in vivo,* a glucan extraction scheme was formulated by combining extraction methods for beta(1-3) and beta(1-6) glucans used by other workers (1,2,3).

The yeast cells were harvested at the end of the exponential growth phase in order to maximize the glucan: glycogen ratio since glycogen synthesis is turned on during the stationary phase (13,14). The cells were washed twice with citrate-phosphate buffer at pH 5.5. The first step involves a rigorous extraction of the cells in 1l, 1N NaOH at 1ØØ°C for 1 hour. The suspension was then allowed to cool and 1l distilled water was added. The insoluble material was recovered by centrifuging at 2ØØØ RPM for 15 min. This material was then suspended in 1l 3% NaOH and extracted at 75°C for 3 hours. The suspension was allowed to cool to room temperature and the extraction

continued for 16 hours. The suspension was then diluted with 1l distilled water. The insoluble residue was recovered by centrifugation at 2ØØØ RPM for 15 min.

The material was then finally extracted in 3% NaOH brought to pH 4.5 with HCl at 75°C for 1 h. The insoluble residue was recovered by centrifugation and washed 3 times with distilled water, once with ethanol and twice with ethyl ether. The resulting glucan was then air dried at 37°C.

4.5 Infra-red Spectroscopy

I.R. Spectra were obtained for all the glucan fractions. The sample was prepared in solid KBr discs. A 5Ø mg sample size was used with a glucan concentration of 2% w/w. To obtain higher resolution of the characteristic β(1-6) peak, a glucan concentration of 8% w/w was used in the KBr disc.

Standard glucan spectra were obtained using Laminarin (isolated from Laminaria) as a β(1-3) standard and β-gentiobiose as β(1-6) standard.

4.6 Capillary Viscometry

The principle of the capillary viscometer is to relate the flow-rate of fluid through a narrow capillary to the viscosity of that fluid (25). In this viscometer, the driving force is the hydrostatic head of the sample fluid,

hence kinematic viscosity is measured directly.

A Cannon-Fenske Routine viscometer (size 75) was used for all the viscometer measurements. The viscometer was immersed in a well-stirred water bath at 25°C. The glucan samples were all suspended in distilled, deionized water, and the latter was used as a control. The concentration range for each glucan was determined so as to give efflux times in the range 2-5 minutes approximately. The measurements were repeated to obtain 4 consistent results per concentration. After running each concentration, the viscometer was cleaned with chromic acid and dried with acetone.

4.7 Laminarinase Digest of Glucan

A 400 ml solution containing 1 mg/ml glucan and 0.25 mg/ml Laminarinase (endo β(1-3) glucanase) was prepared in phosphate buffer at pH 7.0. The solution was incubated at 37°C for 4 hours. At the end of the incubation the solution was held at 70°C for 15 minutes to deactivate the enzyme. The remaining residue was recovered by centrifugation at 5000 rpm for 20 min. 380 ml of supernatant were removed in order to bring the glucan residues back to an original concentration of 20 mg/ml. This solution is diluted into range of concentrations in order to obtain viscosity measurements of the Laminarinase

degraded glucan samples. Since the enzyme could not be effectively removed from solution, a control experiment was performed as above where the incubated enzyme contained no glucan. Such readings were then used to correct the solvent viscosity accounting for the contribution of the enzyme to the macroscopic solution viscosity.

4.8 Acetic Acid Extraction

Repeated extraction of alkali insoluble glucan preparations in acetic acid removes the highly branched β(1-3)glucan component(4).

500mg of a whole glucan preparation was suspended in 0.5M acetic acid to a final concentration of 2mg/ml. The suspension was continuously stirred at 90°C for three hours. At the end of the extraction the insoluble glucan was removed by centrifugation at 5000rpm for 20 minutes. The glucan residue was washed in distilled, de-ionized water, ethanol and ether, and was then air dried at 37°C. The initial suspension and the supernatant were assayed for total carbohydrate.

Total Carbohydrate Assay

Total carbohydrate was measured using the phenol method. In bacterial or yeast cell walls certain carbohydrate constituents (glucose, mannose) predominate to such an extent that the effects of other constituents on the assay become negligible. Hence, this assay was chosen to quantitate β-glucan preparations.

The protocol used is described by Langer and Thilly(26). The carbohydrates in the sample are dehydrated in strong (98%) sulphuric acid to give derivatives known as furfurals. These derivatives form complexes with phenol which absorb ligt at 488nm.

5. RESULTS AND DISCUSSION

The growth of strains A364A, 374, 377 are shown in Figs. 13,14,15. The temperature shift for strains 374 and 377 was made at the early exponential growth phase at about 30 Klett. In this case an increased specific growth rate was observed but the cells moved into the stationary phase shortly after.

Table 4

Yeast Fermentation

Strain	Temperature (^{o}C)	Specific Growth Rate (h^{-1})	Doubling Time (min)
A364A	30	0.45	92
374	28	0.16	246
374	37	0.27	154
377	28	0.25	162
377	37	0.32	129

The morphologies of the strains used are illustrated on Figs. 16,17,18. Figures 17[b] and 18[b] clearly illustrate the incomplete budding process which has resulted in elongated buds remaining attached to the parent cell.

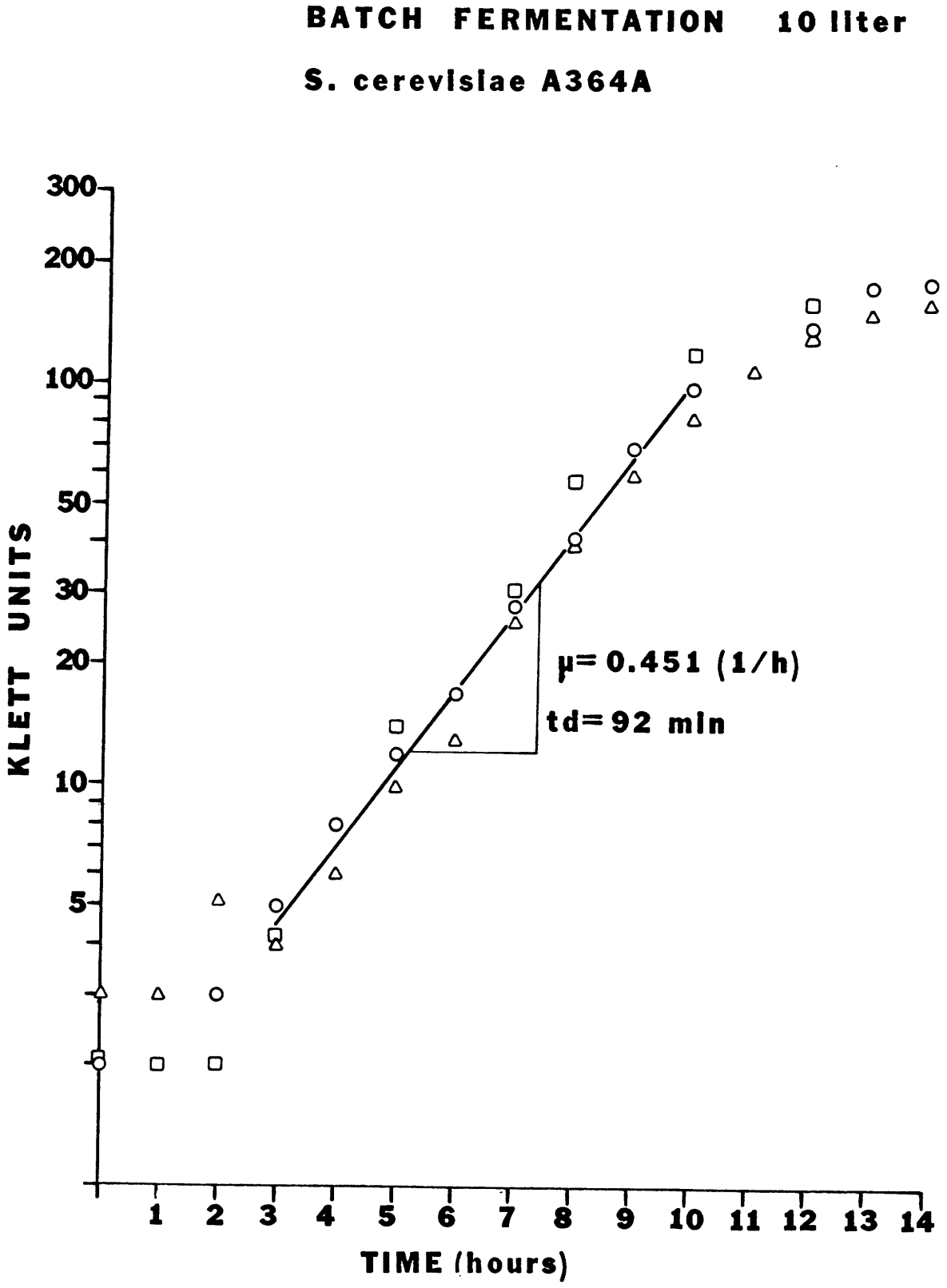
BATCH FERMENTATION 10 liter
S. cerevisiae A364A
KLETT UNITS
300
200
100
50
30
20
10
5
μ= 0.451 (1/h)
td= 92 min
1
2
3
4
5
6
7
8
9
10
11
12
13
14
TIME (hours)

Figure 13.

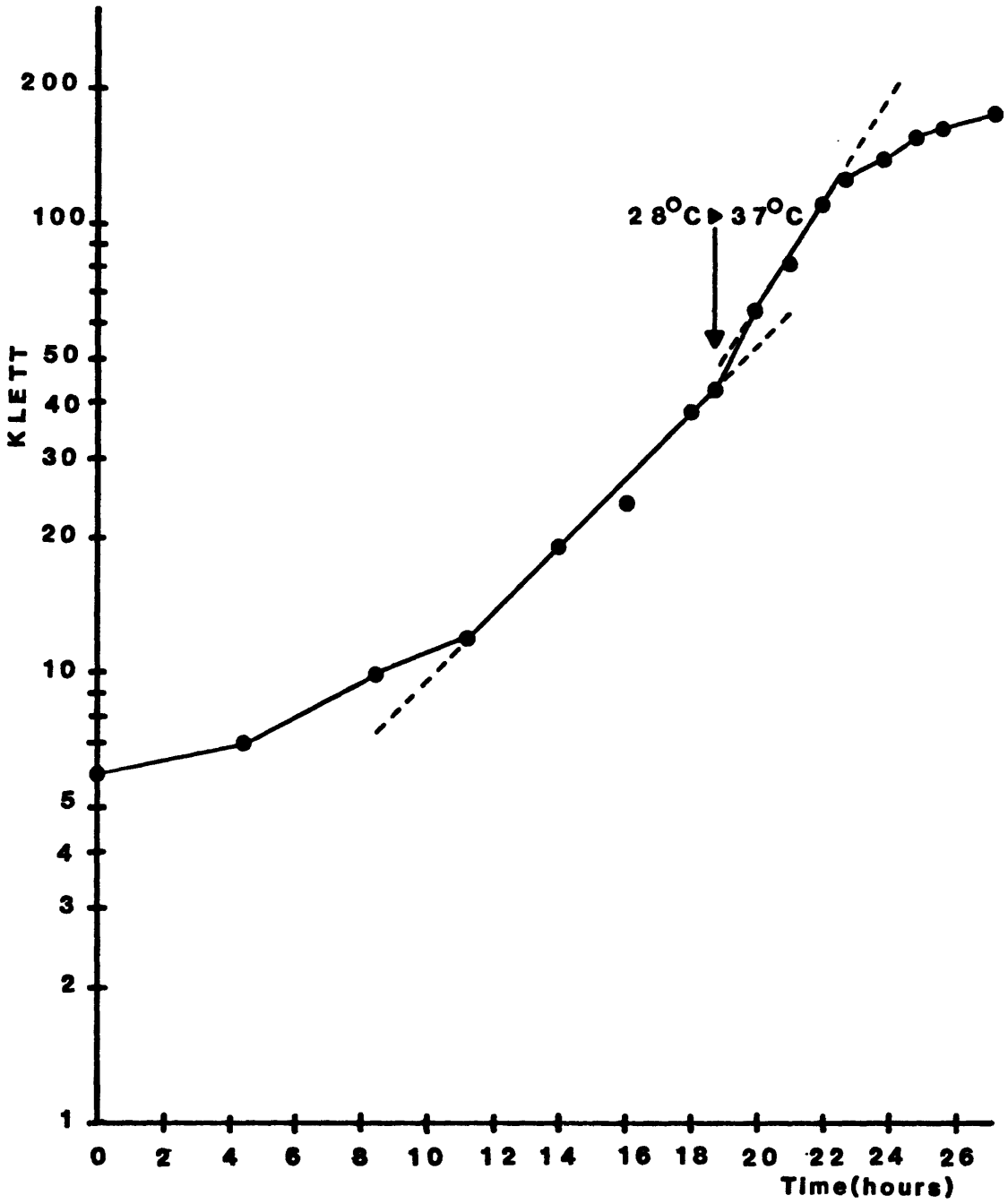

Figure 14: **Growth curve with temperature shift**
Saccharomyces cerevisiae 374

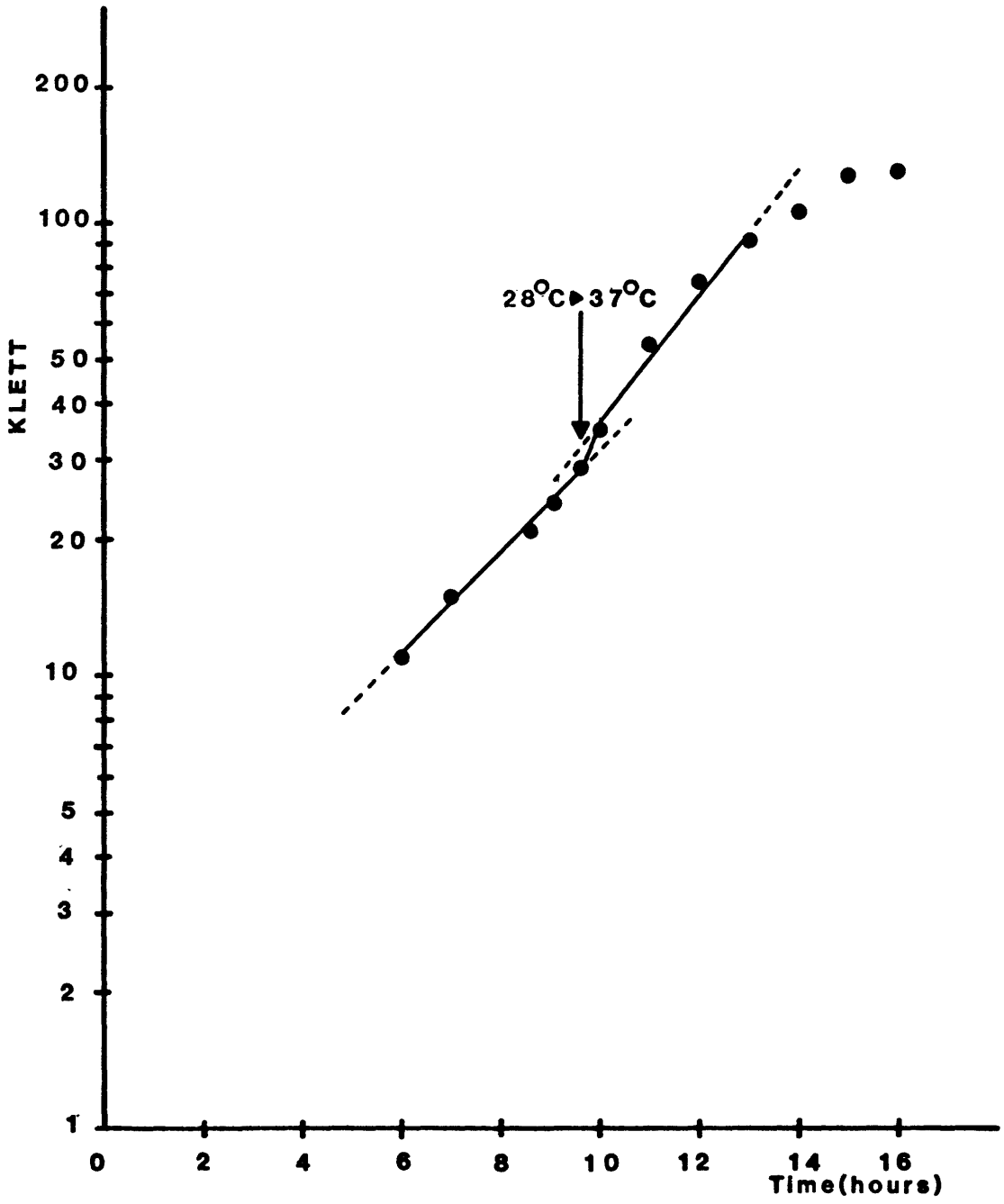

Figure 15: **Growth curve with temperature shift**
Saccharomyces cerevisiae 377

Figure 16. Morphology of Saccharomyces cerevisiae A364A

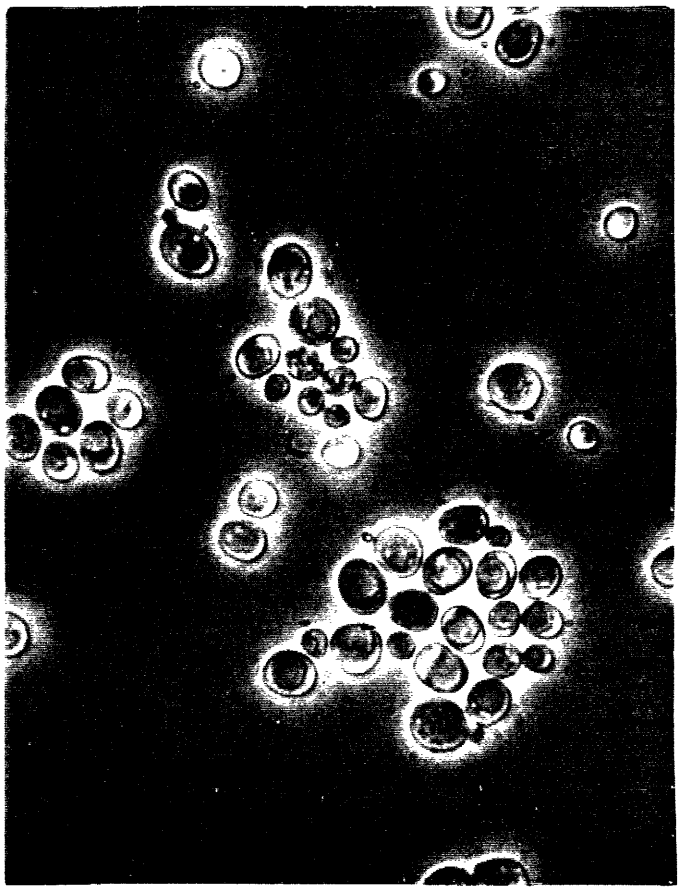

Figure 17[a]. Morphology of Saccharomyces cerevisiae 374 Grown at 28°C

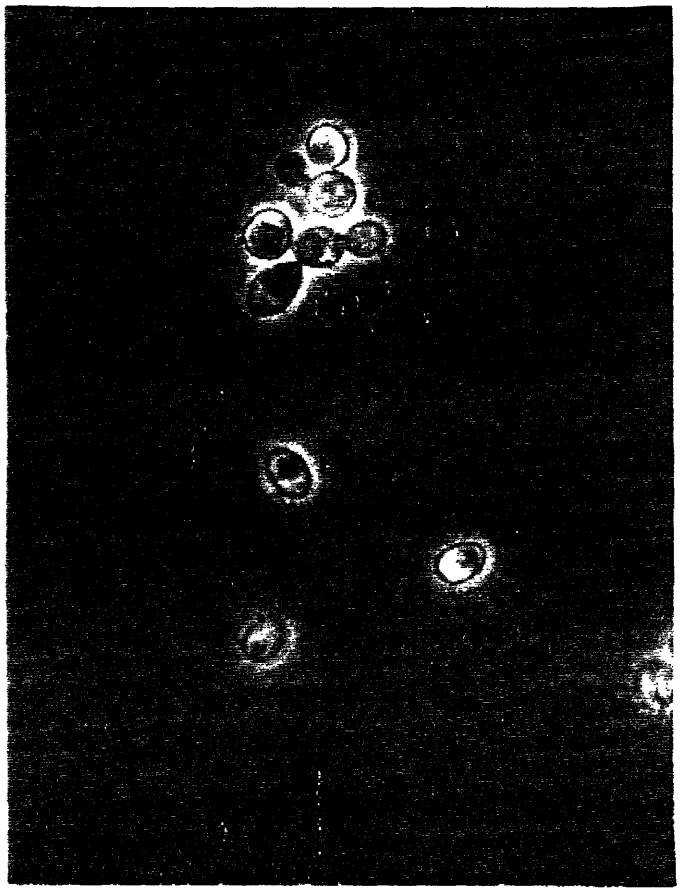

Figure 17[b]. Morphology of Saccharomyces cerevisiae 374 Grown at 37°C

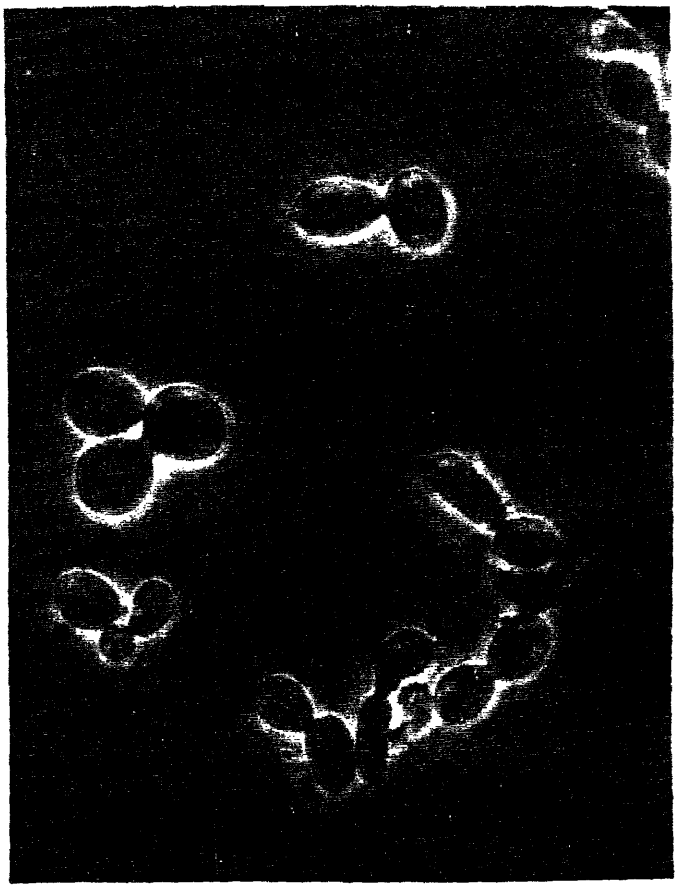

Figure 18[a]. Morphology of Saccharomyces cerevisiae 377 Grown at 28°C

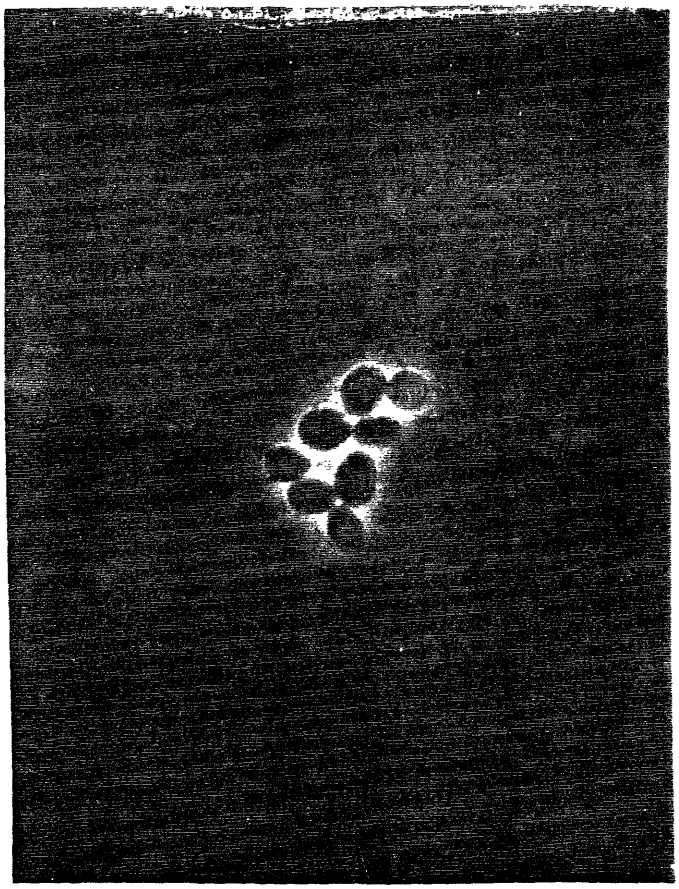

Figure 18[b] Morphology of Saccharomyces cerevisiae 377 Grown at 37°C

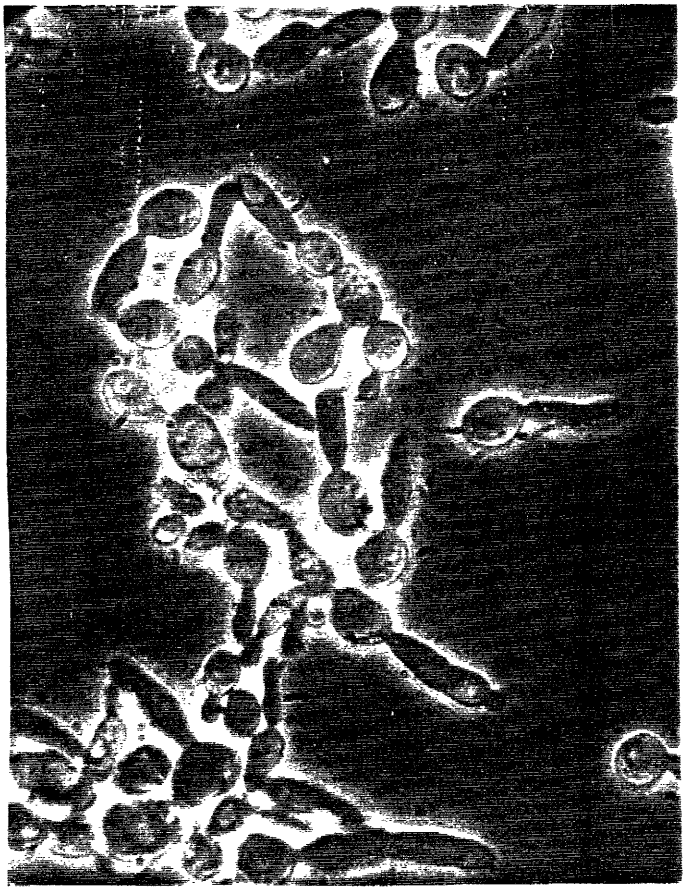

Figure 19. A364A Glucan

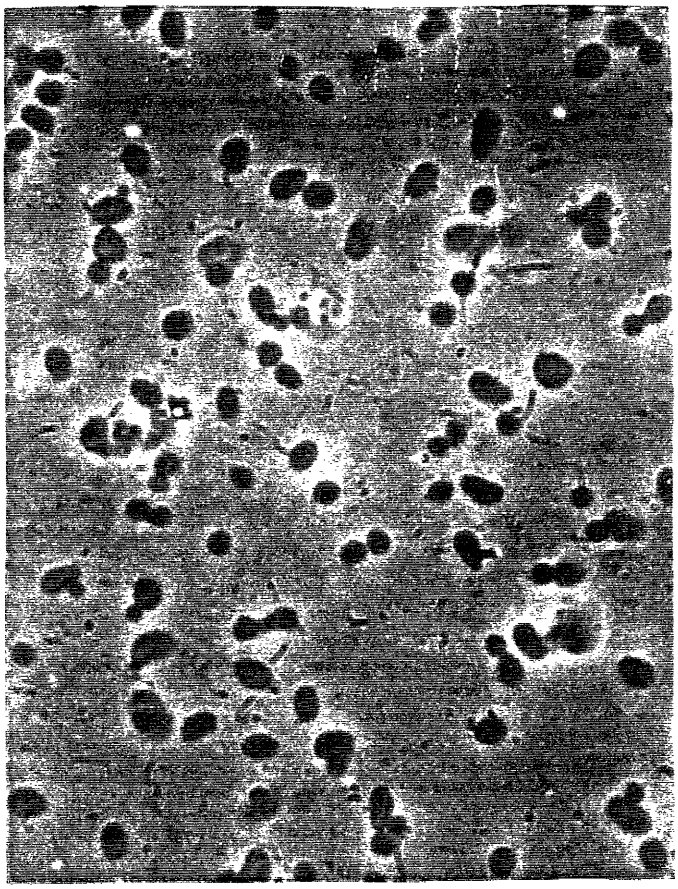

Figure 20. 374 Glucan

Figure 21. 377 Glucan

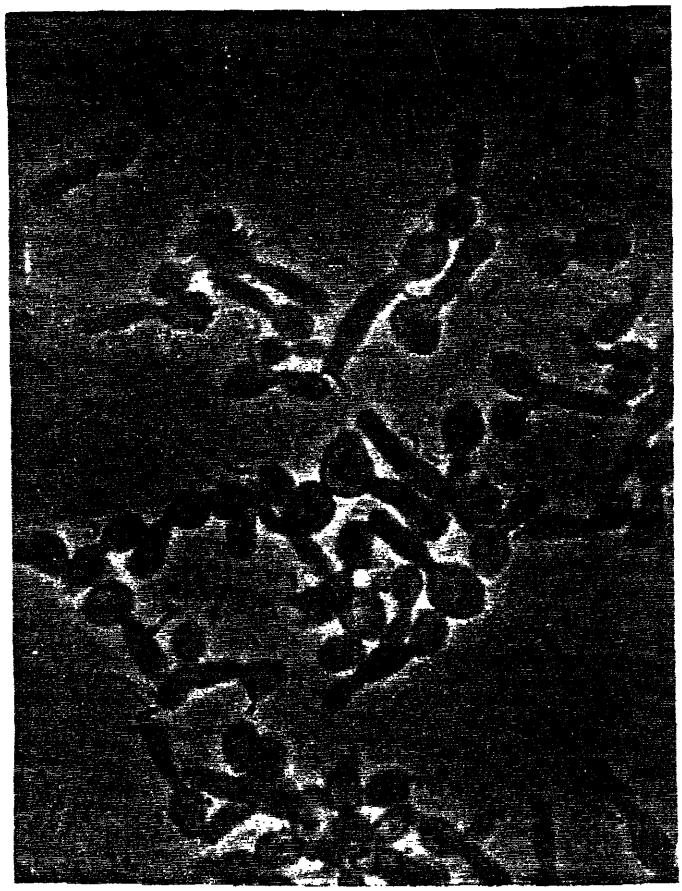

Table 5

GLUCAN EXTRACTION
(Alkali Insoluble)

DRY CELL WEIGHT (g)	14.03	15.25	9.78
GLUCAN FRACTION (g)	1.86	1.64	1.53
%DCW EXTRACTED	13	11	15
TOTAL CELL GLUCAN (12% dcw)	1.68	1.83	1.17
AA CONTENT Lysine equiv. (mg/g glucan)	7.33	8.07	8.77

The yields from the glucan extraction could not be accurately determined due to loss of sample during the lengthy extraction process. However, Table 5 gives an overall view of the yields obtained in 3 different extractions of A364A glucan. It was interesting to observe (Fig. 19,20,21) that the glucan preparations retained the cell shape confirming glucans role as the major structural biopolymer in the yeast cell wall. Ninhydrin protein assays made on the glucan samples clearly indicated the presence of amino acids as observed by other workers (6,7).

The whole glucan samples from all three strains gave characteristic spectra of glucans (see Figures 22,23,24,25,26). All the peaks characteristic of β(1-3) glucosidic bonds(11) at 7.95, 8.35, 8.7 and 11.3μm were obtained for both laminarin and the glucan samples. The whole glucan preparations also exhibited a slight peak at 11.0 μm which is characteristic of β(1-6) glucosidic bonds as illustrated in the β-gentiobiose spectra (Figure 23). owever, the 377 glucan sample only gave a very small shoulder at this wavelength indicating a possible lower degree of β(1-6) glucan. To magnify the peak intensity, the glucan concentration in the sample was increased from 2% w/w to 8% w/w. The spectra obtained are shown in Figures 27,28,29. Even at this concentration 377 glucan only gave a slight β(1-6) shoulder.

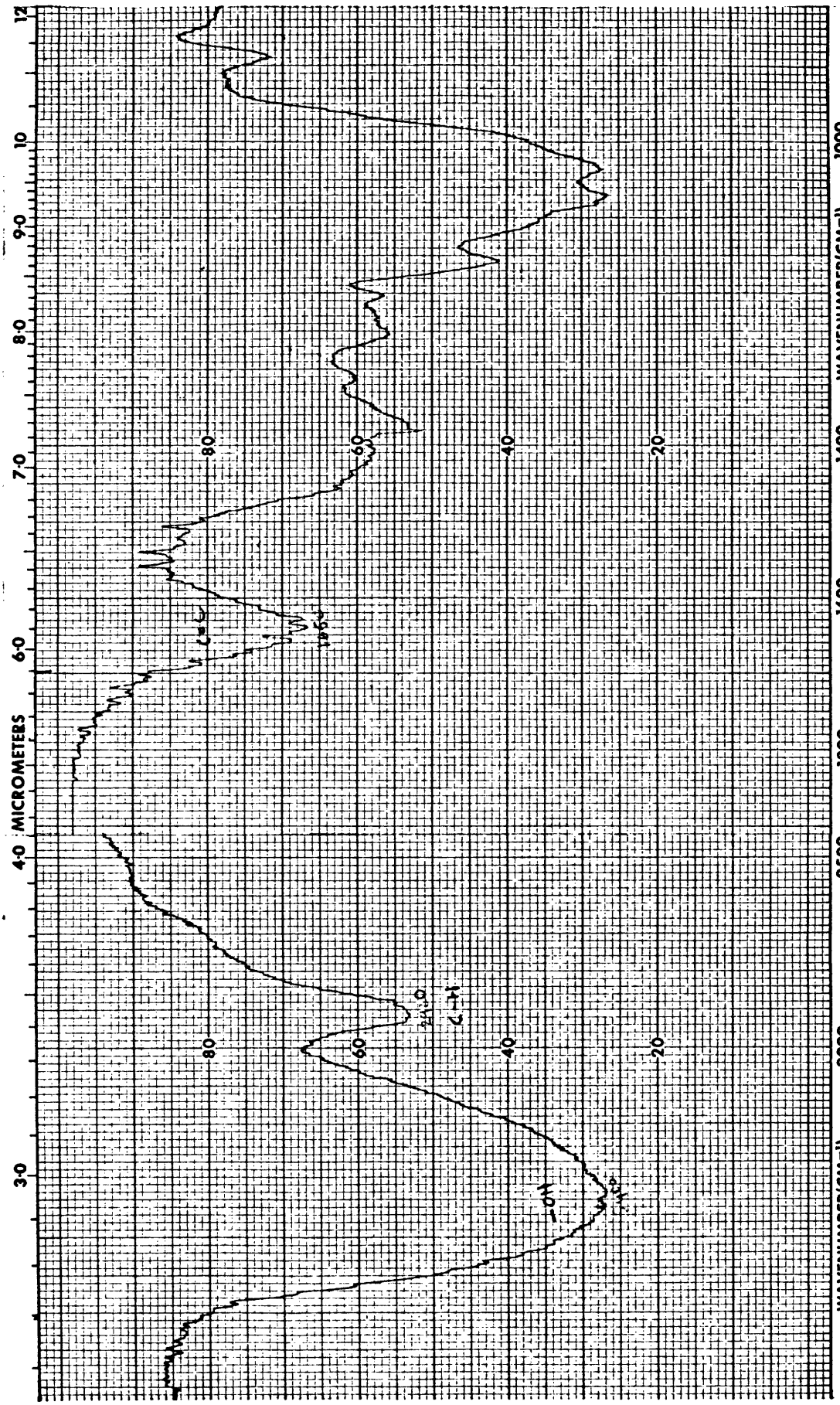

Figure 22. I.R. Spectrum of Laminarin
(2% w/w sample concentraion)

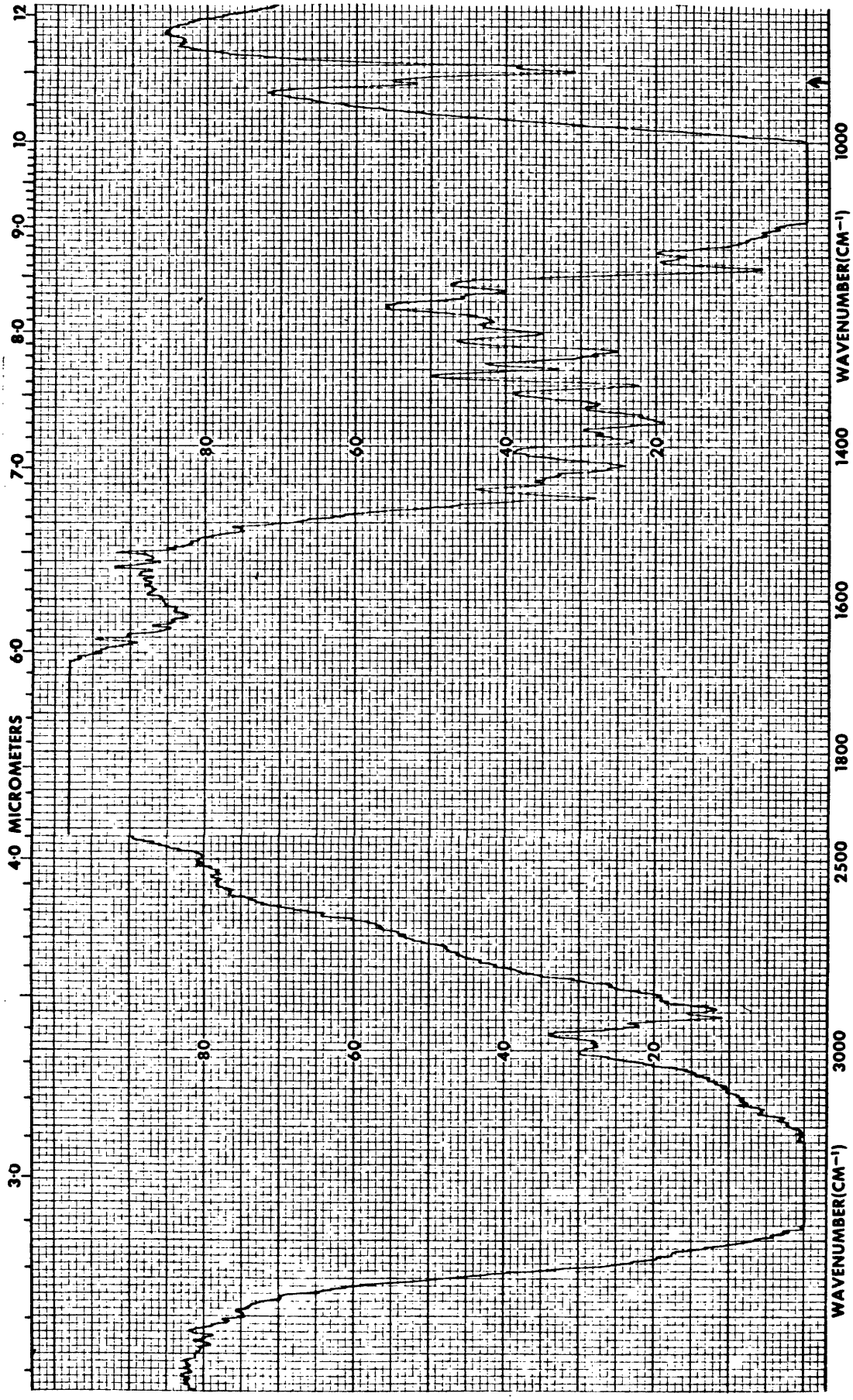

Figure 23. I.R. Spectrum of β-Gentiobiose
(2% w/w sample concentration)

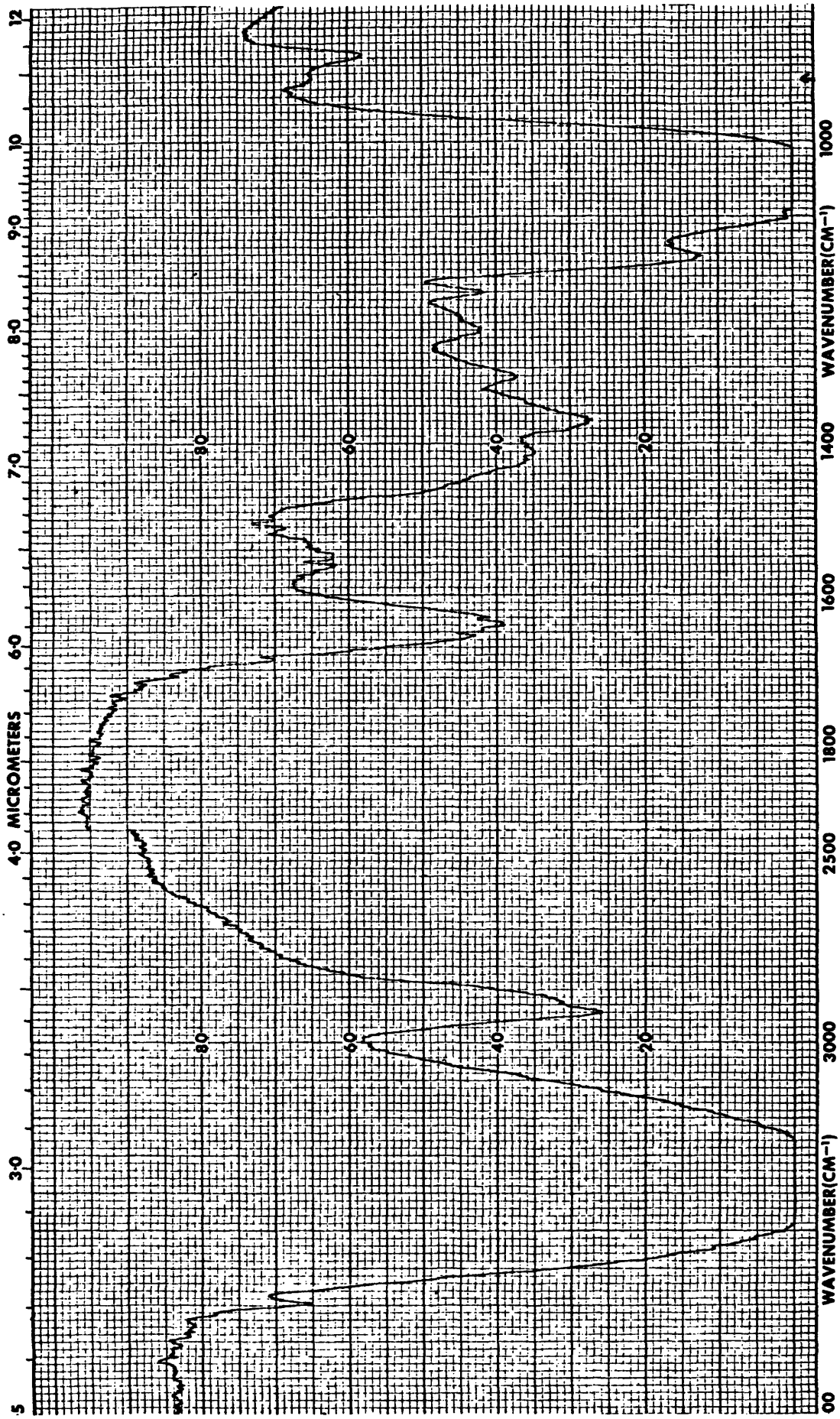

Figure 24. I.R. Spectrum of A364A Glucan
(2% w/w sample concentration)

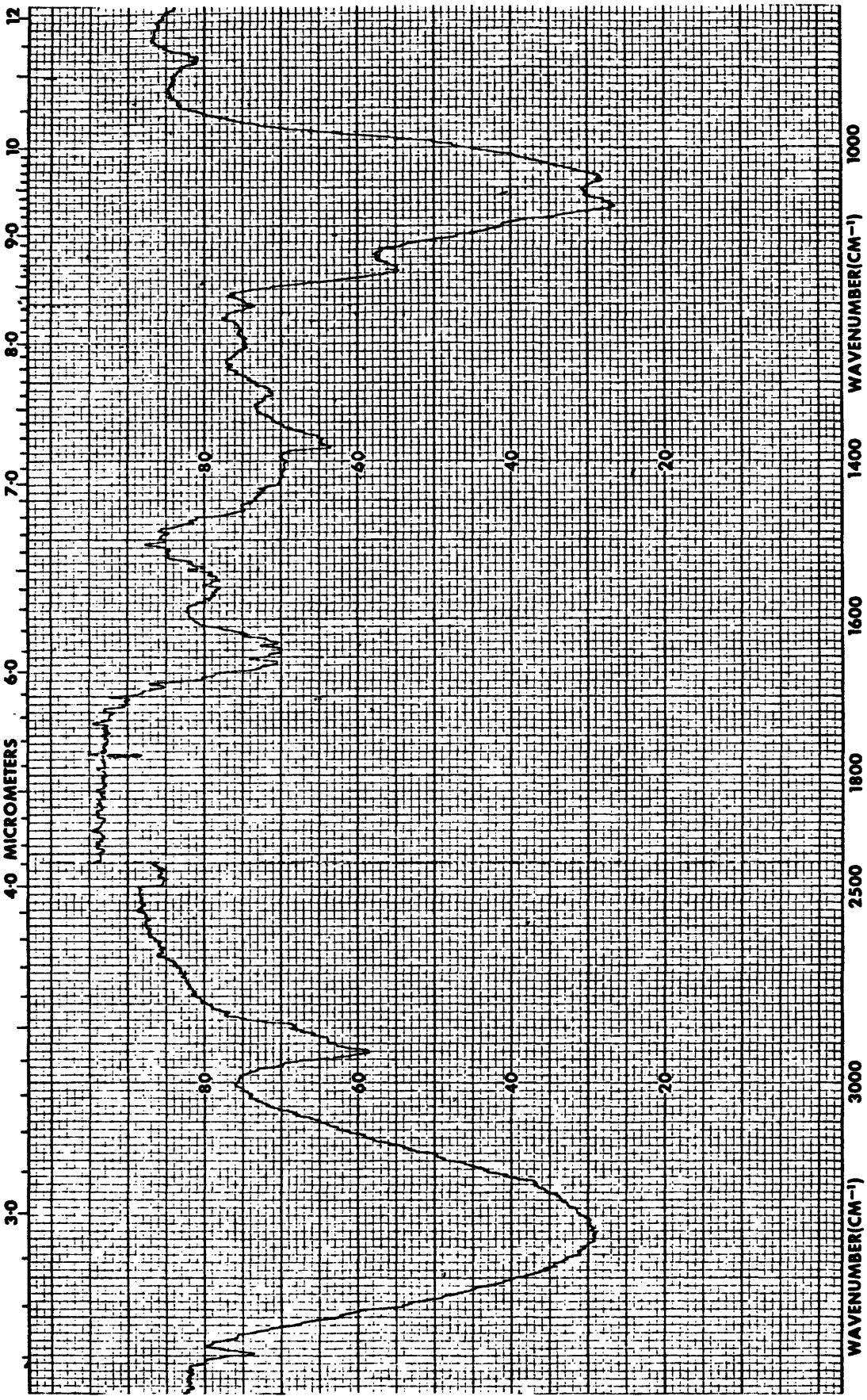

Figure 25. I.R. Spectrum of 374 Glucan
(2% w/w sample concentration)

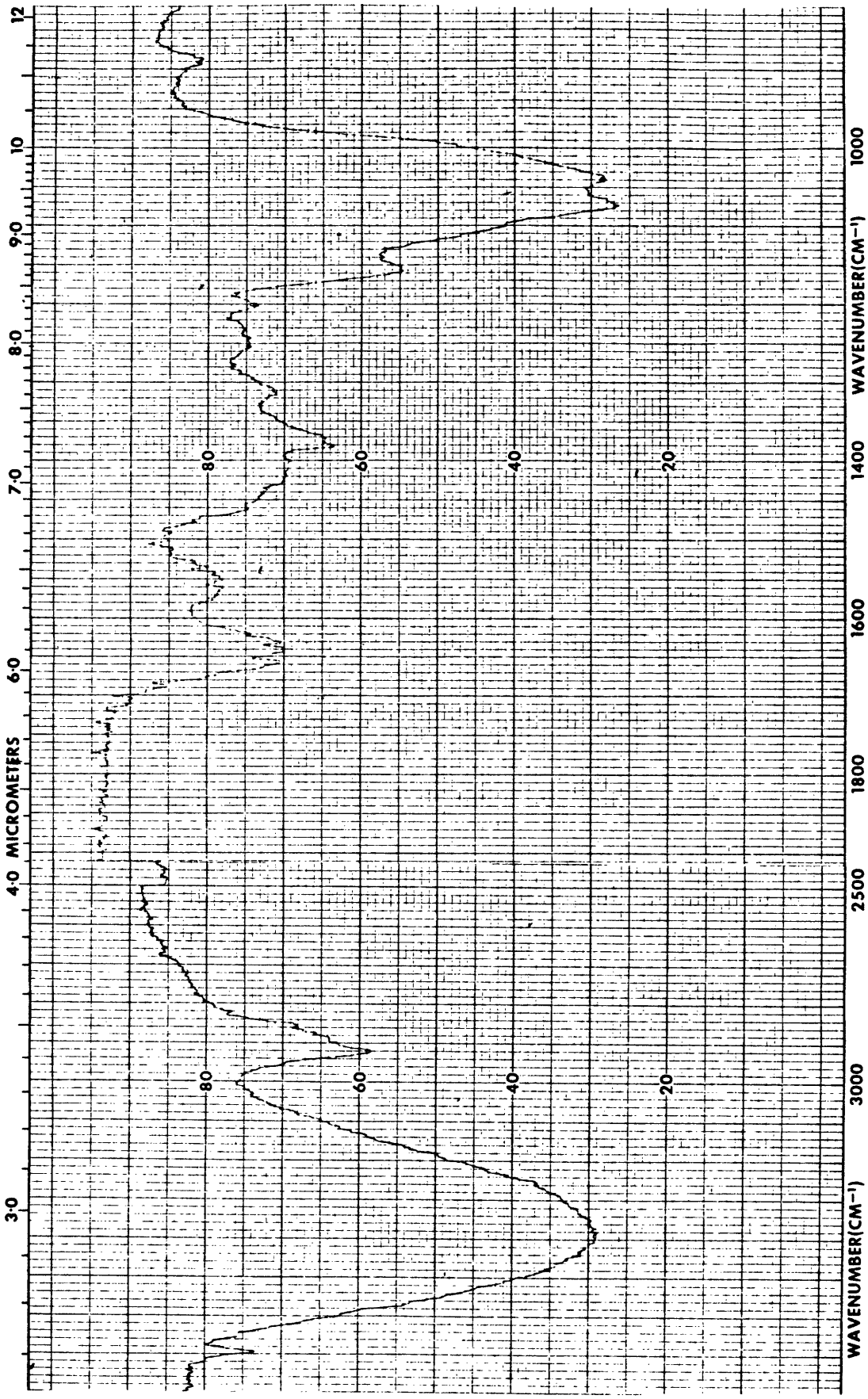

Figure 26. I.R. Spectrum of 377 Glucan
(2% w/w sample concentration)

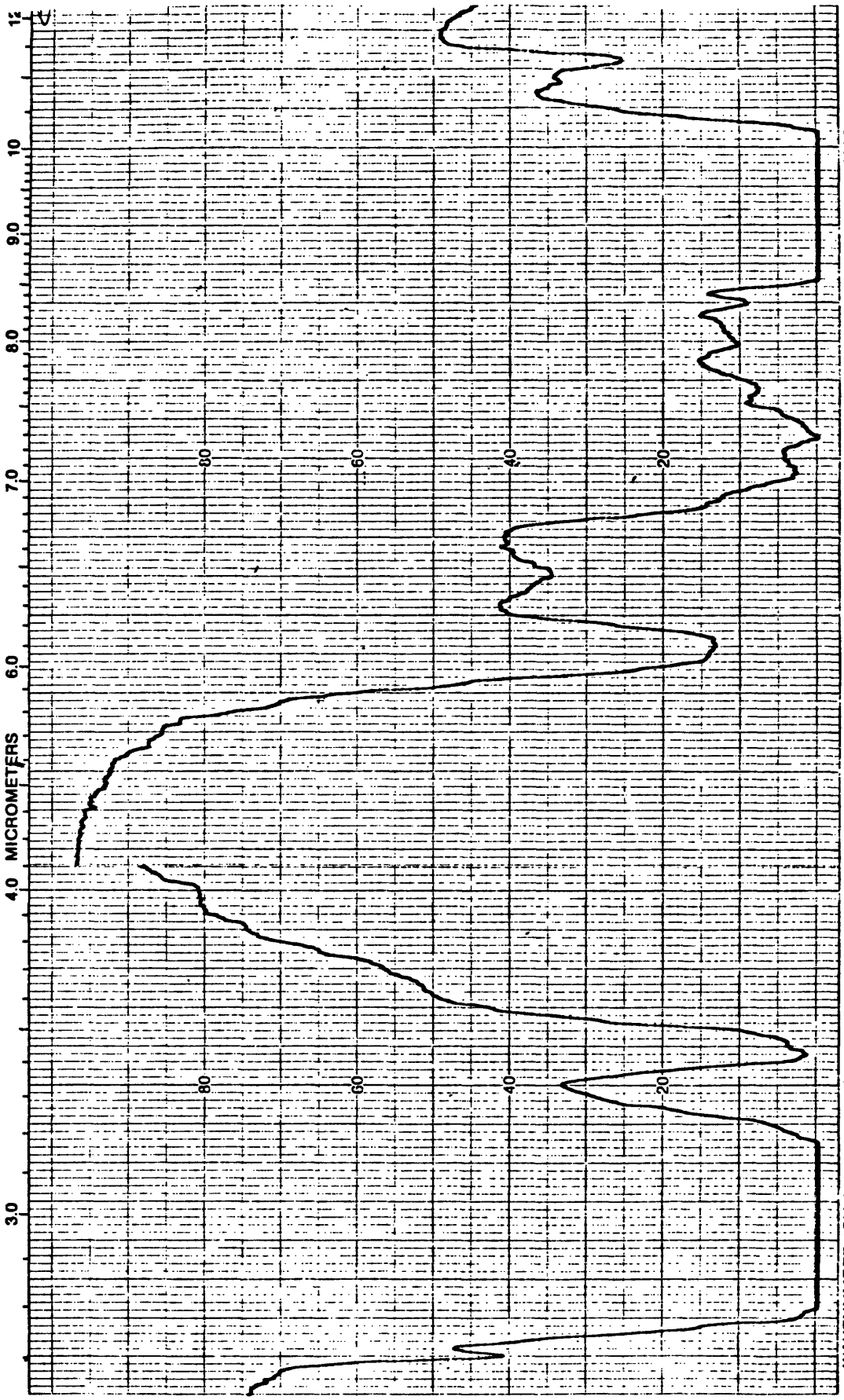

Figure 27. I.R. Spectrum of A364A Glucan
(8% w/w sample concentration)

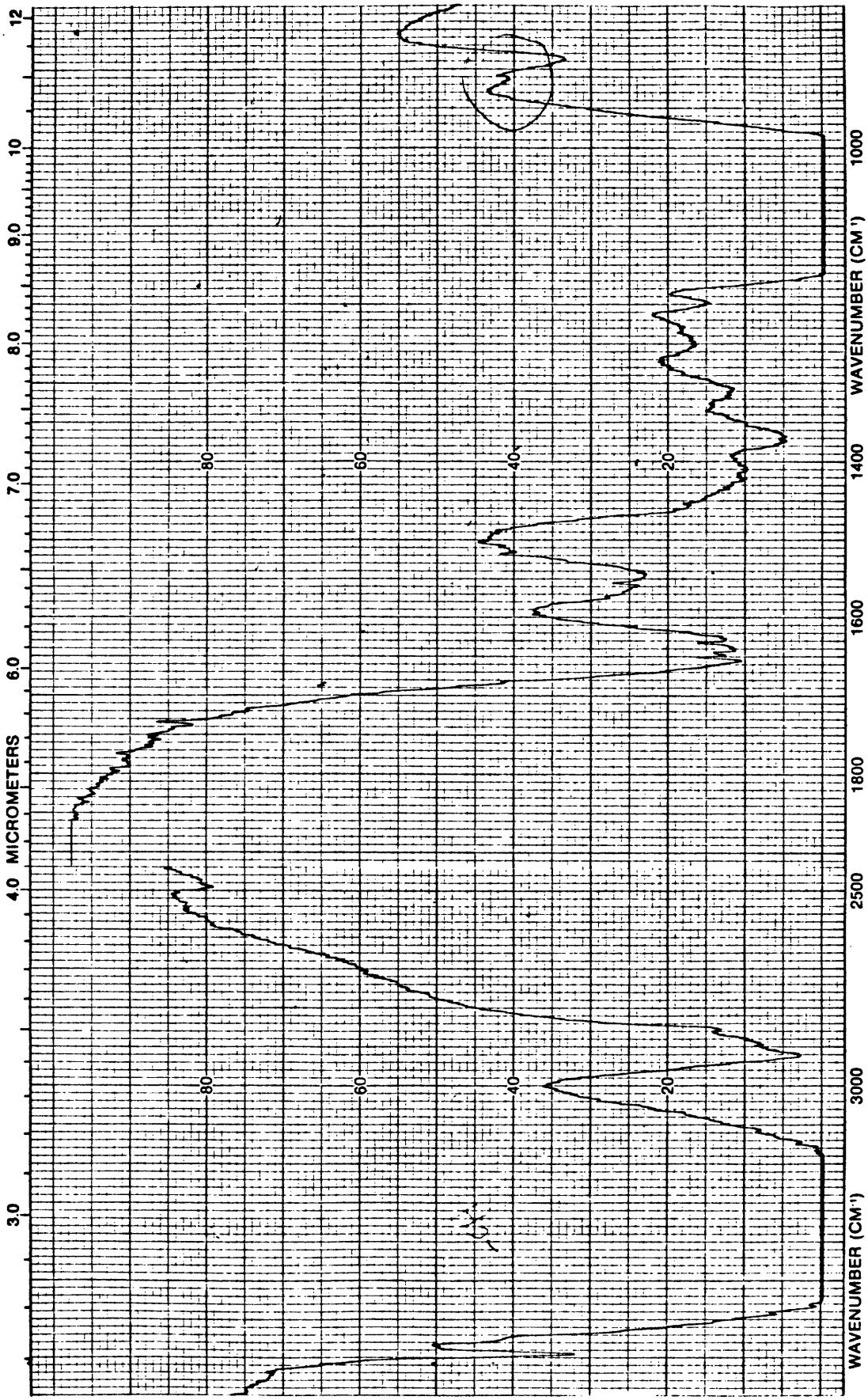

Figure 28. I.R. Spectrum of 374 Glucan
(8% w/w sample concentration)

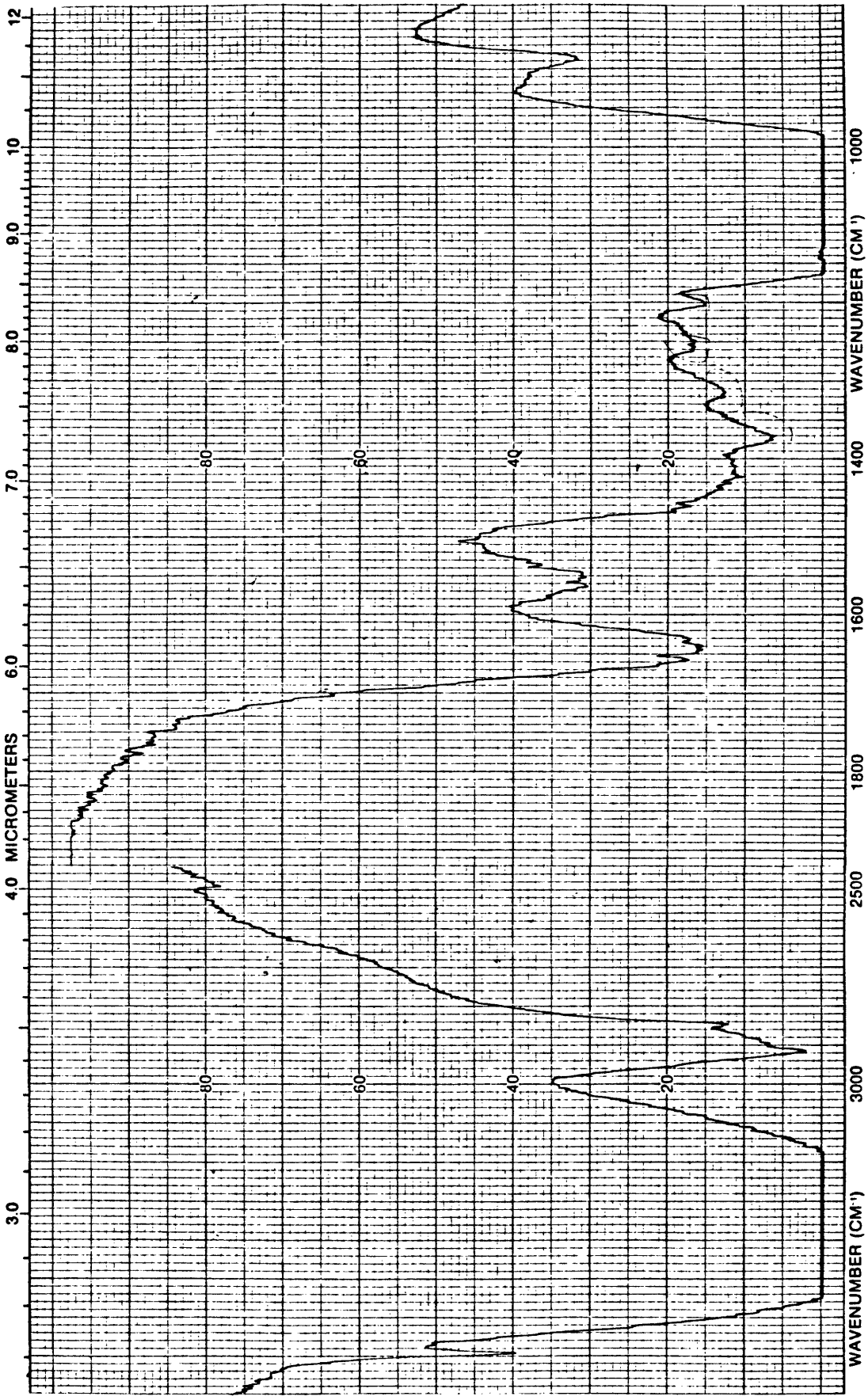

Figure 29. I.R. Spectrum of 377 Glucan
(8% w/w sample concentration)

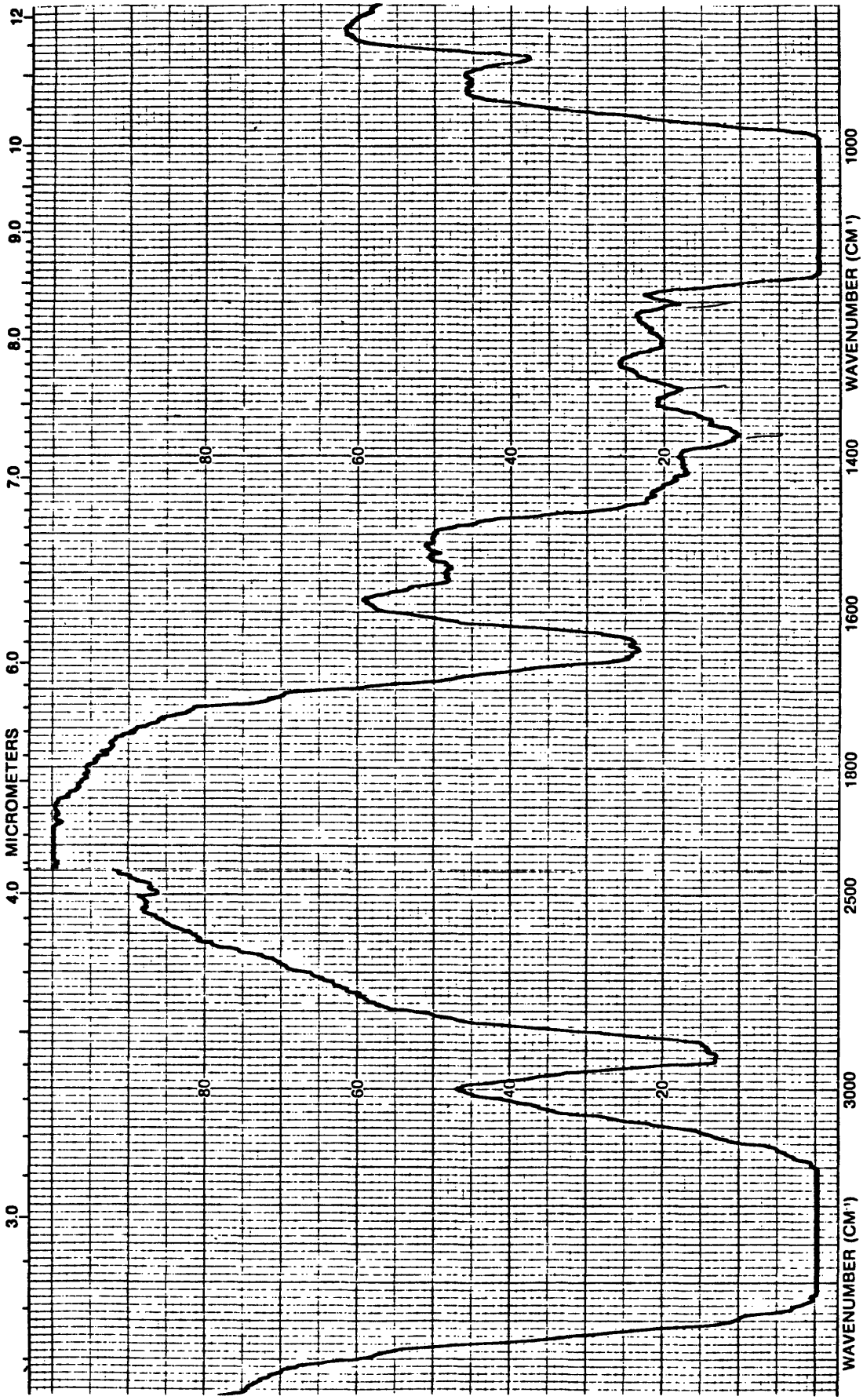

Figure 30 . I.R. Spectrum of A364A Glucan after Acetic Acid Extraction (8%w/w sample concentration)

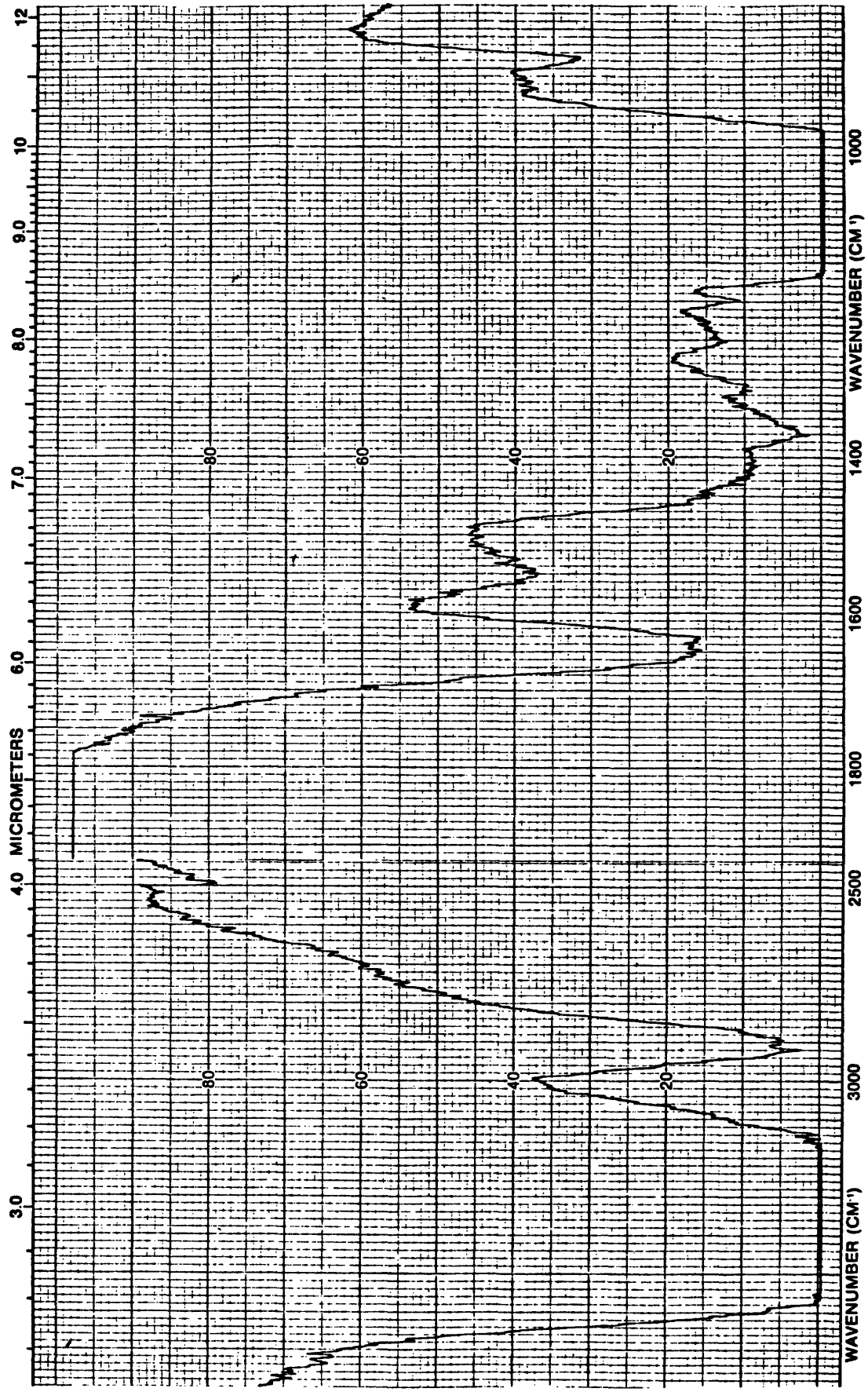

Figure 31 . I.R. Spectrum of 374 Glucan after Acetic Acid Extraction (8% w/w sample concentration)

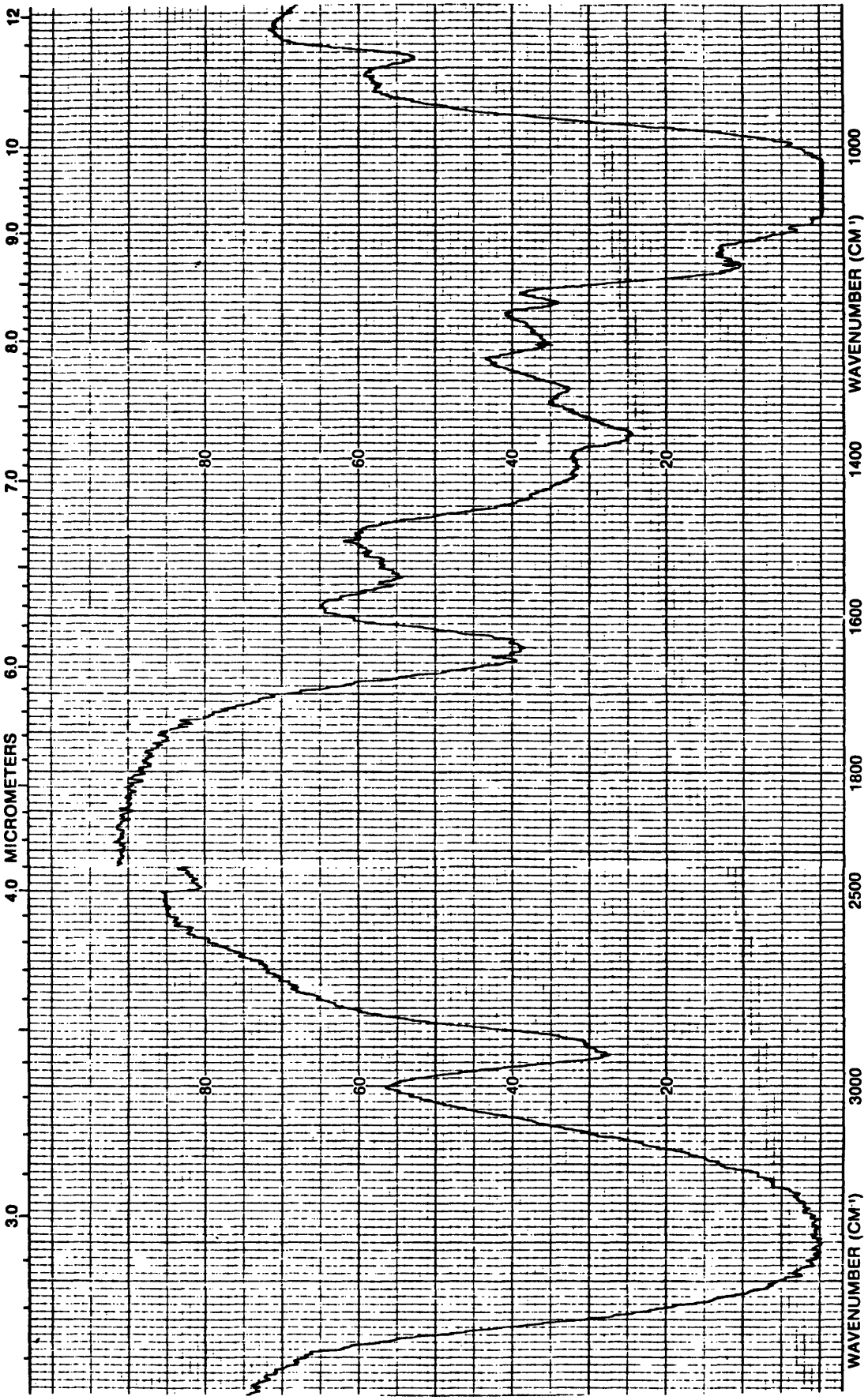

Figure 32 . I.R. Spectrum of 377 Glucan after Acetic Acid Extraction (8% w/w sample concentration)

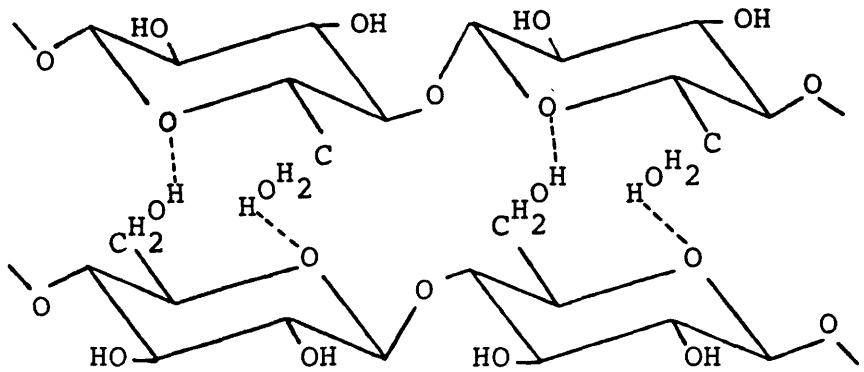

Figure 33. Cooperative Hydrogen Bonding in adjacent Cellulose Molecules

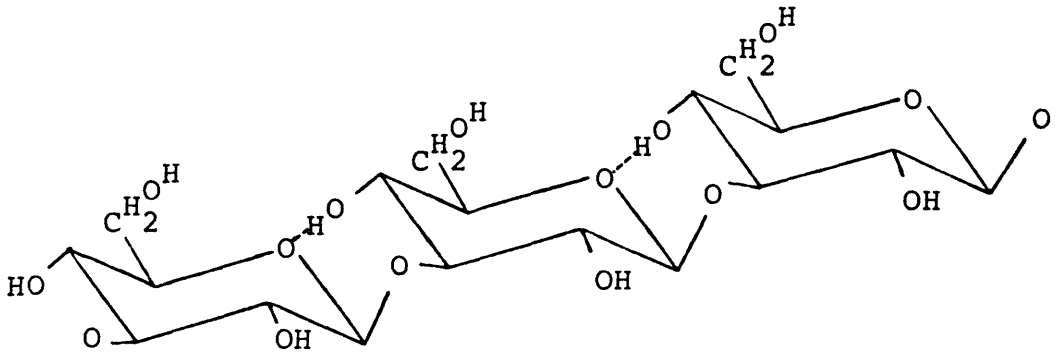

Figure 34. Inter-Molecular Hydrogen Bonding within a β(1-3) Glucan Molecule

An important observation from these spectra is that all gave a peak at 2.7μm adjacent to the strong hydroxide (-OH) peak (3.Ø μm), which indicates the presence of hydrogen bonded hydroxyl groups. Since the spectra obtained were of dry samples in KBr discs the H-bonding observed probably occurs inter- or intra-molecularly in the glucans. It is possible therefore, that glucan chains arrange themselves geometrically to allow this H-bonding to occur. Given the fact that glucan chains are very large molecules of molecular weight 25Ø,ØØØ , the cooperative formation of H-bonds along the length of a chain will explain its reluctance to go into solution. For example, consider cellulose which is a β(1-4)-D-glucosidically linked polysaccharide. Cooperative H-bonding between the closely stacked adjacent chains makes this compound insoluble in water (Figure 33). However, laminarin, a β(1-3)-D-glucan of molecular weight approximately 8ØØ, is readily soluble in water. This can be explained by the fact that the β(1-3) orientation of the bonds brings the oxygen in the glucose ring close to the hydroxide on the 4^{th} carbon of the adjacent glucose unit thus promoting inter-molecular H-bonding. The electronegative O -atoms in the glucose rings are therefore H-bonded to hydroxyl hydrogens of the same glucan molecule (Figure 34). Cooperative H-bonding between chains is therefore not strong enough to resist H-bonding to water molecules, hence, laminarin goes into, solution.

The above criteria however, are not sufficient to explain the physical properties of the yeast glucan matrix since this is composed of more complex branched chains. The rheological studies have elucidated these properties and will be discussed later.

As shown in Figures 30,31,32 extraction of the whole glucan samples in acetic acid resulted in partial removal of the β(1-6) glucan component in addition to destruction of H-bonding. The relation of the β(1-6) glucan component to H-bonding in the whole glucan matrix has not been studied to date. The only information available(4) is that this minor component is closely associated to the insoluble β(1-3) glucan matrix. It is not known if this association is through covalent bonds or electrostatic attractions. The results provided above infer that the highly branched β(1-6) glucan extracted by the acetic acid treatment has a relatively high H-bonding potential. This supposition is supported by the fact that this component becomes soluble after the extraction.

Only one model can be proposed by taking all the above experimental evidence into consideration. The model is that the major alkali insoluble β(1-3) glucan component - with the aid of β(1-6) inter-molecular crosslinking and cooperative H-bonding - provides a rigid insoluble matrix into which the highly branched β(1-6) component is strongly bound through H-bonding. In the presence of this

macroscopic matrix, the β(1-6) component does not go into solution. However, upon rigorous chemical treatment the cooperative H-bonding is disrupted and the minor component becomes soluble in water.

An additional comment that can be made is that the insoluble nature of the β(1-3) glucan (in contrast to laminarin) is due to two factors:

1. the tight geometric arrangement of the chain due to β(1-6) crosslinks(28)
2. a high density of cooperative H-bonding (a function of chain length/molecular weight)

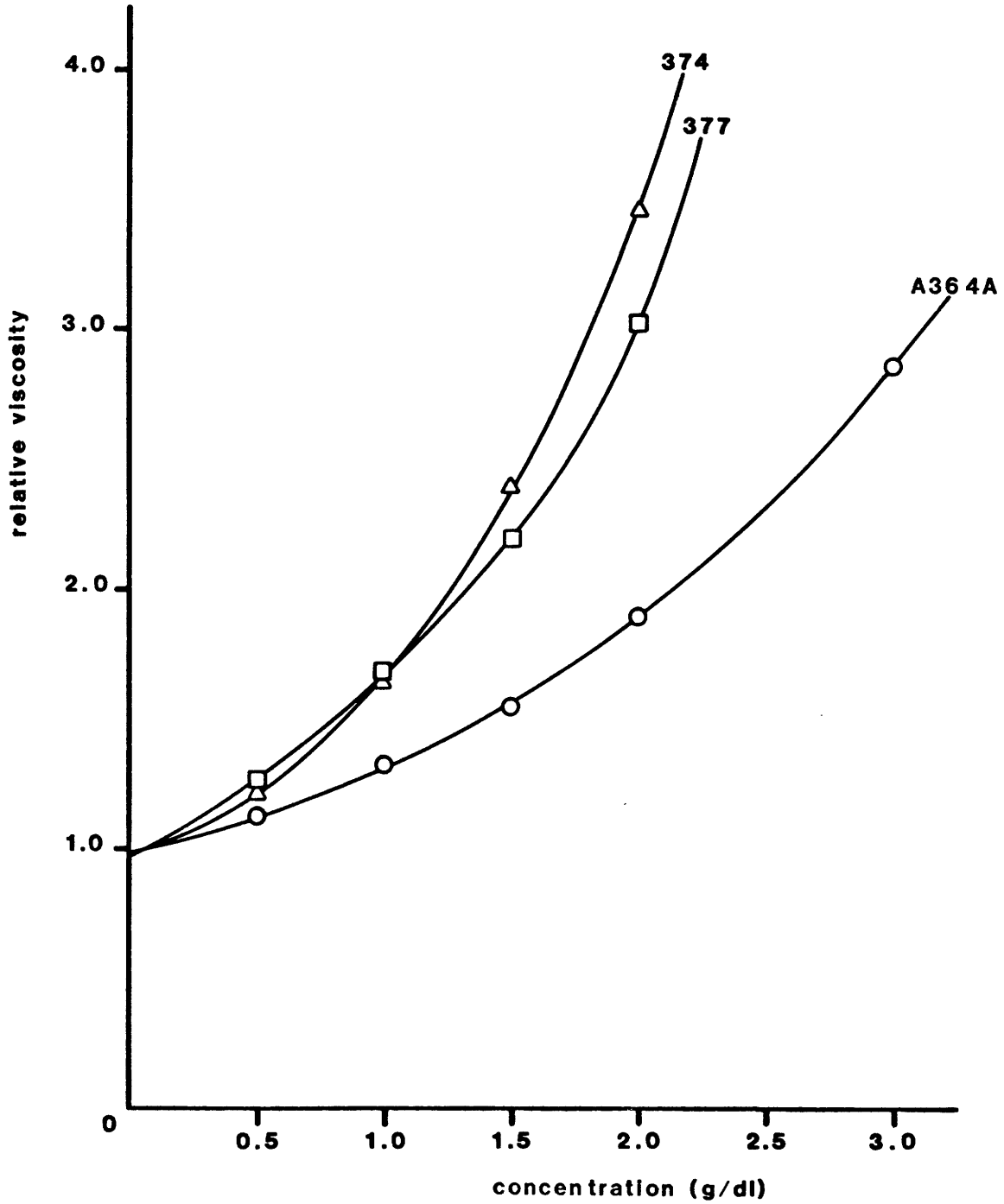

Figure 35 : **Viscosity profiles of yeast glucan comparing different cell morphologies**

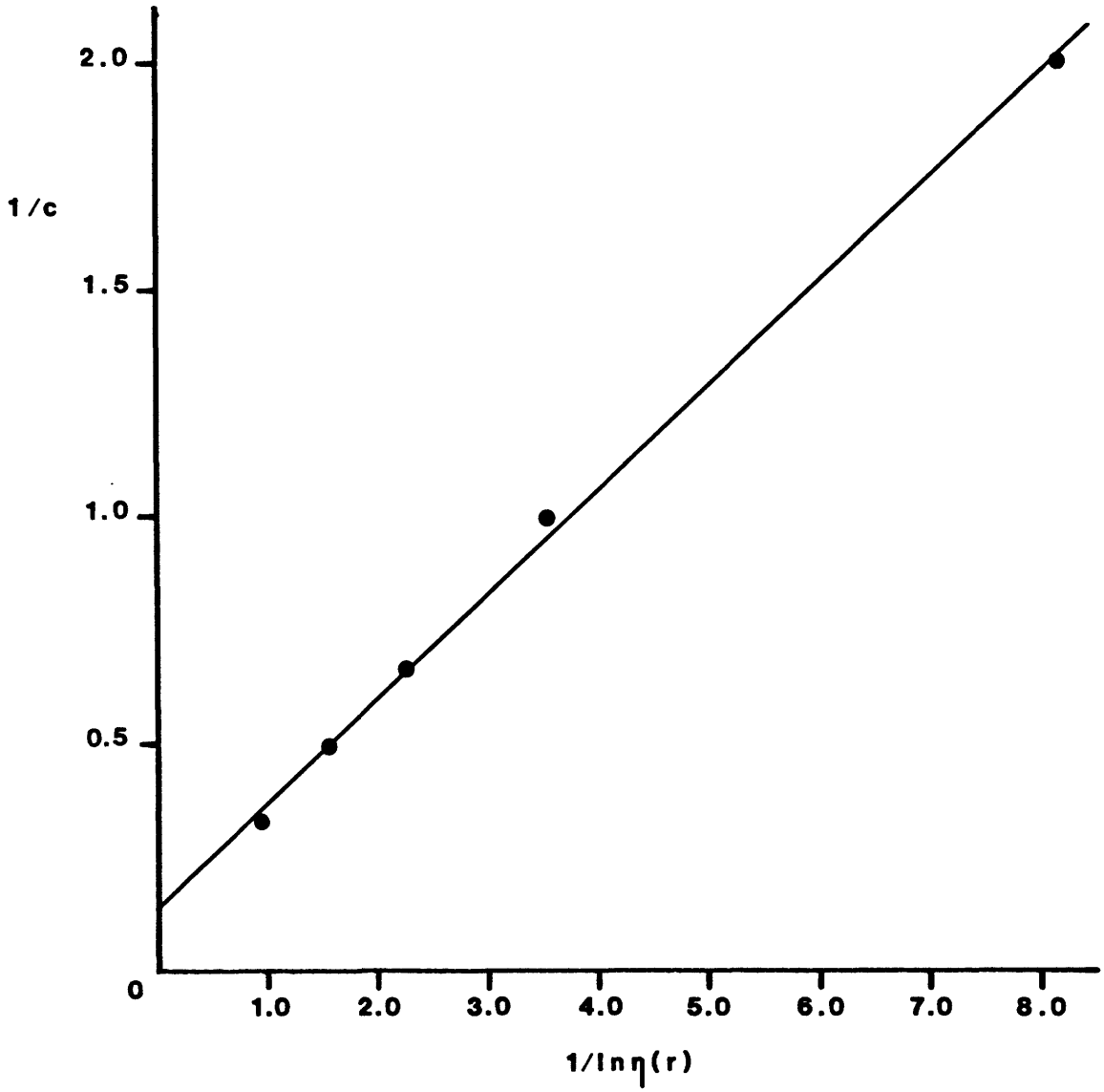

Figure 36 : **Plot of the modified Mooney equation for A364A glucan**

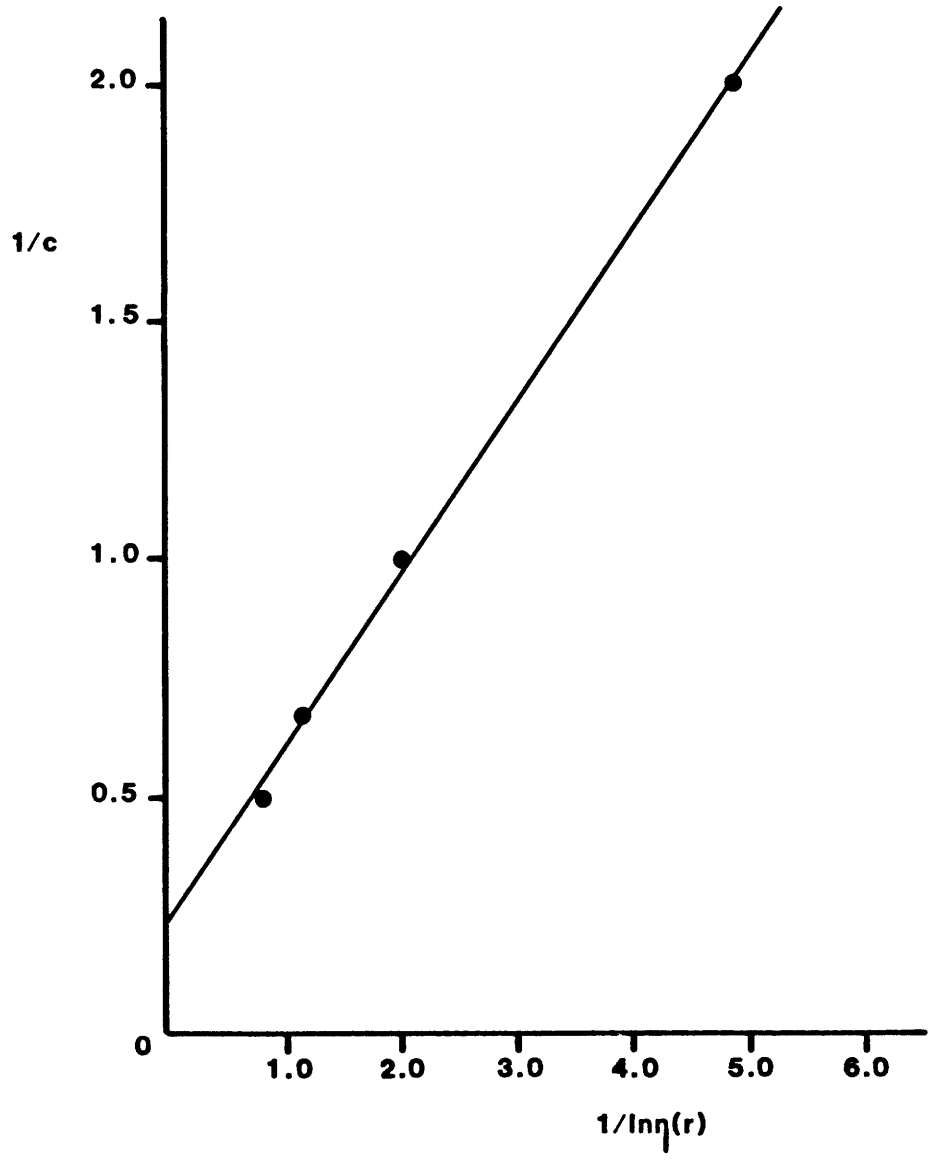

Figure 37. **Plot of the modified Mooney equation for 374 glucan**

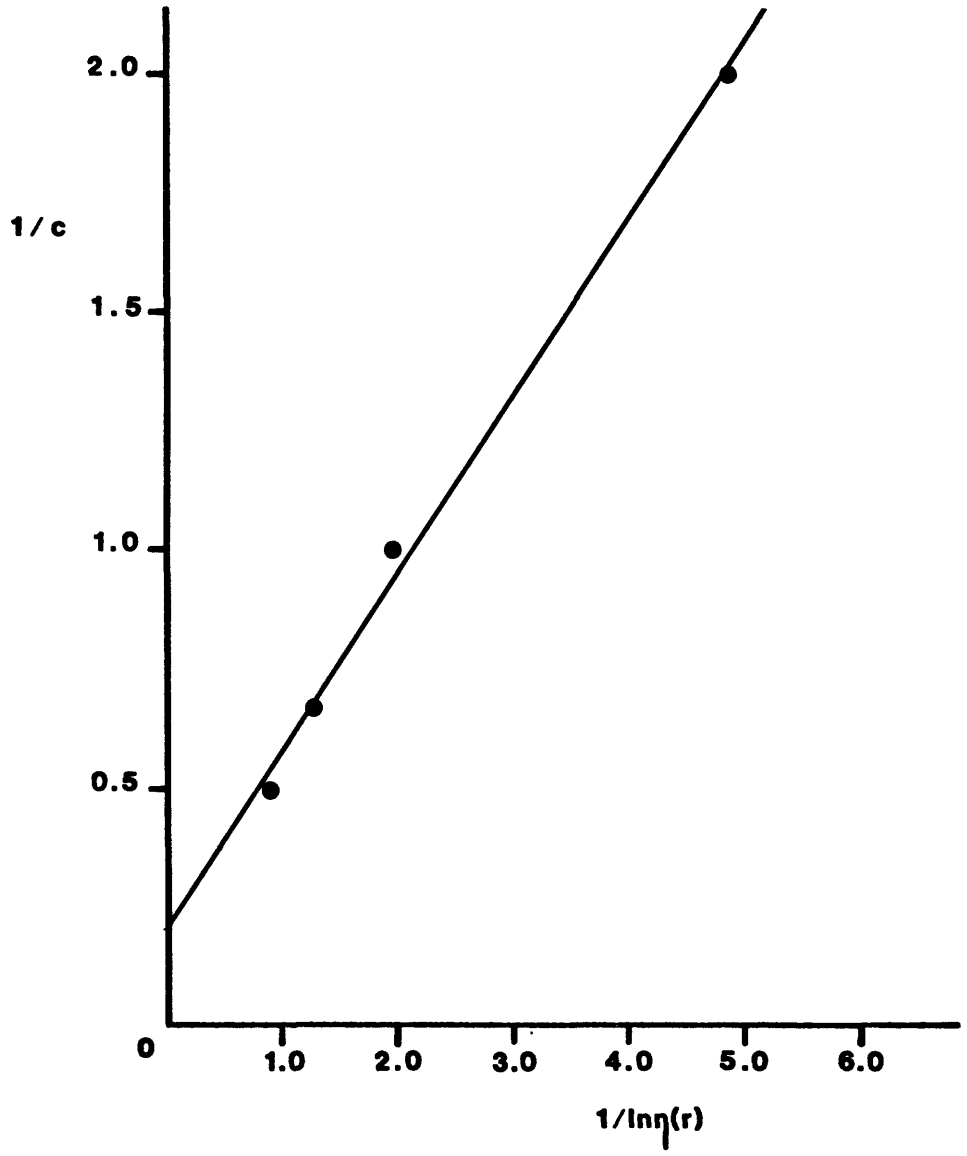

Figure 38 : **Plot of the modified Mooney equation for 377 glucan**

Figure 35 illustrates the viscosity profiles of A364A glucan compared to 374 and 377 glucan after inducing the cell division cycle block. It can be clearly seen that 374 and 377 glucans impart higher viscosities in suspension to A364A glucan and reach an inflection (critical concentration) at a much lower concentration. In fact, the viscosity profile of A364A glucan does not appear to reach an inflection point in the concentration range used. This behaviour can be grossly explained by the shape differences of the glucan particles. A more concise explanation of these results with respect to macrosopic glucan structure can be arrived at by using the plots of the linear model that was developed in the theory section (see Figs. 36,37,38). Table 6 summarizes the obtained information.

Table 6

Hydrodynamic Properties of Whole Yeast Glucan

Glucan Sample	Regression Coefficient r	k_1	k_2	Shape Factor V	Hydrodynamic Volume $\bar{v}$ (dl/g)	$\emptyset_m$
A364A	Ø.9986	Ø.23	Ø.15	2.5	Ø.Ø92	Ø.63
374	Ø.9987	Ø.36	Ø.24	4.1	Ø.Ø88	Ø.36
377	Ø.9974	Ø.37	Ø.2Ø	4.1	Ø.Ø91	Ø.45

We can observe that wild type glucan from spherical A364A cells has a higher hydrodynamic volume, $\bar{v}$ than glucan from the elongated 374 and 377 cells. From Mooney's equation it can be seen that relative viscosity increases with $\bar{v}$. Therefore, an adverse behavior is observed, since we would expect 374 and 377 glucan to have higher hydrodynamic volume than A364A glucan. (This effect is overpowered by the considerably higher shape factor, V, since n_r is proportional to exp (V)). Furthermore, coulter counter studies on the various glucan samples showed that 377 and 374 glucan have a higher mean effective diameter than A374A glucan.

The above observations therefore indicate that the 374 and 377 glucan particles are denser structures than A364A glucan, possibly containing a higher proportion of β(1-6) crosslinks between the β(1-3) backbone chains. These points will be elucidated and have been confirmed with other experiments discussed below.

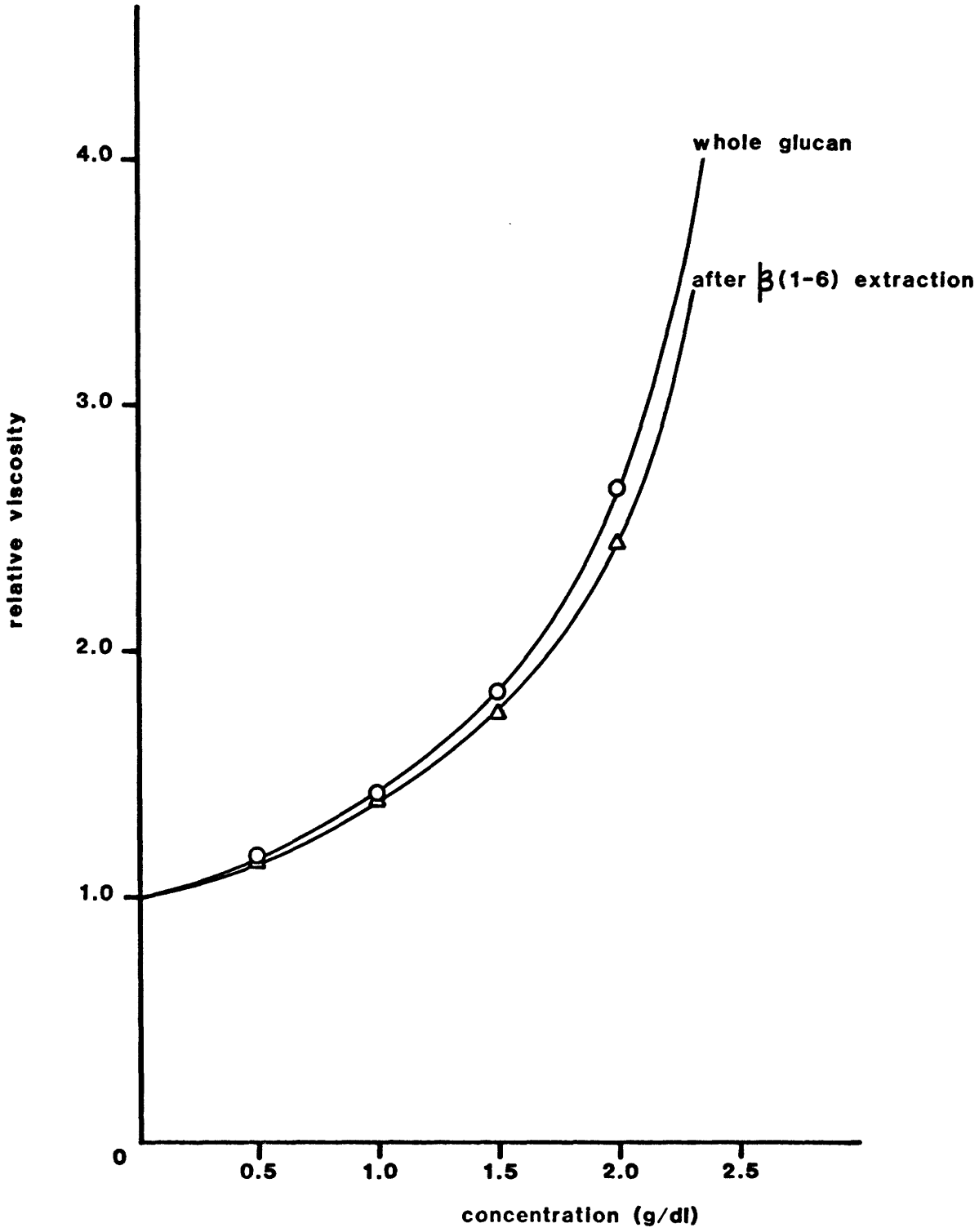

Figure 39 : **Viscosity profile of A364A glucan showing the effect of 3h. extraction in acetic acid**

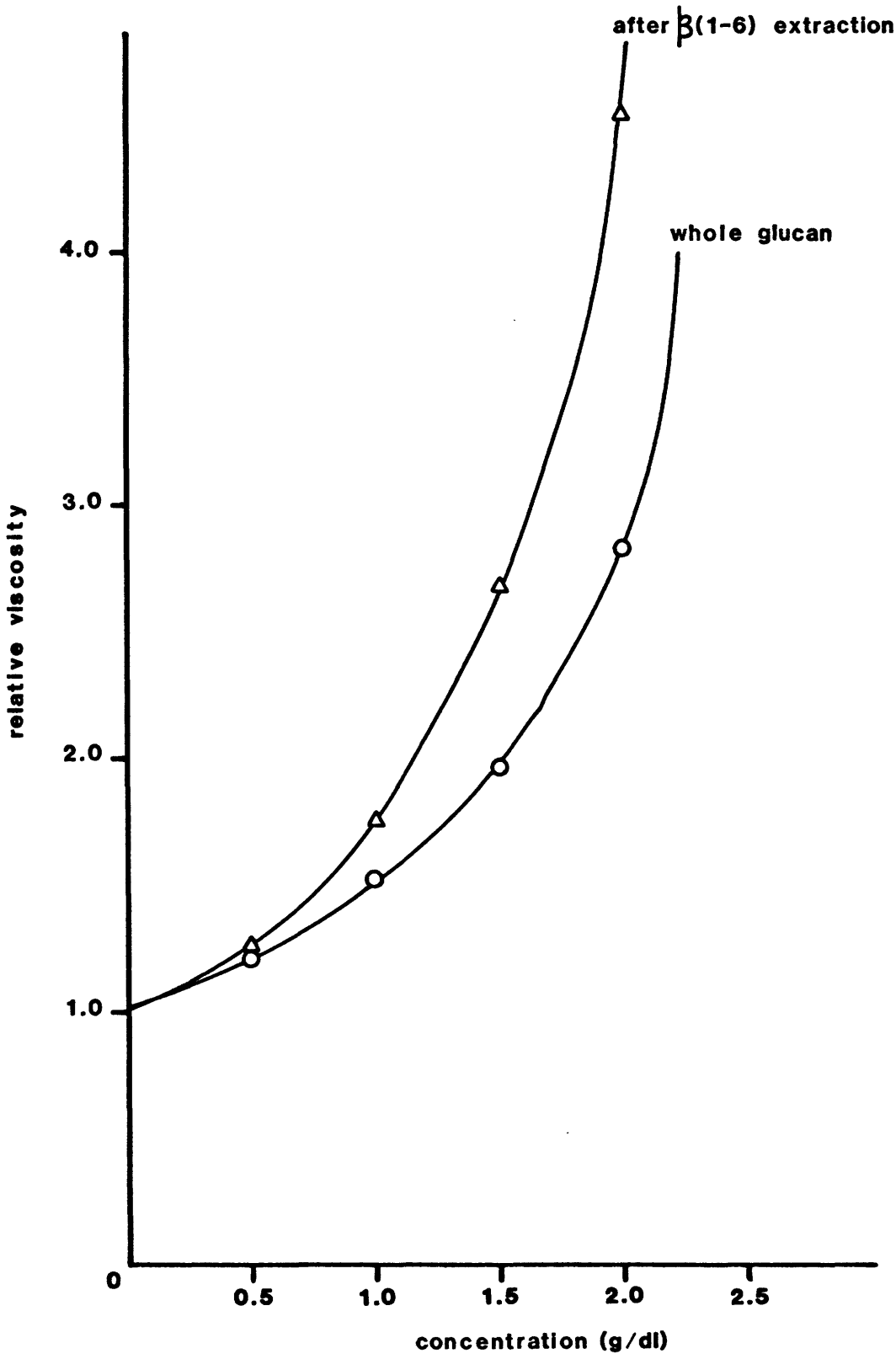

Figure 40: **Viscosity profile of 374 glucan showing the effect of 3h. extraction in acetic acid**

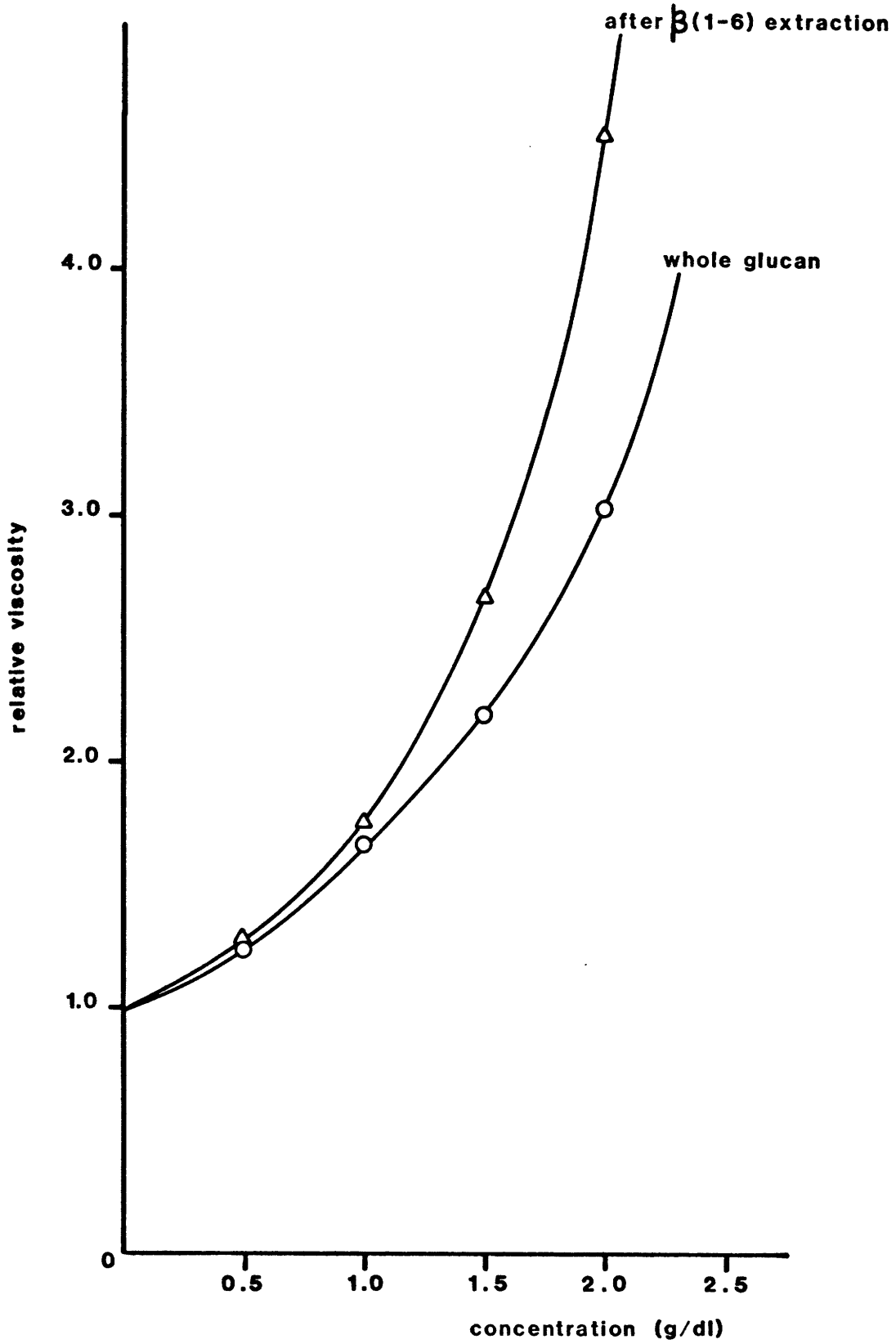

Figure 41 : **Viscosity profile of 377 glucan showing the effect of 3h. extraction in acetic acid**

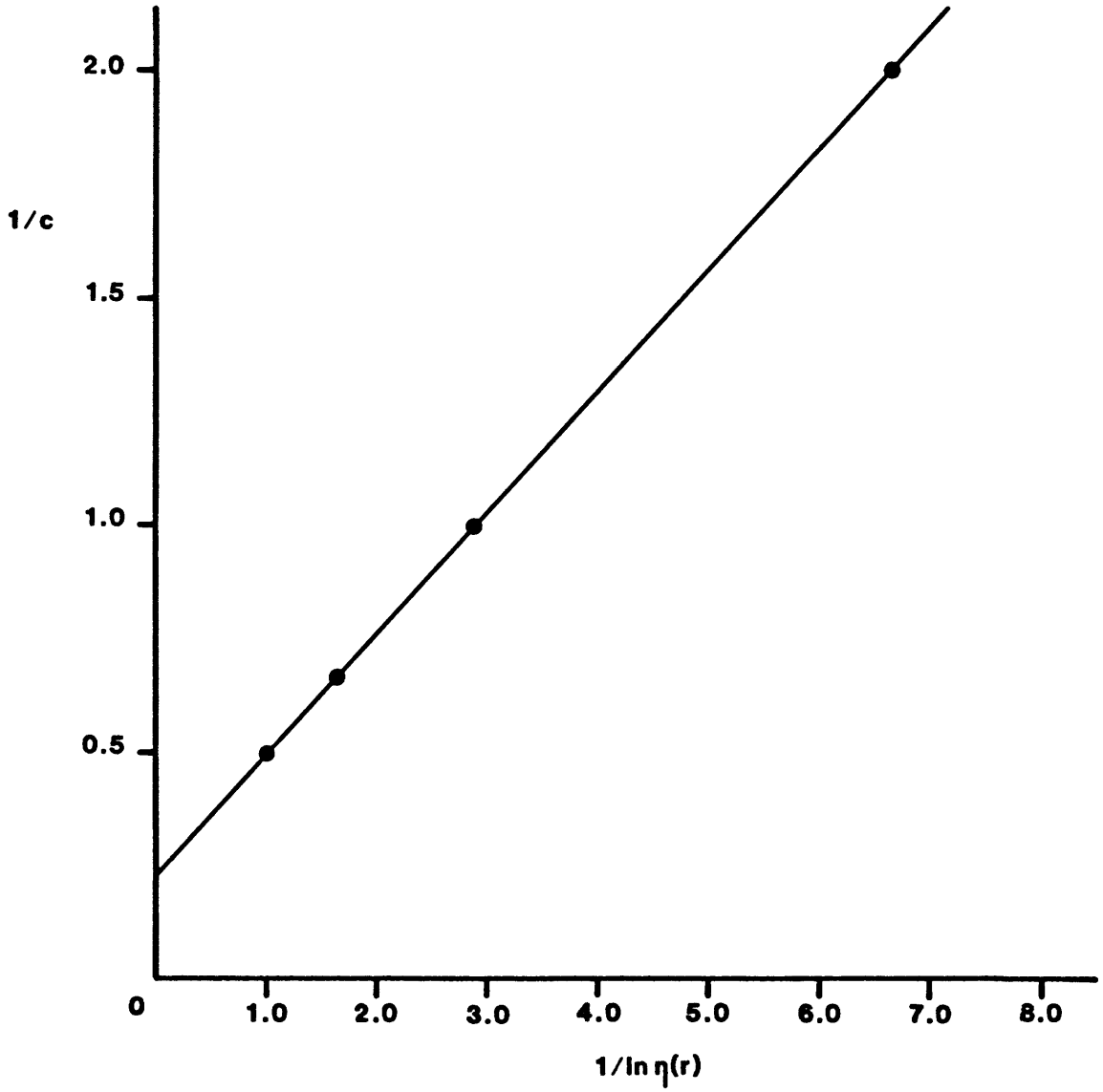

Figure 42 : **Plot of the modified Mooney equation for A364A glucan**

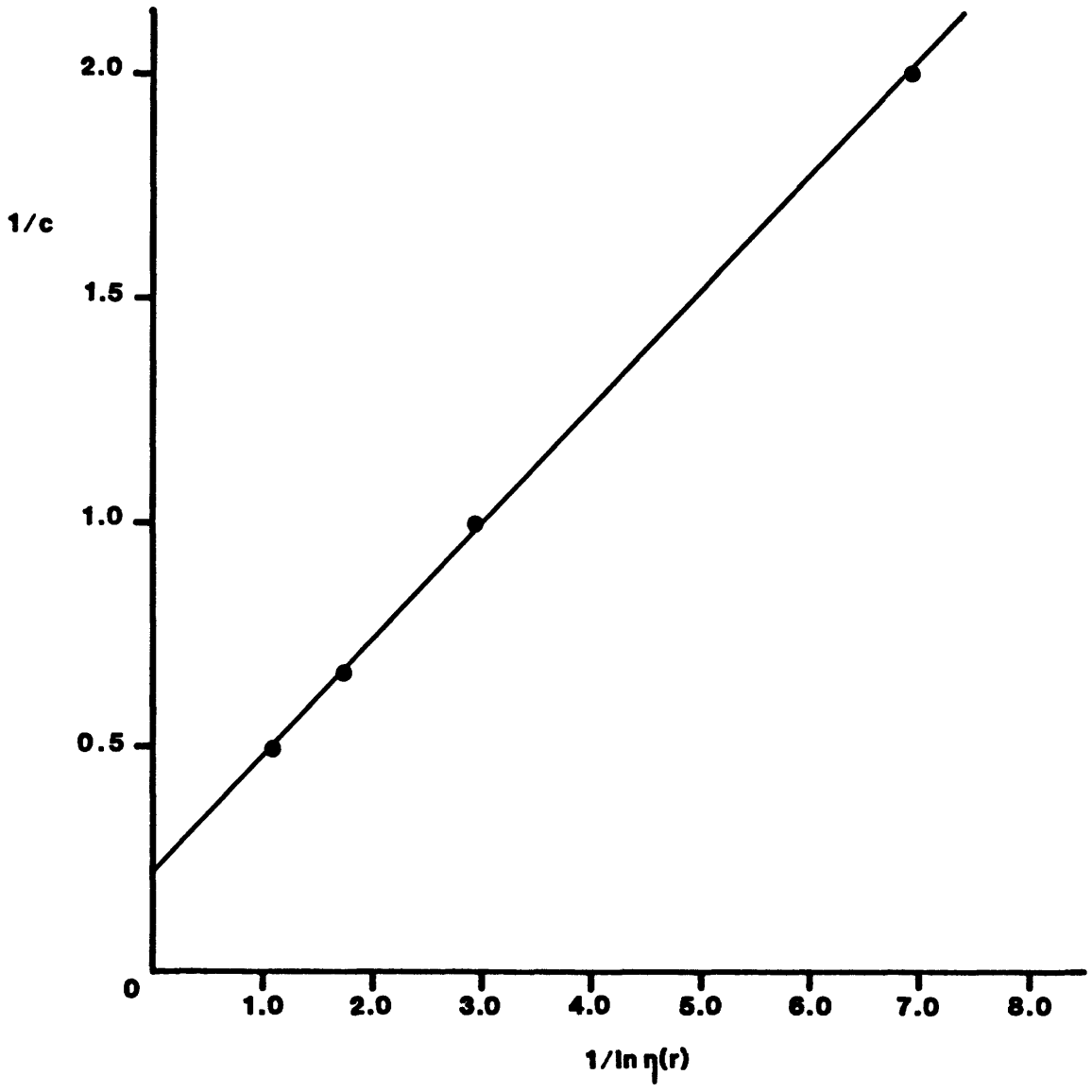

Figure 43 : **Plot of the modified Mooney equation for A364A glucan after 3h. extraction in acetic acid**

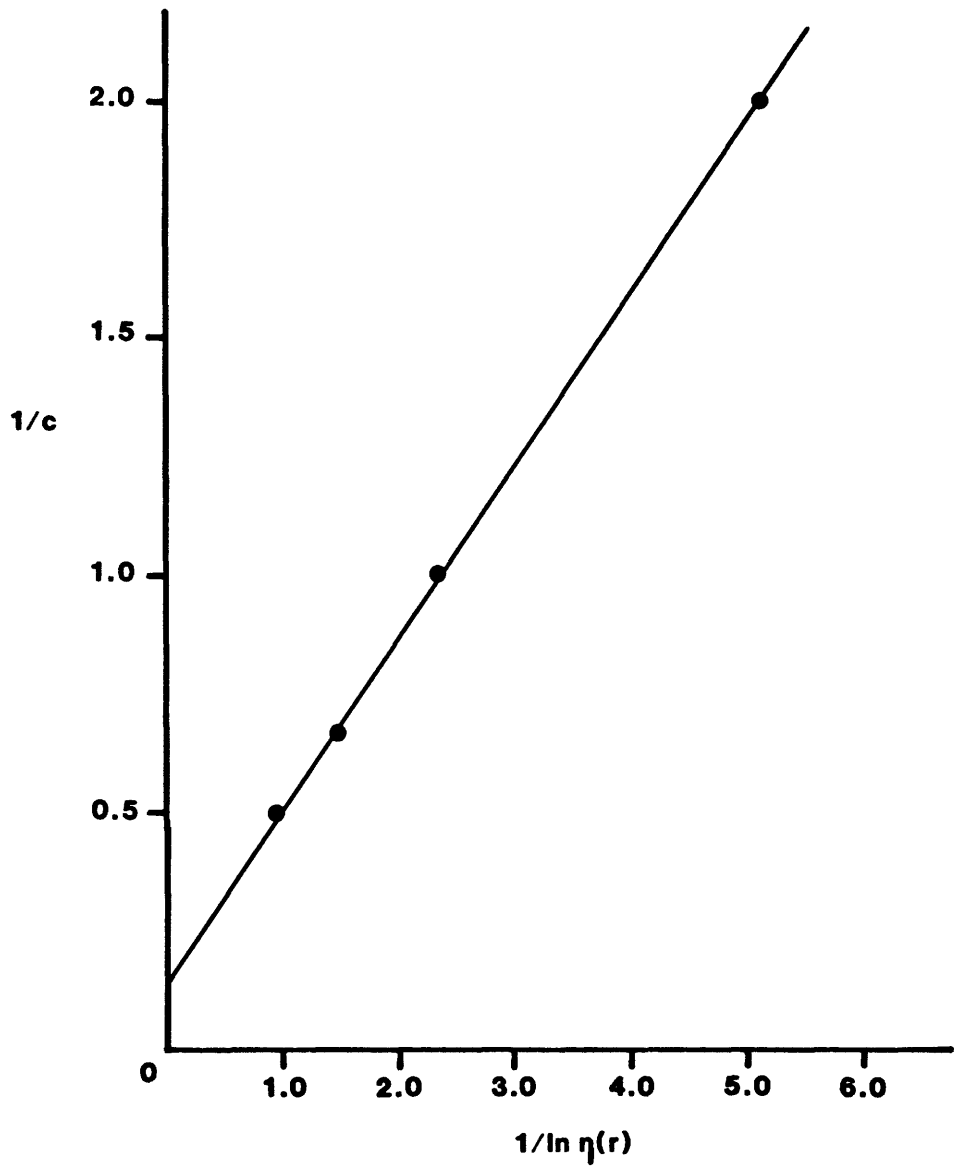

Figure 44 : **Plot of the modified Mooney equation for 374 glucan**

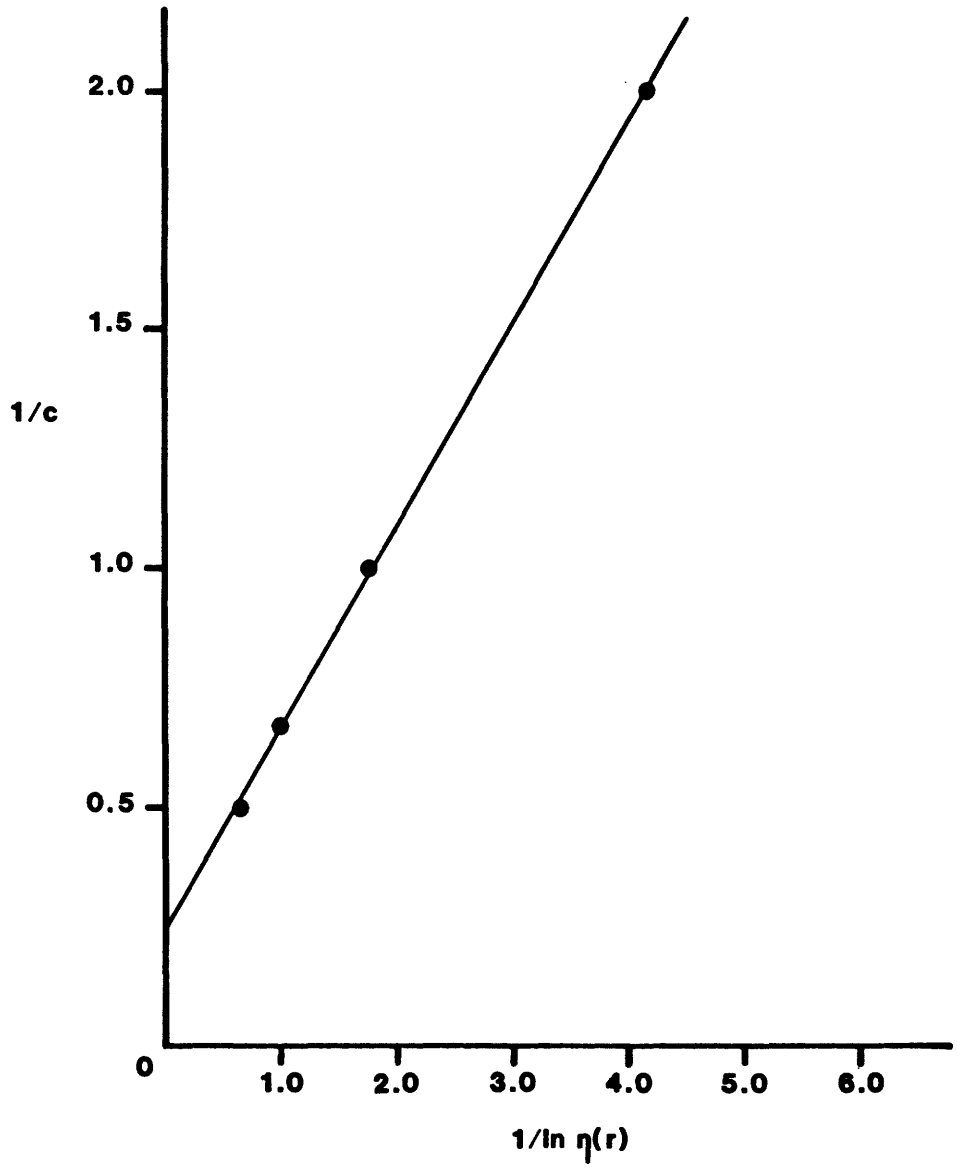

Figure 45 : **Plot of the modified Mooney equation for 374 glucan after 3h. extraction in acetic acid**

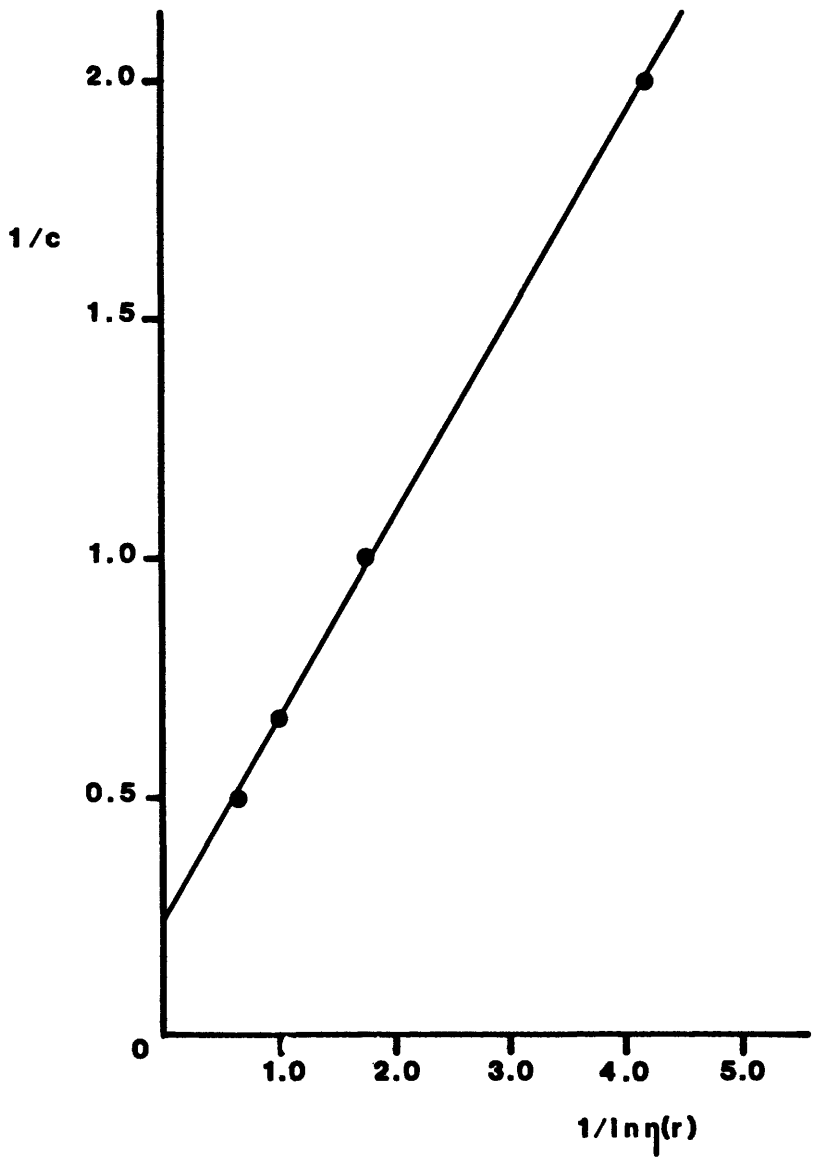

Figure 46: **Plot of the modified Mooney equation for 377 glucan after 3h. extraction in acetic acid**

The β(1-6) glucan extraction in Ø.5M acetic acid was performed to clarify the role of this fraction in the structural integrity of yeast cell wall glucan. Figures 39, 4Ø, and 41 illustrate the effects of this extraction on 377 and A364A glucan. Before proceeding on the discussion of this particular experiment it must be noted that microscopic observation of the glucan samples before and after the extraction revealed no visual (shape related) differences. This allowed us to assume that the shape factor, V remained constant throughout the experiment, and enabled calculation of the hydrodynamic parameters from the 1/c vs. 1/ln (n_r) plots (see Figs. 42,43,44,45,46). Table 7 summarizes these results.

Table 7

Hydrodynamic Properties of Glucan after Acetic Acid Extraction

Sample	r	k_1	k_2	Shape Factor V	Hydrodynamic Volume $\bar{v}$ (dl/g)	ϕ_m
A364A Whole glucan	Ø.9999	Ø.27	Ø.23	2.5	Ø.1Ø6	Ø.46
A364A After extn.	Ø.9974	Ø.26	Ø.22	2.5	Ø.1Ø3	Ø.47
374 whole glucan	Ø.9981	Ø.36	Ø.15	4.1	Ø.Ø88	Ø.6Ø
374 after extn.	Ø.9995	Ø.42	Ø.23	4.1	Ø.1Ø3	Ø.44
377 Whole glucan	Ø.9997	Ø.37	Ø.2Ø	4.1	Ø.Ø91	Ø.45
377 After extn.	Ø.9995	Ø.42	Ø.23	4.1	Ø.1Ø3	Ø.44

An initial observation is that β(1-6) extraction has a very small effect on the viscosity profile of A364A glucan and in fact a slight decrease in the thickening properties of the glucan occurs. The values of $\bar{v}$, ϕ_m also remain

essentially constant. These results indicate that β(1-6) glucan has a minor structural role in the glucan matrix of A364A cell walls and is possibly present in relatively small quantities with respect to β(1-3) glucan.

On the contrary a significant and converse effect was observed on 374 and 377 glucan after the β(1-6) extraction. The β(1-6) extracted 374 and 377 glucans exhibited considerably higher thickening properties with a critical concentration 1Ø% and 25% respectively, lower than for whole glucan. The extraction of the β(1-6) glucan can also be reflected in the increase of the value for hydrodynamic volume (see Table 7). This increase indicates a drop in the density of the glucan matrix in suspension. Furthermore, the fact that the maximum packing fraction, ϕ_m , remains essentially unchanged indicates that the overall shape and size of the glucan particle remains unchanged. In other words, the difference in rheological properties observed with β(1-6) extraction is not due to shape and size effects but due to more subtle structural alterations.

Hence we can conclude that β(1-6) glucan plays an important structural role in 374 and 377 glucan and is present in relatively high proportions.

It must be mentioned that I.R. spectra of the glucan samples were used to follow the extraction in acetic acid. Before the extraction, the spectra showed the characteristic β(1-6) peak at 11.Ø μm. I.R. spectra of glucan samples after

the extraction clearly showed only a very low background response at 11.Ø μm, thus confirming that the extraction was effective. The peaks characteristic of β(1-3) glucan remained unchanged.

Table 8

Extraction of β(1-6) Glucan

Sample	Total Carbohydrate before extn. (mg/ml)	Total Soluble Carbohydrate (mg/ml)	β(1-6) / β(1-3) %
A364A	4.31	Ø.18	4.2
374	3.23	Ø.13	4.Ø
377	4.75	Ø.15	3.3

The laminarinase digest of the glucan samples can also be used to obtain structural information. Since laminarinase has only β(1-3) lytic activity, information on the availability of β(1-3) glucosidic sites can be established. Figures 47,48,49 illustrate the effect of the 4 hour enzyme digest on the glucan samples. In all three cases a decrease in viscosity imparting ability is observed and inflection points occur at higher concentrations. However, it is clearly shown that this treatment has a more pronounced effect on A364A glucan than on 374 and 377 glucan.

For example, at 2.Ø g/dl concentration, the viscosity of the A364A glucan suspension drops by 38% whereas for 374 glucan the drop is 19% and for 377 glucan an 11% drop is observed. These results agree with the earlier conclusion that 377 and 374 glucan particles have a denser matrix than A364A glucan, thus having a lower availability of β(1-3) sites for cleavage by the enzyme. Furthermore, an increased proportion of β(1-6) crosslinks in the mutants will also decrease the availability of β(1-3) sites and provide a more resistant matrix.

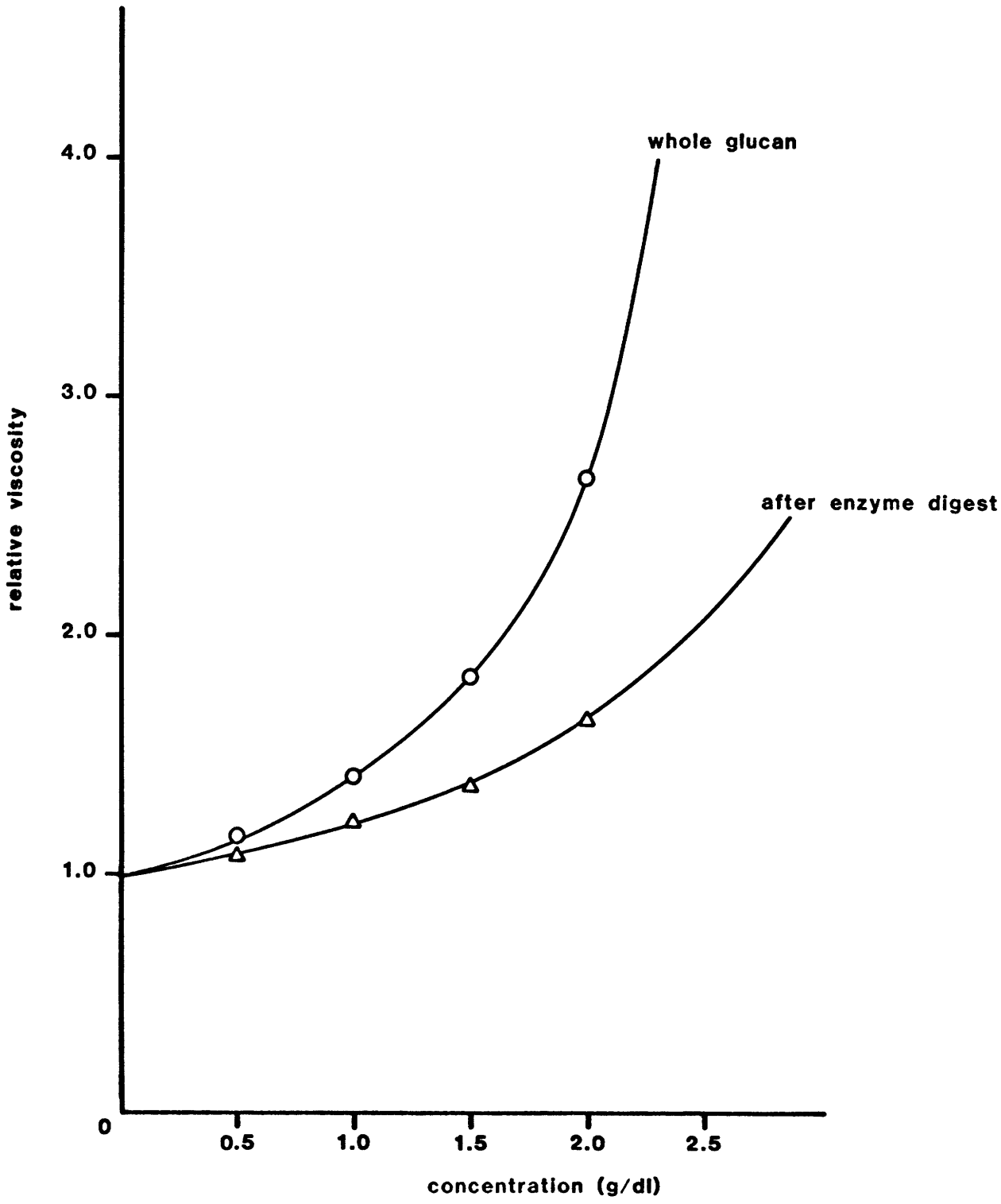

Figure 47: **Viscosity profile of A364A glucan showing the effect of 4h. laminarinase digest**

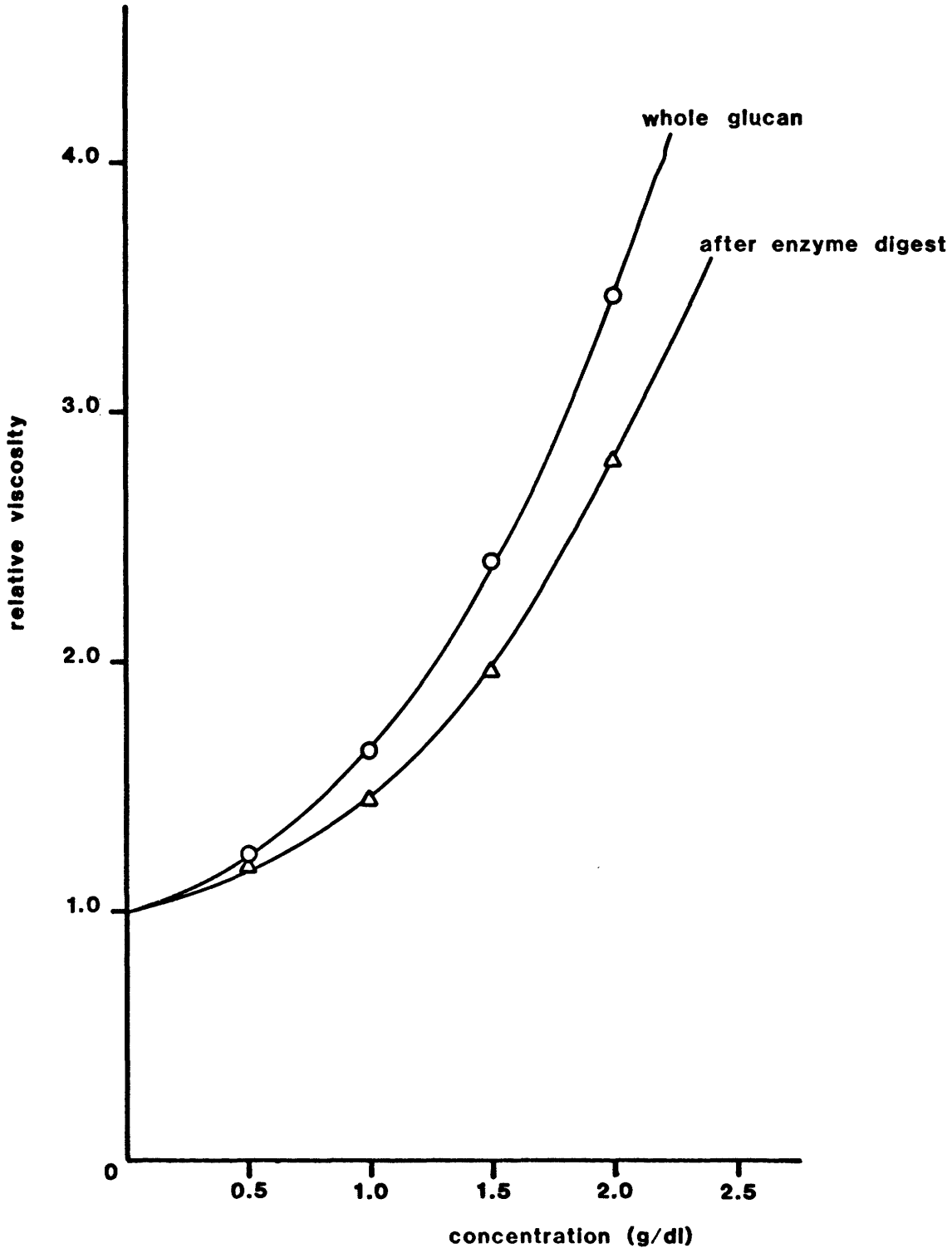

Figure 48: **Viscosity profile of 374 glucan showing the effect of 4h. laminarinase digest**

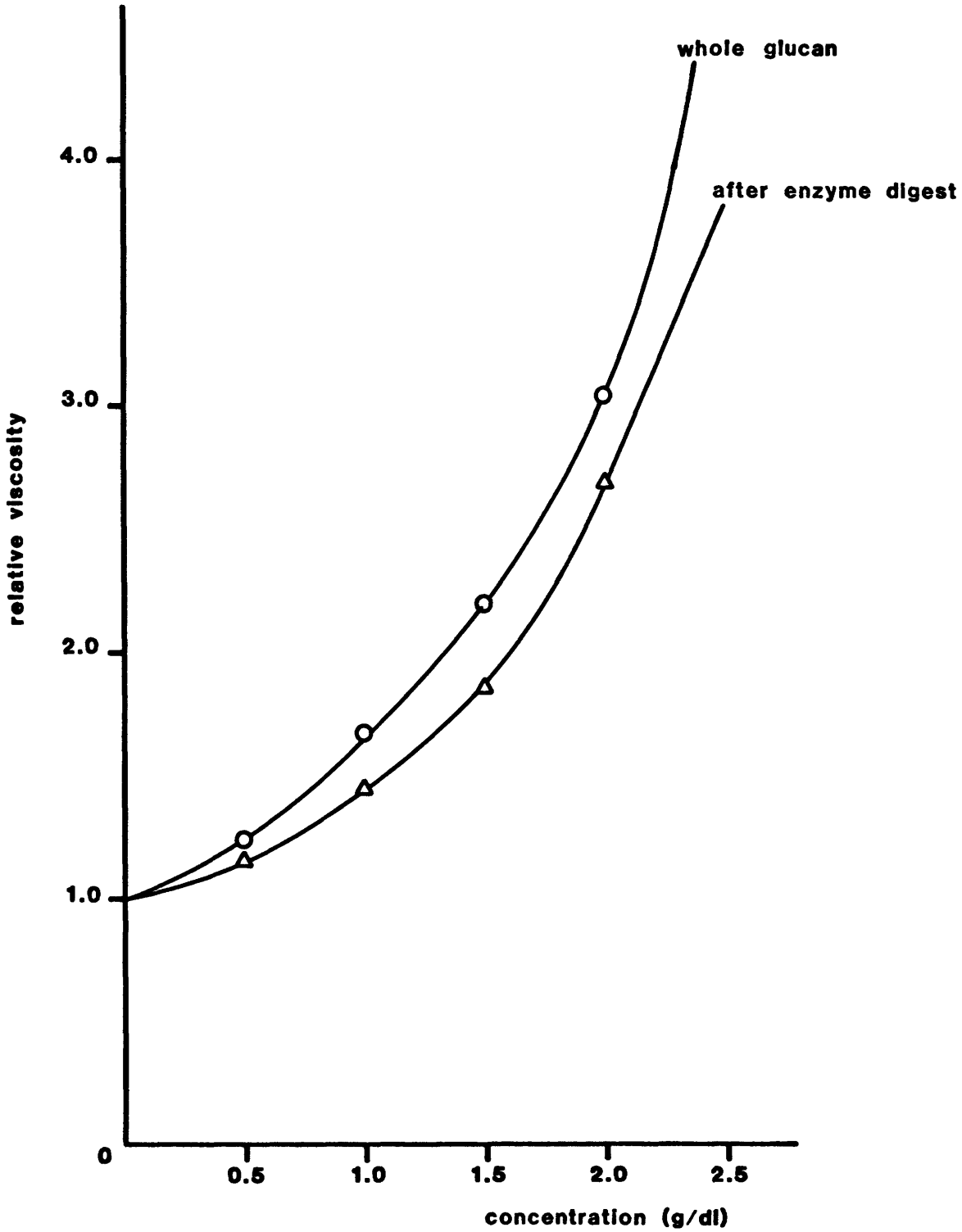

Figure 49: **Viscosity profile of 377 glucan showing the effect of 4h. laminarinase digest**

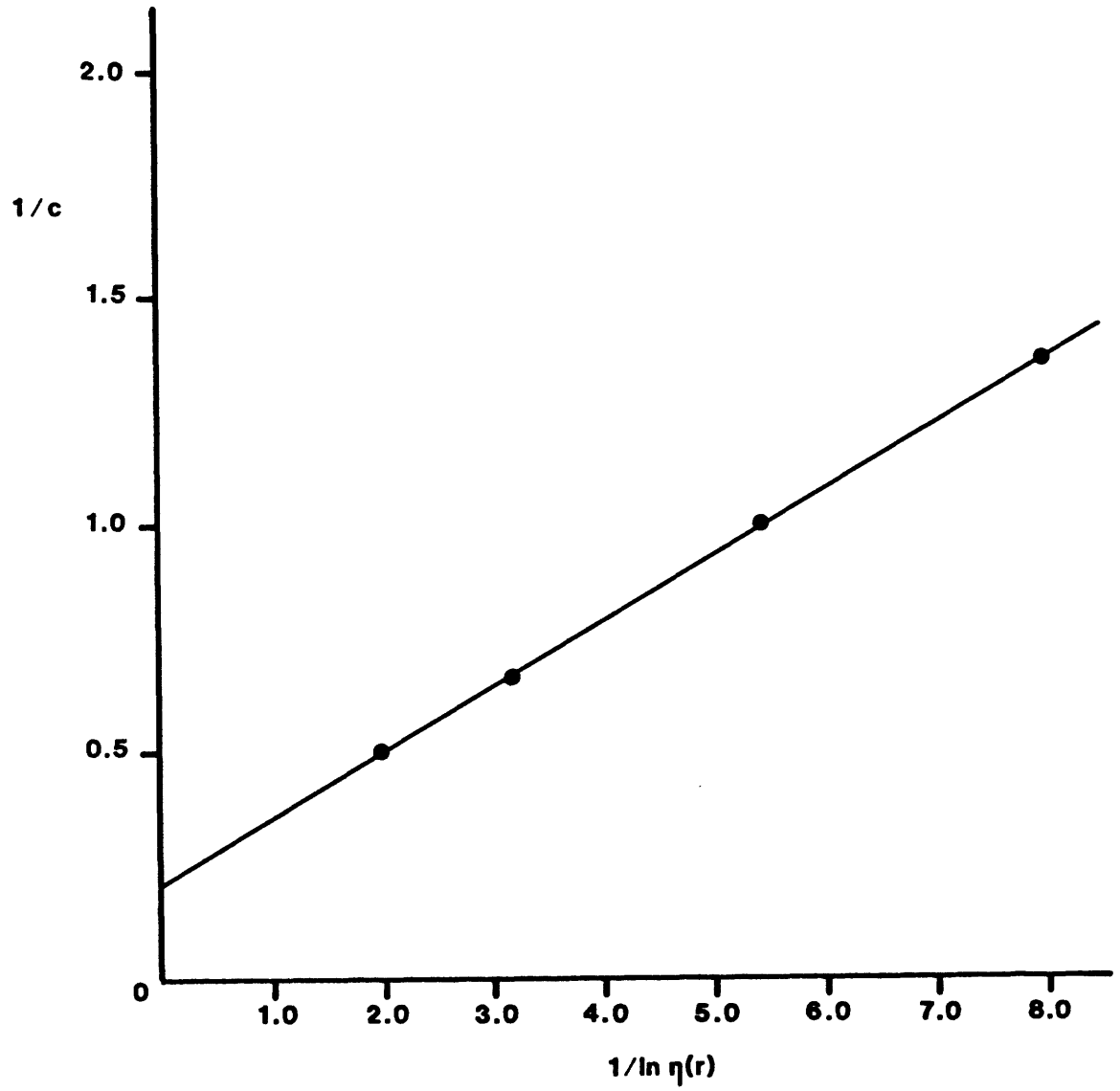

Figure 50: **Plot of the modified Mooney equation for A364A glucan after 4h. laminarinase digest**

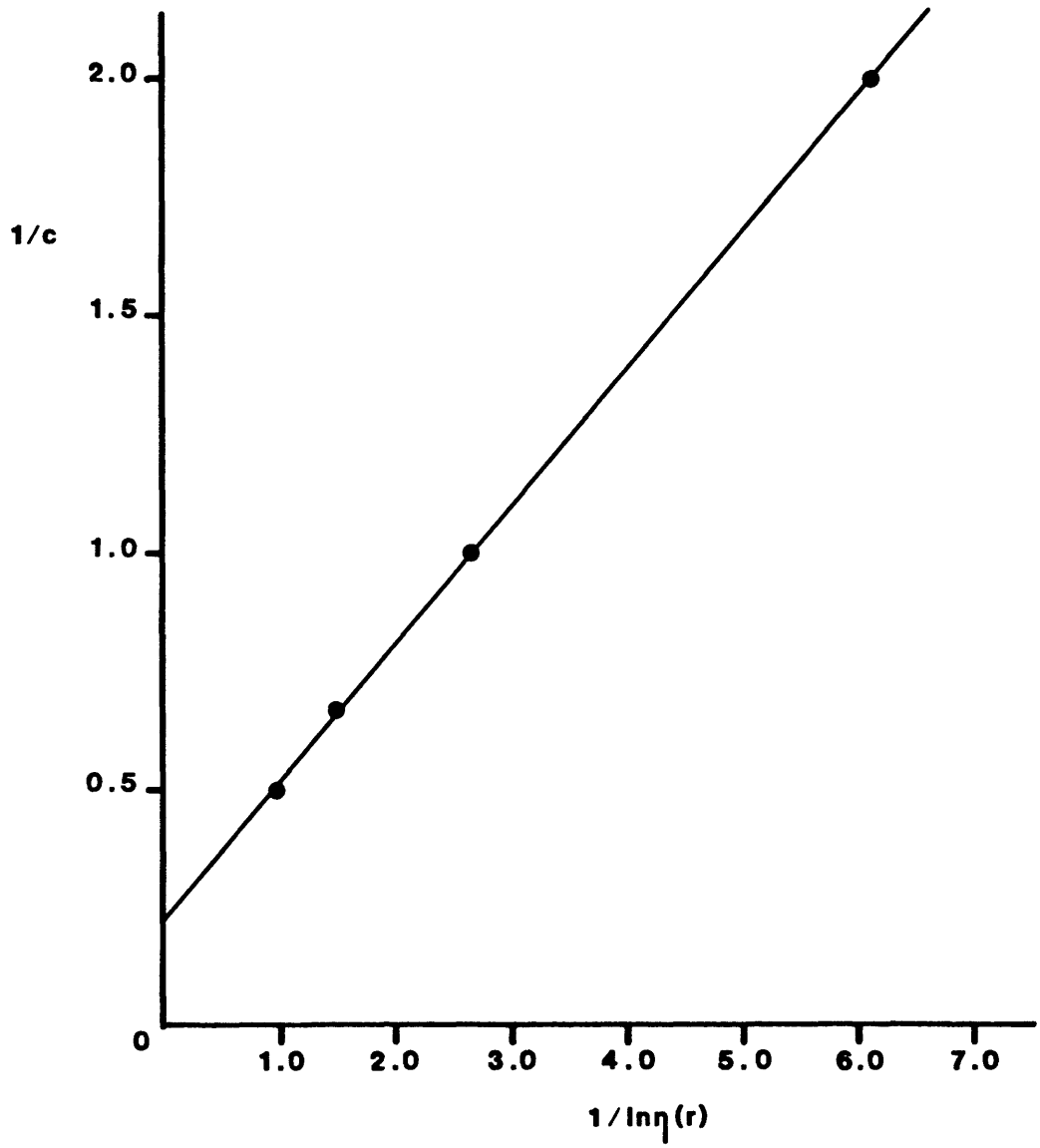

Figure 51: **Plot of the modified Mooney equation for 374 glucan after 4h. laminarinase digest**

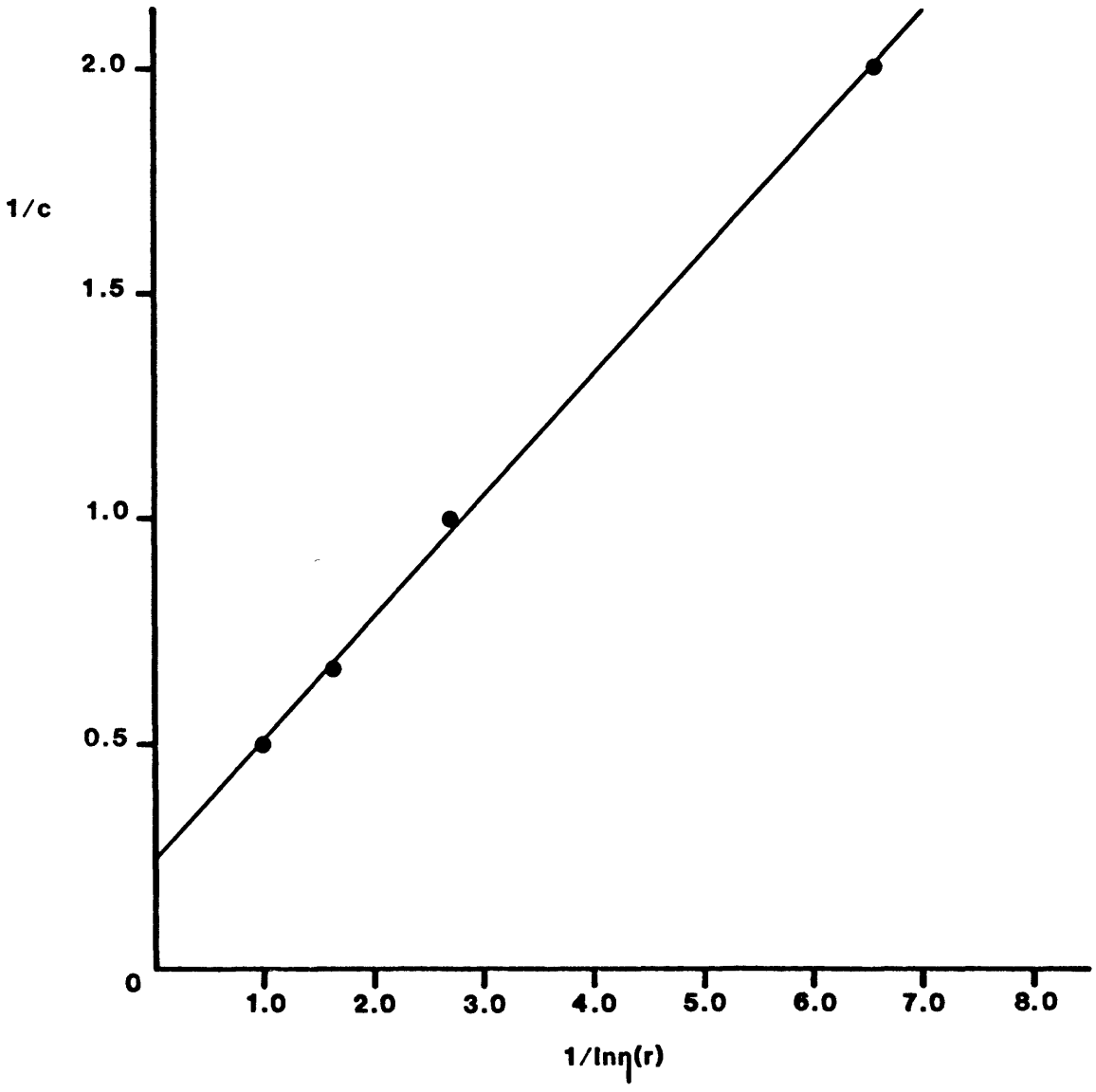

Figure 52 : **Plot of the modified Mooney equation for 377 glucan after 4h. laminarinase digest**

The plots of the linear model (see Figs. 50,51.52) provide the following information.

Table 9

Hydrodynamic Properties of Glucan after Laminarinase Digest

Sample	r	k_1	k_2	Shape Factor V	$\bar{v}$(dl/g)	ϕ_m
A364A Whole glucan	Ø.9999	Ø.27	Ø.23	2.5	Ø.1Ø6	Ø.46
A364A After digest	Ø.9998	Ø.14	Ø.21	2.5	Ø.Ø57	Ø.27
374 Whole glucan	Ø.9987	Ø.36	Ø.24	4.1	Ø.Ø88	Ø.36
374 After digest	Ø.9985	Ø.23	Ø.23	4.1	Ø.Ø7Ø	Ø.3Ø
377 Whole glucan	Ø.9974	Ø.37	Ø.2Ø	4.1	Ø.Ø91	Ø.45
377 After digest	Ø.9989	Ø.27	Ø.24	4.1	Ø.Ø65	Ø.27

The effect of laminarinase is reflected in a significant decrease in both the hydrodynamic volume and

maximum packing fraction for all three glucan samples. The decrease in hydrodynamic volume is due to the lysis of β(1-3) glucosidic bonds on the surface of the glucan particles. This yields particles with a higher proportion of crosslinking in a densely packed matrix resistant to the enzyme. The decrease in ϕ_m is a result of this effect.

An important observation of the results in Table 9, is that for each glucan sample, the value of k_2 (the intercept on the modified Mooney plot), remains essentially constant after the laminarinase digest. The effect of the enzymatic degradation on the hydrodynamic properties of the glucan is reflected in the value of the parameter k_1 - the slope of the modified Mooney plot. To establish this fact an experiment was performed in which A364A glucan was subjected to laminarinase digest for a range of incubation times. The viscosity profile of each sample was obtained. The results are plotted on Figure 53. This plot only illustrates the continuous action of the enzyme on the substrate. The activity of the enzyme is essentially lost after 1 hour since no further degradation of the glucan occured in the 4 hour incubation. However, the plot of the modified Mooney equation (Figure 54) for these results gives an important piece of information. The intercept (k_2) has remained essentially constant and the effect of the incubation time is clearly reflected in the slope which is a hydrodynamic

parameter consisting of the shape factor, V, and the hydrodynamic volume, $\bar{v}$. These results are shown in Table 1Ø.

Table 1Ø

Effect of Laminarinase Digestion Time on the Hydrodynamic Properties of A364A Glucan

Incubation Time (min)	$k_1 = \bar{v}V$
Ø	Ø.27
15	Ø.23
3Ø	Ø.18
6Ø	Ø.14
24Ø	Ø.14

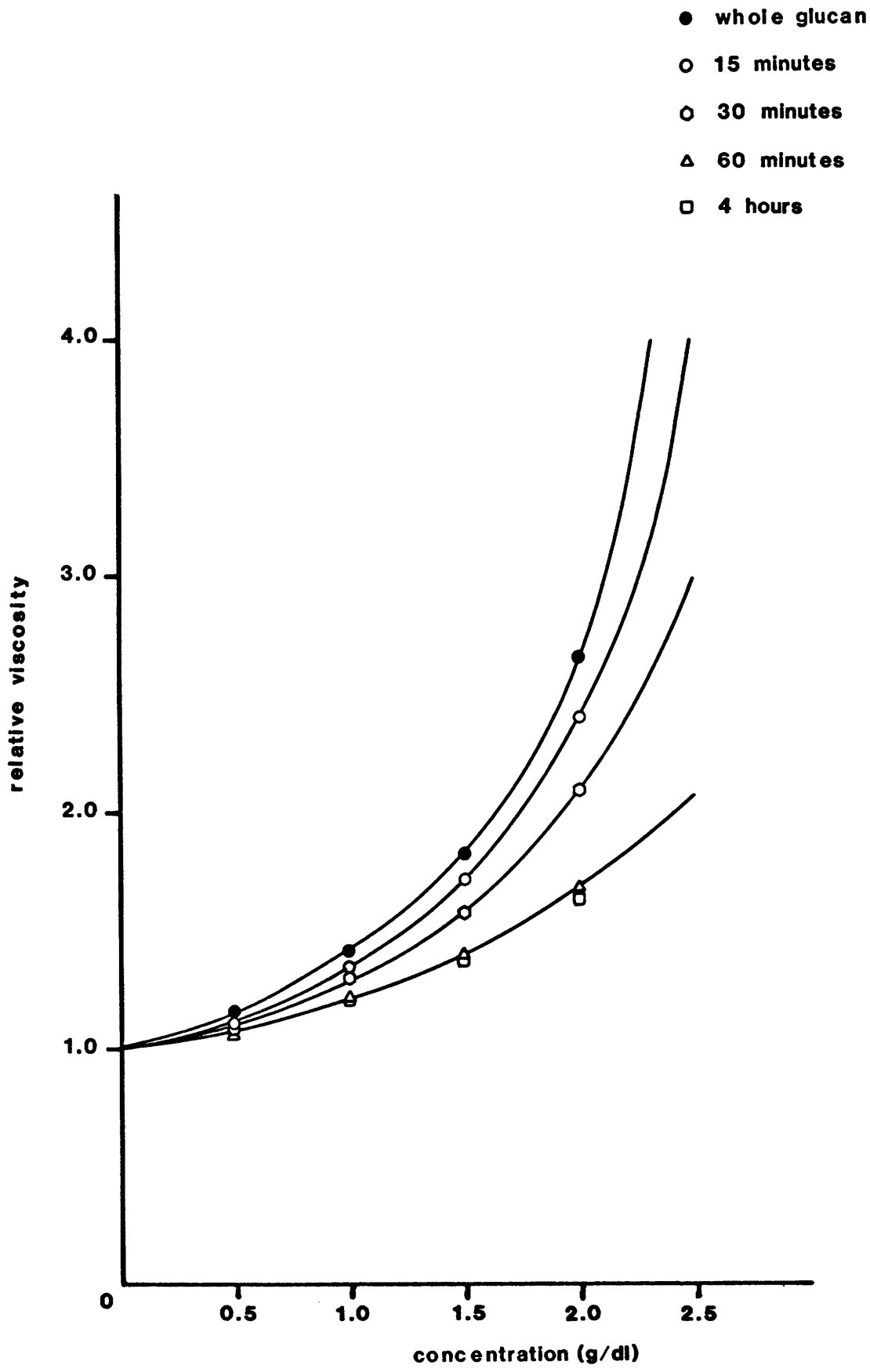

Figure 53: **Viscosity profile of A364A glucan showing the effect of incubation time with laminarinase**

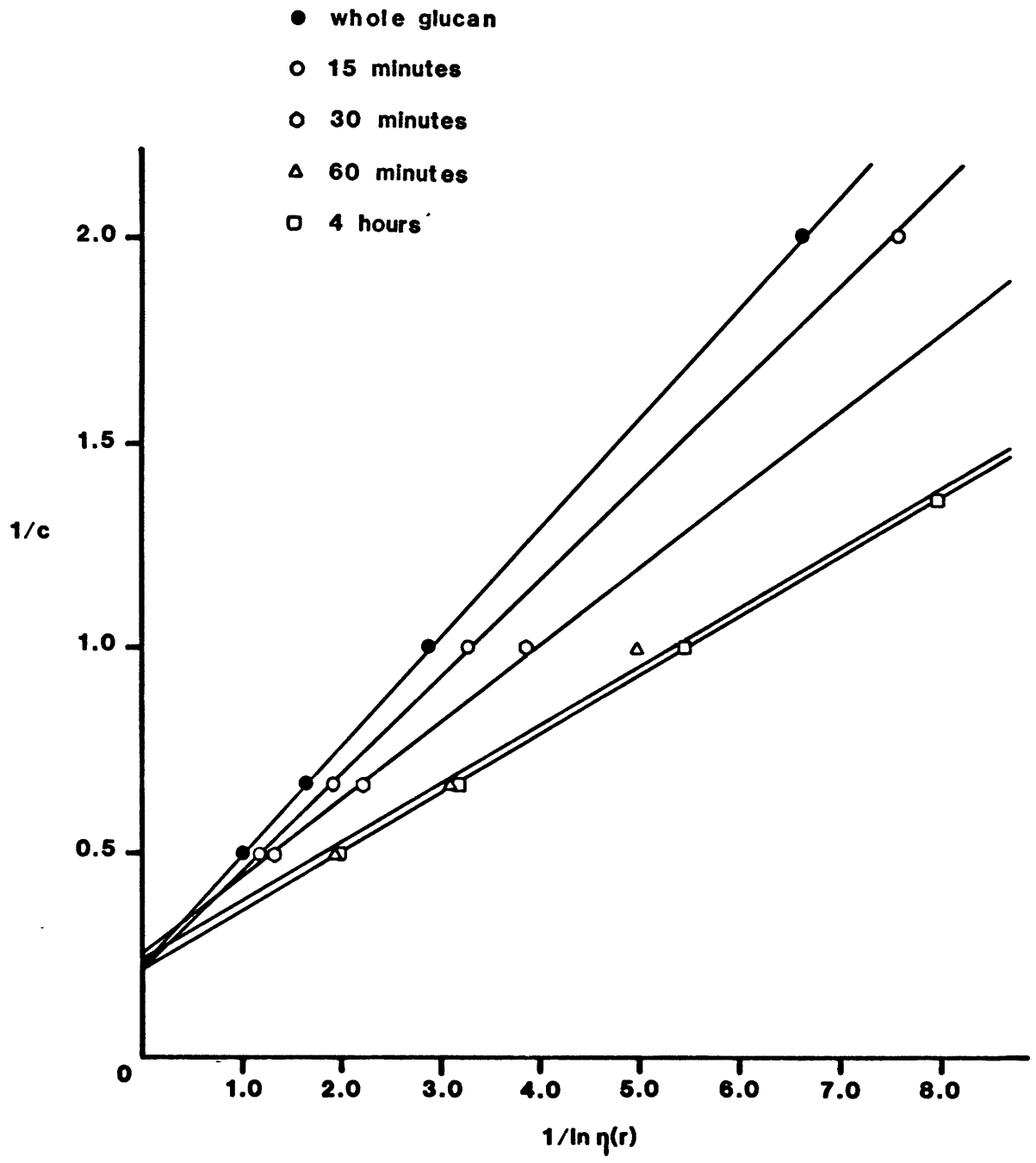

Figure 54 : **Plot of the modified Mooney equation for A364A glucan - the effect of incubation time with laminarinase**

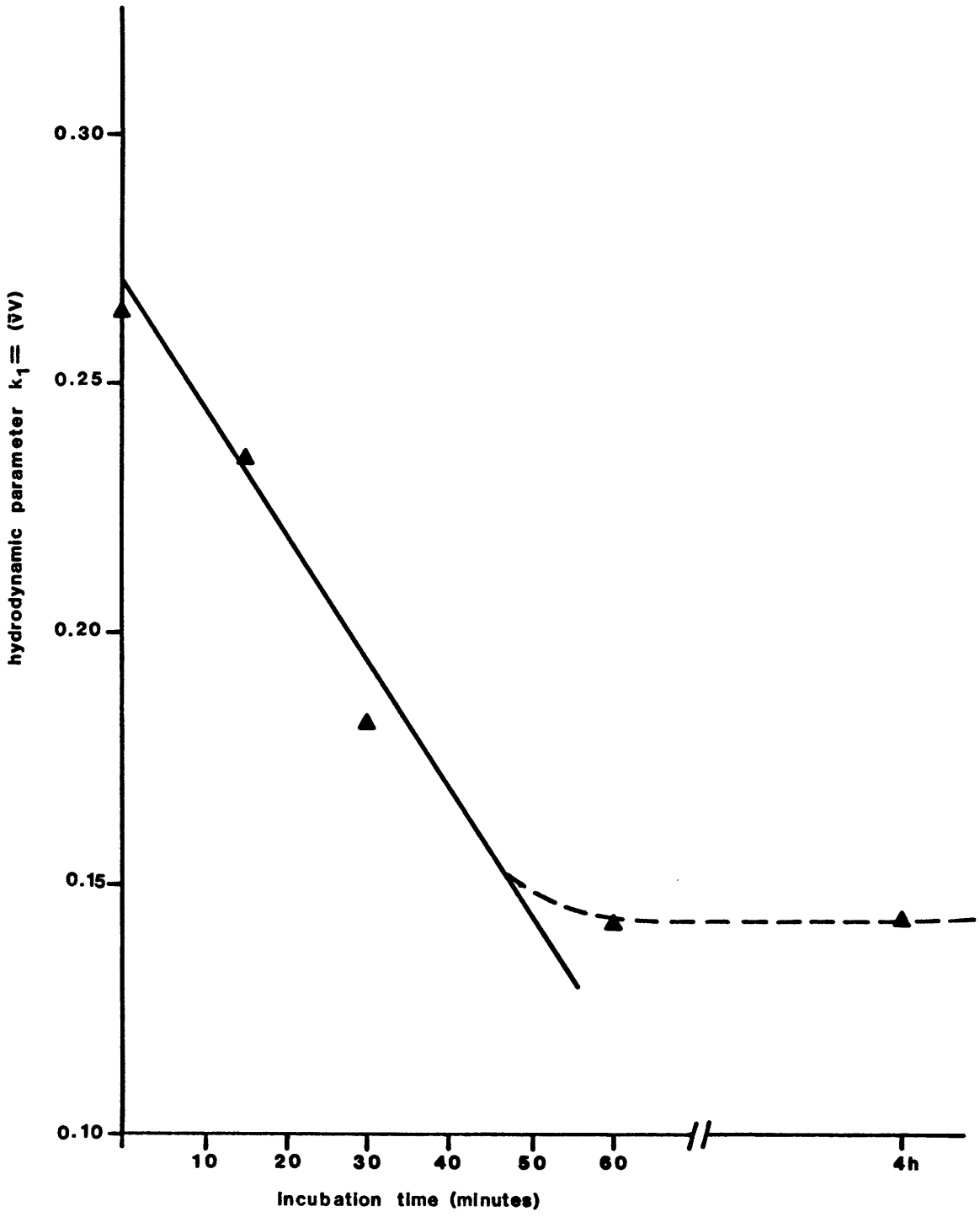

Figure 55 : **Linear correlation of a hydrodynamic parameter of A364A glucan to incubation time with laminarinase**

A plot of the data in Table 10 is shown in Figure 54. Using linear regression, incubation time can be correlated to k_1 for times up to 60 minutes.

The correlation obtained is:

$$k_1 = -0.0021(\text{ time }) + 0.26$$

$$\text{regression coefficient} = -0.98$$

The implication of this result is that for a given glucan sample (in this case A364A glucan) the thickening properties can be adjusted to desired levels. This requires the previous knowledge of the initial hydrodynamic properties (shape factor, maximum packing fraction) of the glucan which were obtained using capillary viscometry.

6. SUMMARY AND CONCLUSIONS

The alkali-insoluble glucan fractions of the cdc mutants 374, 377 exhibit higher thickening properties than the wild-type A364A glucan.

Glucan isolated from Saccharomyces cerevisiae 374 and 377 have denser matrices than wild type A364A glucan.

β(1-6) glucosidic crosslinking plays an important structural role in the glucan isolated from the mutants. It was also found to be related to H-bonding in the whole glucan samples. This H-bonding is, however, not responsible for the rheological properties of the glucans since it was also present in A364A glucan which was not affected by its absence.

Chemical extraction of the β(1-6) glucan fraction has an insignificant effect on the rheological properties of A364A glucan.

Chemical extraction of the β(1-6) glucan fraction from 377 glucan enhanced its thickening properties without altering its gross size and shape.

Laminarinase digestion of the glucan samples decreased

the viscosity imparting characteristics in all 3 cases. The effect was more pronounced for the wild type A364A glucan.

The effect of laminarinase treatment on yeast glucan can be correlated directly to the hydrodynamic parameters of the glucan. This enables accurate design of glucan with prespecified thickening properties.

7. SUGGESTIONS FOR FUTURE RESEARCH

The ultimate objectives of this line of research is to develop:

1. genetic techniques to control/direct glucan biosynthesis
2. a system for the production of yeast glucan using spent yeast or a continuous regeneration model

It is therefore necessary to formulate a research program firstly in the areas of yeast genetics with respect to cell division cycle events and cell wall biosynthesis, and secondly for the optimal extraction of glucans from the yeast cell wall.

The work presented in this thesis establishes a simple yet unique method to characterize glucan structure. Therefore, by utilizing the existing Saccharomyces cerevisiae cell division cycle mutants, the structural differences of glucan at different stages of the cell cycle can be determined. This will provide two pieces of important information:

1. mode of glucan biosynthesis during the cell division cycle in yeast
2. extensive understanding of the structure-function relationships of yeast glucan

The research approach for the second objective will

utilize a similar strategy. The major problem associated with glucan extraction is that the bulk of the glucan is located in the inner cell wall and is covered by an outer mannan layer. It is therefore unavailable for cleavage by enzymes or chemical extraction. Saccharomyces cerevisiae mutants blocked in mannan biosynthesis have been isolated and characterized(5). These mutants can therefore be used to study glucan extraction/regeneration. Furthermore, mannan mutants can be mutagenized and screened for temperature sensitivity, cell division cycle mutants or mutants with altered glucan structure. For example, mutants with a block in the β(1-6) glucosyl transferase activity will contain a higher proportion of β(1-3) glucan which is more susceptible to cleavage by β(1-3) glucanases.

Although a two part research approach has been described, a combination of the two approaches will yield a more conclusive understanding of glucan formation and its structure-function relationships.

References

1. Pei-Syan, L. (1981), Rheological Properties of Yeast Wall Glucan. S.M. Thesis, Dept. of Nutrition and Food Science, M.I.T.

2. Fleet, G.H., and Manners, D.J. (1976), Isolation and composition of an alkali soluble glucan from the cell walls of Saccharomyces cerevisiae .J.Gen.Micro. 94, 180-192.

3. Manners, D.J., Masson, A.J., and Patterson, J.C. (1973a), The structure of a β(1-3)-D-glucan from yeast cell walls. Biochem. J. 135, 19-30.

4. Manners, D.J., Masson, A.J., Patterson, J.C., Bjorndahl, H., and Lindberg. (1973b), The structure of (1-6)-D-glucan from yeast cell walls. Biochem. J. 135, 31-36.

5. Ballou, C.E. (1976), Structure and biosynthesis of the Mannan component of the yeast cell envelope. Adv. Microb. Physiol. 14, 93-158.

6. Sietsma, J.H., and Wessels, J.G.H. (1979), Evidence for covalent linkages between chitin and β-glucan in a fungal wall. J. Gen. Micro. 114, 99-108.

7. Sietsma, J.H., and Wessels, J.G.H. (1981), Solubility of (1-3)- β -D/(1-6)- β -D-glucan in fungal walls: Importance of presumed linkage between glucan and chitin. J. Gen. Micro. 125, 209-212.

8. Cabib, E., and Robert, R. (1982), Synthesis of the yeast cell wall and its regulation. Ann. Rev. Biochem. 51, 763-793.

9. Rogers, H.J., Perkins, H.R., and Wand, J.B. (1980), Microbial Cell Walls and Membranes. Chapman and Hall (editors), London, New York.

10. Molano, J., Bowers, B., and Cabib, E. (1980), Distribution of chitin in the yeast cell wall. J. Cell Biol. 85, 199-212.

11. Kopecka, M., Phaff, H.J., and Fleet, G.H. (1974), Demonstration of a fibrillar component in the cell wall of the yeast Saccharomyces cerevisiae and its chemical nature. J. Cell Biol. 62, 66-76.

12. Phaff, H.J. (1971), Structure and Biosynthesis of the Yeast Cell Envelope. The Yeasts. A.H. Rose and J.S. Harrison (editors), New York: Academic Press, 2, 135.

13. Sentandreu, R.,Victoria Elorza, M., and Villanueva, J.R. (1975), Synthesis of yeast wall glucan. J. Gen. Micro., 90, 13-20.

14. Victoria Elorza, M., Lostau, C.M., Villanueva, J.R., and Sentandreu, R. (1976), Cell wall synthesis regulation in Saccharomyces cerevisiae. Effect of RNA and protein inhibition. Biochimica et Biophys. Acta, 454, 263-272.

15. Lopez-Romero, E., and Ruiz-Herrera, J. (1977), Biosynthesis of β-glucan by cell-free extracts from Saccharomyces cerevisiae. Biochem. Biophys. Acta, 500, 372-784.

16. Shematek, F.M., Braatz, J.a., and Cabib, E. (1980), Biosynthesis of the yeast cell wall. 1. Preparation and properties of β(1-3) glucan synthetase. J. Biol. Chem. 255, 888-894.

17. Shematek, F.M., and Cabib, E. (1980), Biosynthesis of the yeast cell wall. 2. Regulation of β(1-3) glucan synthetase by ATP and GTP. J. Biol. Chem. 255, 895-902.

18. Hartwell, L.H. (1967), Macromolecule synthesis in temperature-sensitive mutants of yeast. J. Bact. 93, 1662-1670.

19. Hartwell, L.H., Mortimer, R.K., Culotti, J., and Cullotti, M. (1973), Genetic control of the cell division cycle in yeast. V. Genetic analysis of CDC mutants. Gen. 74, 267-286.

20. Nurse, P. (1981), Genetic Analysis of the Cell Cycle. In: Genetics as a Tool in Microbiology. 31st Symposium of Soc. for Gen. Microb., Cambridge.

21. Bird, R.B., Stewart, W.E., and Lightfoot, E.N., (1960), Transport Phenomena. John Wiley and Sons, ed.

22. Einstein, A. (1906), Eine neue bestimmung der molekuldimmensionen. Ann. Phys., Paris IV , 19, 289-306.

23. Mooney, M. (1951), The viscosity of a concentrated suspension of spherical particles. J. Colloid. Sci., 6, 162-170.

24. Biomaterials Science and Engineering Laboratory, Food Rheology: Principles and Practice, 1982.

25. Van Wazer et al. (1963), Viscosity and flow measurement, Ed., Interscience.

26. Langer, R.S., and Thilly, W.G. (1981), Analytical Practices in Biochemistry. M.I.T. Department of Nutrition and Food Science.